



UvA-DARE (Digital Academic Repository)

Interactive adsorption of phenolic acids and amino acids on soil minerals

Implications for the formation and properties of soil mineral–organic associations

Gao, J.

Publication date

2017

Document Version

Final published version

License

Other

[Link to publication](#)

Citation for published version (APA):

Gao, J. (2017). *Interactive adsorption of phenolic acids and amino acids on soil minerals: Implications for the formation and properties of soil mineral–organic associations*. [Thesis, fully internal, Universiteit van Amsterdam].

General rights

It is not permitted to download or to forward/distribute the text or part of it without the consent of the author(s) and/or copyright holder(s), other than for strictly personal, individual use, unless the work is under an open content license (like Creative Commons).

Disclaimer/Complaints regulations

If you believe that digital publication of certain material infringes any of your rights or (privacy) interests, please let the Library know, stating your reasons. In case of a legitimate complaint, the Library will make the material inaccessible and/or remove it from the website. Please Ask the Library: <https://uba.uva.nl/en/contact>, or a letter to: Library of the University of Amsterdam, Secretariat, P.O. Box 19185, 1000 GD Amsterdam, The Netherlands. You will be contacted as soon as possible.

Interactive adsorption of phenolic and amino acids on minerals: Implications for the formation and properties of soil mineral–organic associations

Jiajia Gao



Jiajia Gao

Interactive adsorption of phenolic and amino acids on minerals

2017

**Interactive adsorption of phenolic and amino acids
on minerals: Implications for the formation and
properties of soil mineral–organic associations**

Jiajia Gao

Gao J. 2017. Interactive adsorption of phenolic and amino acids on minerals: Implications for the formation and properties of soil mineral–organic associations.

PhD thesis, University of Amsterdam

Cover illustration: A simple display of natural soil system with plantation. Compared with light color soils in desert and agriculture field, the dark soils in forest have better quality (three stars). Cover designed by Jiajia Gao.

The research reported in this thesis was carried out at the research group of Earth Surface Science (ESS) of the Institute for Biodiversity and Ecosystem Dynamics (IBED) of the University of Amsterdam and at the Institute of Soil Science of the Leibniz Universität Hannover. This work was funded by the China Scholarship Council and the Deutsche Forschungsgemeinschaft DFG (FOR1806, “The Forgotten Part of Carbon Cycling: Organic Matter Storage and Turnover in Subsoils (SUBSOM)”).

ISBN 978-94-91407-50-5 / Copyright © 2017

Printed by Ipskamp Printing.

Interactive adsorption of phenolic acids and amino acids on soil minerals: Implications for the formation and properties of soil mineral–organic associations

ACADEMISCH PROEFSCHRIFT

ter verkrijging van de graad van doctor

aan de Universiteit van Amsterdam

op gezag van de Rector Magnificus

prof. dr. ir. K.I.J. Maex

ten overstaan van een door het College voor Promoties ingestelde

commissie, in het openbaar te verdedigen in de Agnietenkapel

op dinsdag 21 november 2017, te 14:00 uur

door

Jiajia Gao

geboren te Shanxi, China

Promotiecommissie:

Promotors: Prof. dr. P.C. de Ruiter, Universiteit van Amsterdam

Prof. dr. K. Kalbitz, Technische Universität Dresden

Copromotor: Dr. B. Jansen, Universiteit van Amsterdam

Overige leden: Prof. dr. W.P. de Voogt, Universiteit van Amsterdam

Prof. dr. R.A.P.F. Bol, Universiteit van Amsterdam

Prof. dr. W. Bouten, Universiteit van Amsterdam

Prof. dr. R. Mikutta, Martin-Luther-Universität Halle-Wittenberg

Dr. K. Heister, Universiteit Utrecht

Faculteit der Natuurwetenschappen, Wiskunde en Informatica

Table of Contents

Chapter 1 General introduction	1
Chapter 2 Ten-year anniversary of the “multilayer model” — a mini-review	11
Chapter 3 Robust analysis of underivatized free amino acids in soil by hydrophilic interaction liquid chromatography coupled with electrospray tandem mass spectrometry	23
Chapter 4 Competition and surface conditioning alter the adsorption of phenolic and amino acids on soil minerals	49
Chapter 5 Organic matter coatings of soil minerals affect adsorptive interactions with phenolic and amino acids	69
Chapter 6 Synthesis	93
Appendices	101
References	137
Summary	157
Samenvatting	161
Acknowledgements	165
List of publications	167

Chapter 1

General introduction

Soil as the interface between lithosphere, hydrosphere and atmosphere and hosting most of the biosphere, makes great contributions by maintaining the stability of various ecosystem on earth, e.g. (i) providing food, biomass and raw material, (ii) storing, filtering and transforming water, nutrients and carbon, (iii) playing a central role as a biodiversity pool and (iv) serving as archive of geological and archaeological heritage (European Commission (EC), 2006; Keesstra *et al.*, 2016). Among these functions, the significance of soil as the largest terrestrial carbon pool (Lal, 2004; FAO and ITPS, 2015) is of particular importance in a world with a changing climate.

1.1 Importance of SOM

The global soil carbon pool (2500 Pg) is much larger than the atmospheric pool (760–829 Pg) and vegetation pool (420–620 Pg) combined (Lal, 2004; Lehmann & Kleber, 2015). The soil carbon pool can be divided into a pool of soil organic carbon (SOC) and a pool of soil inorganic carbon (SIC). The former accounts for > 60% of the total soil carbon pool (Lal, 2004). Given the vast size of the SOC pool and its role in global carbon cycling, processes regulating SOC dynamics have a great and direct influence on the concentration of greenhouse gases (e.g. CO₂ and CH₄) in the atmosphere and thus on global climate change (Lal, 2004; Schmidt *et al.*, 2011; FAO and ITPS, 2015; Luo *et al.*, 2015).

Due to land use change (e.g. expansion of agriculture), the global decrease of the SOC pool over the last two centuries was estimated at 136–160 Pg, which was the second-largest source of CO₂ emission to the atmosphere following combustion of fossil fuel (Ruddiman, 2003; Lal, 2004; Le Quéré *et al.*, 2009). Although the global carbon sequestration potential in soils is supposed to be finite in capacity and time, many studies have showed that the decreasing trend of SOC was reversible and soils have great potential to mitigate climate change via sustainable soil management and sequestration of more carbon in the soil (Lal, 2004; Fischlin *et al.*, 2007; Smith *et al.*, 2008; Stockmann *et al.*, 2013; Minasny *et al.*, 2017). Therefore, great efforts need to be taken to mitigate soil carbon loss and increase SOC storage on a global scale. In order to achieve these targets and predict the changes of soil carbon under climate change, one of the prerequisites is to understand the mechanisms underlying the retention of soil organic matter (SOM) that protect them against decomposition and increase the turnover time (Schmidt *et al.*, 2011).

1.2 Retention mechanism of SOM

The traditional theory argues that humic substances, operationally extracted OM in alkaline solution, make up the majority of SOM and they are thought to be the most stable OM fraction because of the large molecular size and complex molecular structure (Stevenson, 1994; Swift, 1999). However, this theory is increasingly questioned due to lack of evidence to verify the existence of humic substances by modern techniques and their formation process in natural environments (Schmidt *et al.*, 2011; Lehmann & Kleber, 2015). Recently, substantial evidence leads to an emerging view on SOC dynamics that progressive decomposing of SOM is primarily controlled by the surrounding environment rather than the intrinsic properties of these compounds (Schmidt *et al.*, 2011; Lehmann & Kleber, 2015). The mechanisms currently proposed to govern the protection of SOM against decomposition include: (i) selective preservation of recalcitrant OM, such as lignin-derived aromatic carbons, tannins and black carbon, (ii) physical protection via occlusion, intercalation, hydrophobicity and encapsulation to achieve spatial inaccessibility of microbes and enzymes to OM and a shortage of O₂ and (iii) stabilization by interaction with mineral surfaces (Fe-, Al-, Mn-oxides and phyllosilicates) and metal ions (Six *et al.*, 2004; Lützow *et al.*, 2006; Mikutta *et al.*, 2006). Although, the relative contribution of these mechanisms is still under debate, there is a consensus that adsorption of OM on mineral surfaces plays an important role in stabilizing SOM (Lützow *et al.*, 2006; Paul, 2016). Many researchers have reported a positive correlation between the contents of fine mineral particles and SOC (Burke *et al.*, 1989; Mayer & Xing, 2001; Kögel-Knabner *et al.*, 2008 and citations). The strongly associated OM with minerals can account for the major fraction of the SOC pool, especially for the subsoil deeper than 10–15 cm (John *et al.*, 2005; Kögel-Knabner *et al.*, 2008; Herold *et al.*, 2014; Schrumppf & Kaiser, 2015). On the global scale the majority of SOC is stored in the subsoil (below 20 cm; Stockmann *et al.*, 2013). Therefore, the dynamics of SOM could be primarily controlled by the association with minerals and metal ions. However, this assumption deserves more tests on a larger spatial and temporal scale.

Despite the fact that the emerging view tends to focus more on the effects of environmental factors on turnover of the SOM, there is no consistent evidence for the contribution of inherent properties of OM to their stabilization. Because the adsorption of organic compounds is highly dependent on their molecular composition and preferential adsorption of specific compounds is a widespread phenomenon (see section 1.3), we propose that the molecular properties of OM largely affect the storage of SOM through indirectly governing the interaction

with soil minerals rather than a direct effect on the turnover time by the inherent chemical recalcitrance.

1.3 Interaction of SOM with soil minerals and metal ions

Theoretically, the interaction of OM with soil minerals is dominated by adsorption and the involved mechanisms include: ligand exchange, electrostatic interaction, Van der Waals forces, hydrophobic forces, H-bonding, cation bridging and surface ion chelation (Schlautman & Morgan, 1994; Feng *et al.*, 2005; Mikutta *et al.*, 2007; Philippe & Schaumann, 2014). The prevailing mechanisms involved in the formation of mineral–organic associations (MOAs) in the natural environment include: (i) ligand exchange, i.e. displacement of superficial hydroxyl/water groups of minerals by organic carboxyl groups; (ii) cation bridging, i.e. bridging polar functional groups of OM to permanently negative-charged siloxane surface or to hydroxyls of oxides and phyllosilicates via polyvalent metal ions; (iii) electrostatic and Van der Waals interactions and (iv) hydrophobic interactions (Gu *et al.*, 1994; Mikutta *et al.*, 2007; Philippe & Schaumann, 2014; Kleber *et al.*, 2015). The varied adsorption energy for these mechanisms would produce MOAs with different stability and the larger adsorption energy of chemisorption than physisorption indicates a weaker desorbability and thus a smaller bioavailability of OM bound through ligand exchange and cation bridging (Gatta, 1985; Gu *et al.*, 1994; Kleber *et al.*, 2015). Not only the properties of soil minerals and OM, such as mineral surface charge, reactive surface area, crystalline phase, surface coating, OM molecular structure, hydrophobicity and conformation, but also the surrounding environmental conditions, such as soil moisture, solution pH, ionic strength, temperature and valence of ions can influence the adsorption process (Hunter, 2001; Sposito, 2008; Kleber *et al.*, 2015). Several modes of interaction can operate simultaneously in a system (Kleber *et al.*, 2014). In order to fully understand the stabilization of OM adsorbed on the mineral surface, it is pivotal to identify the dominant mechanisms involved in the adsorptive protection of SOM.

In general, soil mineral surfaces can be divided into three categories: uncharged, permanently charged and variable-charge surfaces (Sposito, 2008; Kleber *et al.*, 2015). Uncharged siloxane surfaces, typically derived from kaolin group minerals, are expected to adsorb nonpolar organic molecules or moieties such as alkyl and aromatic compounds via Van der Waals forces and hydrophobic interactions (Sposito, 2008; Kleber *et al.*, 2015). These interactions

were suggested to play an important role in the adsorption of proteins, hydrophobic organic compounds from soil dissolved organic matter (DOM) and polymers such as cutin and carboxymethyl cellulose (Jardine *et al.*, 1989; Servagent-Noinville *et al.*, 2000; Feng *et al.*, 2005; Cuba-Chiem *et al.*, 2008). Negatively charged siloxane surfaces triggered by isomorphic substitution, can promote the adsorption of organic compounds via cation bridging and electrostatic interaction (Barré *et al.*, 2014). For example, the adsorbed polyvalent cations on negatively charged siloxane can link negatively charged functional groups (amino, carbonyl, carboxyl, or hydroxyl groups) with mineral surfaces to form inner-sphere or outer-sphere complexes (Sposito, 2008). Cation bridging could also be established between charged siloxane surfaces and aromatic π -systems (Keiluweit & Kleber, 2009). Moreover, the negatively charged siloxane surfaces can attract positively charged functional groups (e.g. amines) and organic cations (e.g. quaternary ammonium and pyridinium) via electrostatic interaction (Yeasmin *et al.*, 2014; Kleber *et al.*, 2015). This process may be coupled with a process of cation exchange, i.e. replacement of the bound metal ions such as Na^+ and Ca^{2+} (Kleber *et al.*, 2014). Variable-charge surfaces, derived from metal oxides and broken edge sites of phyllosilicates, can facilitate ligand exchange reactions between hydroxyl groups of mineral surfaces and carboxyl or hydroxamate groups of organic compounds, resulting in formation of inner-sphere complexes via covalent metal–O–C bonds (Liu *et al.*, 2008; Kleber *et al.*, 2015). Outer-sphere complexation and H-bonding may also contribute to the adsorption of organic compounds to the edge sites of phyllosilicates (Liu *et al.*, 2008).

1.4 Distribution and structure of bound organic matter on mineral surfaces

Some studies display that OM can homogeneously coat mineral surfaces (e.g. Heister *et al.*, 2012). However, most studies reveal a patchy distribution of OM on mineral surfaces. This was observed via both direct approaches (e.g. microscopy and mass spectrometry) and indirect approaches (e.g. specific surface area (SSA) measurements (Arnarson & Keil, 2001; Mayer & Xing, 2001; Kaiser & Guggenberger, 2003; Dümig *et al.*, 2012; Ransom *et al.*, 1997; Chenu & Plante, 2006; Heister *et al.*, 2012; Vogel *et al.*, 2014). This is in line with the interactions between OM and the mineral phase as described in the previous paragraph. Based on those, adsorption of OM would be expected to occur at specific reactive sites of mineral surfaces. As a result, the discrete distribution of organic compounds on mineral surfaces could be ascribed to the

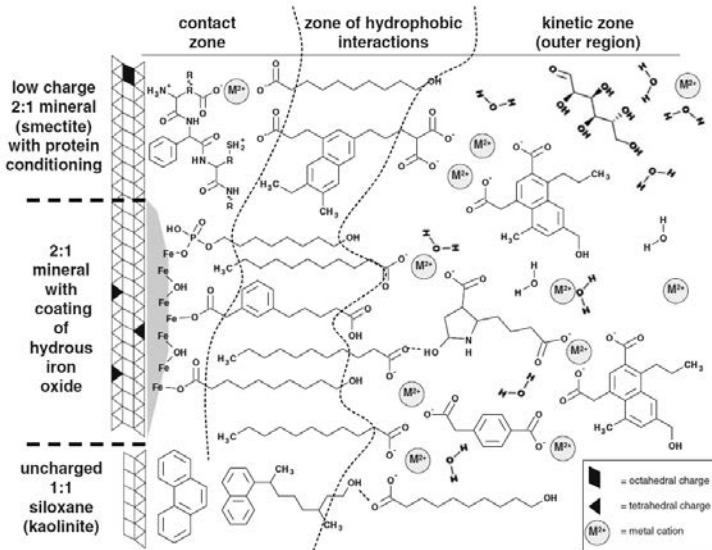


Figure 1.1 The multilayer structure model of mineral-organic associations. Figure adapted from Kleber *et al.* (2007) with reused permission.

heterogeneous distribution of reactive surface hydroxyl groups in phyllosilicates or oxyhydroxide mineral structures and uneven distribution of isomorphic substitution sites in 2:1 clay mineral structures (Kaiser & Guggenberger, 2003; Spósito, 2008).

An important advancement in our understanding of the interactions between SOM and minerals is the introduction of a layer-structure adsorption theory, as first proposed by Schmidt *et al.* (1990). Then a bilayer model of associated OM was suggested by Wershaw (1993). The second important advancement came with the improvement into a multilayer conceptual model (Figure 1.1) by Kleber *et al.* (2007). In this model the structure of bound OM can be self-organized and separated into three layers: (i) the contact zone, i.e. the OM that directly contacts with mineral surfaces; (ii) the intermediate region or zone of hydrophobic interaction and (iii) the outer or kinetic zone. This model reconciles all the prevailing mechanisms that potentially govern the association of OM with soil minerals. It is widely used as the research motivation and explanation for experimental findings (see **chapter 2**). However, there is still no direct and reliable evidence to support this conceptual model.

1.5 Adsorptive protection of phenolic and amino compounds

Substantial evidence supports the preferential adsorption of carboxylated phenolic compounds to various soil minerals (Kaiser & Guggenberger, 2000; Kalbitz *et al.*, 2005; Kothawala *et al.*, 2012). This contradicts the assumption that N-containing amphiphilic compounds are selectively immobilized to form the so called inner layer in the model of Kleber *et al.* (2007). Experimental information about the adsorption of carboxylated phenolic and N-containing compounds to different mineral surfaces and their interaction with respect to competition and surface conditioning is lacking. The proposed multilayer structure regulating the adsorption of organic compounds on mineral surfaces has not yet been tested experimentally, nor has the potentially important role of N-containing compounds therein been tested for the development of a multilayer adsorption structure. This may be achieved by using model compounds, representing nitrogenous and lignin-derived SOM species.

Phenolic acids (PAs) and amino acids (AAs) as degradation products of lignin and organic nitrogen, respectively, play a central role in our current understanding how MOA is formed. Interaction of AAs with soil minerals has been recognized as an important process that may influence the bioavailability of AAs in the soil (Yeasmin *et al.*, 2014). Competitive interaction between AAs and other organic compounds during adsorption on mineral surfaces are, however, not well understood. Numerous studies have shown a high affinity of PAs for soil or soil minerals (Cecchi *et al.*, 2004; Chefetz *et al.*, 2011). However, we do not know whether these monomeric aromatic acids are preferentially adsorbed with respect to N-containing compounds. Furthermore, experimental evidence is lacking for the idea that the proposed surface conditioning by AAs would increase the adsorption of aromatic moieties.

Organic compounds are strongly adsorbed on new mineral surfaces with low C loading through multidentate bonding (Kaiser & Guggenberger, 2007). At larger C loading less functional groups of the organic molecules are involved (Kaiser & Guggenberger, 2007), which renders OM more susceptible to desorption and thus vulnerable to microbial decomposition. Adsorption of natural DOM on mineral surfaces modifies their surface properties, such as SSA and surface charge, consequently altering the adsorption behavior of organic contaminants and phosphate (Zhuang & Yu, 2002; Weng *et al.*, 2008). Such changes in surface properties are important for DOM cycling in the soil profile, which is the result of continuous adsorption (i.e. the formation of MOAs), desorption and microbial production of organic compounds (Sanderman *et al.*, 2008; Kaiser & Kalbitz, 2012). However, effects of these changes in surface properties on the

adsorption of AAs and PAs and their interactions in the soil profile are not well understood, besides the above mentioned decrease in chemical bonds of organic compounds on mineral surfaces with increasing C loading.

1.6 Research objectives and outline

Therefore, the aim of this study was to test Kleber's multilayer conceptual model in general, and in particular with respect to the role of nitrogen containing SOM constituents by investigating the interactive adsorption of AAs and PAs on pure and coated soil minerals with natural DOM in batch adsorption experiment. The outcomes would increase our understanding of the stabilization mechanisms involved in soil C cycling and provided inspirations in modelling and predicting the fate of soil C pool under climate change. To this purpose, the following specific objectives were proposed.

In **chapter 2**, we aimed to critically review and summarize the current state of knowledge with respect to the applicability of the multilayer adsorption model by Kleber and the implications for the model and SOM retention in general.

In **chapter 3**, a robust technique was developed to quantify free AAs in soil extracts using hydrophilic interaction liquid chromatography coupled with electrospray tandem mass spectrometry. The goal was to ensure the precise detection of all the model AAs (lysine, glutamic acid, leucine and phenylalanine) used in the batch adsorption experiments.

In **chapter 4**, batch adsorption experiments were conducted to study the interaction between PAs (salicylic, syringic, ferulic and vanillic acid) and AAs (lysine, glutamic acid, leucine, and phenylalanine) during adsorption on goethite and Ca^{2+} -montmorillonite at pH 6 by applying adsorbate concentrations of 0.01, 0.05 and 0.1 mM. The competition experiments aimed to identify the adsorptive competitiveness of PAs and AAs. The conditioning experiments allowed uncovering the potential role of them in developing a multilayer structure of mineral-associated OM.

In **chapter 5**, batch adsorption experiments were conducted to study how the coating of mineral surfaces with DOM (derived from forest leaf litter (L-DOM) and the underlying O horizon (O-DOM)) affects adsorptive interactions of PAs (salicylic, syringic, ferulic and vanillic acid) and AAs (lysine, glutamic acid, leucine and phenylalanine) on goethite, kaolinite, and montmorillonite at pH 6. This experiment aimed to increase our understanding of the influence of natural

DOM coating of mineral surface on the interactive adsorption of AAs and PAs and add first experimental evidence of the existence of a multilayer structure of associated OM on mineral surfaces.

In **chapter 6**, a synthesis of the thesis is given where the findings of this study were discussed within the context of the multilayer model of Kleber.

Chapter 2

Ten-year anniversary of the “multilayer model” — a mini-review

Abstract

Association with soil mineral phases enhances greatly the resistance of soil organic matter (SOM) to microbial decomposition. In addition, the traditional soil humic substances theory is increasingly challenged, whereas the importance of mineral–organic associations (MOAs) in regulating soil carbon cycling is now rigorously demonstrated by empirical evidence. Based on the substantial knowledge of the formation, composition and structure of MOAs, a multilayer conceptual model was proposed ten years ago. According to the model, the associated OM on mineral surfaces is discrete and self-organized into a multilayer structure. In this review paper, we aim to collect and summarize the existing studies that used this model to explain and understand natural observations, and based on this assess the state-of-the-art insights with respect to the performance and applicability of the model. The multilayer model has seen extensive adoption within the soil science and related fields. In general, existing studies strongly support the concept of a patchy distribution of adsorbed OM on the mineral surface. In addition, enrichment of N-rich OM is found to be controlled by mineral surfaces, and the interplay of different classes of organic compounds is found to be an essential factor for the overall adsorptive storage of SOM. Nevertheless, large uncertainty remains with respect to the multilayer organization of associated OM as rigorous testing of the model at the molecular level is still lacking after ten years of using.

2.1 Introduction

Soils play a crucial role in global carbon cycling by storing around two times as much carbon as the global vegetation and atmosphere combined (Lal, 2004). However, the carbon cycling process and the underlying mechanisms for the long-term storage of soil organic carbon (SOC) are still under debate (Schmidt *et al.*, 2011; Lehmann & Kleber, 2015). Considerable efforts have been devoted to understanding the interaction of soil organic matter (SOM) with minerals and demonstrated that the formed mineral–organic associations (MOAs) possess great contribution to the stabilization of SOM (Lützow *et al.*, 2006; Mikutta *et al.*, 2006; Kleber *et al.*, 2014; Paul, 2016).

Based on the initial layer structure ideas for MOAs from previous researchers (Schmidt *et al.*, 1990; Wershaw, 1993; Horne & McIntosh, 2000; Sollins *et al.*, 2006) and the research findings in soil science and related fields, Kleber *et al.* (2007) proposed a complex conceptual model for MOAs. This new model integrated the potential mechanisms involved in the formation of MOAs and visualized the possible structure of associated OM on mineral surfaces. Although the model refers to the experimental paper of Sollins *et al.* (2006), the experimental basis of the model is weak. Poor relationship exists between the findings of Sollins *et al.* (2006) and the multilayer model for MOAs because the data for the calculation of the organic layer thickness across various soil fractions is missing. The model is based on the assumption that SOM consists largely of amphiphilic molecular fragments with the ability to self-assemble into micellar structure on mineral surfaces in aqueous solution. Consequently, the adsorption of SOM on mineral surfaces is arranged in a discrete zonal structure (Figure 1.1, **chapter 1**) consisting of the following three zones: (1) the polar functional groups of organic compounds interact with mineral hydroxyls via ligand exchange to form the contact zone, directing the hydrophobic portions outwards towards aqueous solution. Proteinaceous material can also accumulate on charged mineral surfaces via electrostatic bonding and the process of structural unfolding that takes place upon adsorption increases their bonding strength via additional hydrophobic interactions (Quiquampoix *et al.*, 1995). In addition, some hydrophobic organic compounds may interact with non-charged mineral surfaces; (2) an entropically driven membrane-like bilayer structure is developed via hydrophobic interacting with other amphiphilic compounds, forming the so-called hydrophobic zone and exposing the hydrophilic portions towards aqueous solution. The strong adsorption of proteinaceous molecules with unfolding results in discontinuous distribution of the membrane-like structure and (3) more organic compounds possibly interact

with the hydrophilic moieties in the hydrophobic zone and the adsorbed proteinaceous compounds via cation bridging, hydrogen bonding and other interactions to form an outer region (kinetic zone). The weakly retained compounds in the kinetic zone may depend more on input than the available binding sites and possess high kinetic exchange rates with the surrounding compounds in aqueous solution. The significance of N-containing compounds is highlighted in this model because of the relatively high abundance of such compounds in soils and the ability of these compounds to adsorb irreversibly on mineral surfaces (Kleber *et al.*, 2007).

This review aims to collect and summarize the existing studies that used this multilayer model to explain and understand natural observations, and based on this assess the state-of-the-art insights with respect to the performance, applicability and further development / improvement of the model.

2.2 Application in soil science and related fields

2.2.1 Soil wettability

Soil OM contributes greatly to soil water repellency (SWR), a widespread natural phenomenon (Goebel *et al.*, 2011; Achtenhagen *et al.*, 2015). The formation of SWR is closely related with associated OM on mineral surfaces and the surrounding environment. The multilayer model has been used successfully to explain the dynamic and reversible SWR under drying and wetting cycles (Goebel *et al.*, 2011; Kaiser *et al.*, 2015; Achtenhagen *et al.*, 2015). Other factors that may affect the SWR include soil microorganisms (Achtenhagen *et al.*, 2015) and H₂O molecules remained in dry soils (Kaiser *et al.*, 2015). Similarly, Diehl *et al.* (2009) used the multilayer model to explain the increased normalized C-H peak area of soils with increasing dryness, which indicates an increase in the proportion of outward-oriented hydrophobic moieties in the outer layer of SOM. In addition, the multilayer model was adopted by Bachmann *et al.* (2008) to show the possible mechanisms involved in the development of soil wettability, i.e. the spatial structure of the OM molecules changing from a sparse flat to a dense upright orientation with increasing surface loading. This hypothesis was also made by Kaiser & Guggenberger (2003). At small OM loading, the hydrophobic groups are arranged at the outside of the particle, while at high OM loading, another layer of organic molecules can be attached to the adsorbed OM with upright orientation via hydrophilic functional groups, thus resulting hydrophobic groups

oriented towards outside (Bachmann *et al.*, 2008). However, the different orientation of organic molecules might be explained by their polyelectrolytic character as well. Such molecules can re-arrange under variable water contents. Moreover, Woche *et al.* (2017) reported that the intrinsic properties of surface OM, i.e. the proportion of non-polar C species, played a crucial role in the surface wettability.

2.2.2 SOM storage and dynamics

Many researchers presented the multilayer model merely to provide an overview of the stabilization processes and mechanisms of SOM and the importance of MOAs in storing SOM (e.g. Brüggemann *et al.*, 2011; Khalaf *et al.*, 2014; Swenson *et al.*, 2015; Kaiser *et al.*, 2016). In addition, the multilayer model was widely used to explain the high amount of OC in soils with limited reactive mineral surfaces (O'Brien & Jastrow, 2013; Araujo *et al.*, 2017; Souza *et al.*, 2017). Similarly, the continued accumulation of SOC with increasing C and nutrients inputs (Orgill *et al.*, 2017) and the increased adsorption capacity of dissolved organic matter (DOM) on subsurface soils with increasing original SOC content were also explained by the multilayer model (Mayes *et al.*, 2012). Based on the model, Lin & Simpson (2016) attributed the protection of cutin and suberin components in soils to the indirect interaction with mineral-bound SOM. However, these observations can also be explained by aggregation effects (O'Brien & Jastrow, 2013; Lin & Simpson, 2016).

Based on the multilayer model, Han *et al.* (2016) made a hypothesis that the adsorbed OC on mineral surfaces can be divided into two categories: directly and indirectly associated SOC. The former being in the "contact zone" has a stronger resistance to decomposition, thus slower turnover rate and longer residence time than the latter, i.e. SOC in the "hydrophobic and kinetic zone". A similar idea has been introduced before that and discussed in the following studies: Castanha *et al.* (2008) observed that isolated soil density fractions contained a mix of old and young carbon indicated by ^{14}C data. Using a modelling approach, Torn *et al.* (2013) reported the coexistence of strongly bound (old) and weakly bound, fast-cycling (young) OM in different soil density fractions. Zollinger *et al.* (2013) showed higher ^{14}C -ages for the stable soil C-fraction (with H_2O_2 treatment) compared to the bulk soil. Because physical density fractionation makes only a rough separation between active and passive OC pool (Lützow *et al.*, 2006), the presence of occluded free OM in aggregates across all density fractions can also explain the mix of fast and slow cycling of

OC. Moreover, the residual OC after H₂O₂ treatment often contains pyrogenic material (Mikutta *et al.*, 2005), which possible lead to high ¹⁴C-ages. The higher bioavailability of newly synthesized amino acids (AAs) compared to the original AAs in soils was explained by their retention in the outer layer of MOAs (Zhang *et al.*, 2015). However, the protection of original soil AAs could be also attributed to entrapment in pores which are too small for enzyme access, interaction with and encapsulation in other OM components (Zhang *et al.*, 2015). Based on the multilayer model, Helassa *et al.* (2009) and Feng *et al.* (2014) assumed that adsorption and variation in loading of natural OM, possibly representing different bonding modes for different OM layer on mineral surfaces, alter the thermal and biological stability of natural OM. They found the thermal and biological stability of natural OM upon adsorption on minerals generally increased with C loading which is in contrast to the multilayer model. The reason was attributed to the unsaturated loading of OM on mineral surfaces and absence of an ageing process for the MOAs (Feng *et al.*, 2014).

Bingham & Cotrufo (2016) adopted the multilayer model to support a theory that fresh inputs of N-containing OM into the upper soil horizons are weakly retained on OM coating of mineral surfaces. This enables them to be readily displaced and migrate to deeper horizons, where strong adsorption on mineral surfaces occurs due to the abundant fresh mineral surfaces. Similarly, Macías & Arbestain (2010) used the multilayer model to explain why the importance of MOAs in SOM stabilization increases with soil depth (Von Lützow *et al.*, 2008). The low degree of oxidation of the fresh inputs of OM likely results in weak interaction with the mineral phase in the top soil horizons. With increasing soil depth oxidation of OM and the availability of mineral surfaces increase gradually and results in higher affinity between DOM and mineral phase in the deep horizons (Lehmann & Kleber, 2015). Avneri-Katz *et al.* (2017) used the multilayer model coupled with patchy structure theory to clarify the enhanced adsorption of hydrophobic DOM on mineral soils with increasing DOM concentration. Yet no experimental evidence of the model was included. Vázquez-Ortega *et al.* (2014) used the multilayer model to explain the displacement of weakly bound grassland soil DOM molecules by high-affinity organic molecules from forest soil DOM in soil column experiments. He *et al.* (2016) integrated the model to a theory to illustrate the dynamic exchanges between DOM and particulate organic matter (POM) in coastal and inland aquatic ecosystems. However, the inner- and outer-sphere complexes theory (Sposito, 2008) can be used as well to explain these observations and assumptions.

Some studies used the multilayer model to explain their findings but not necessarily referring to the notion of multilayer structure, such as higher stable C and N concentration in soils from the Alps than that from the Wind River Range (Egli *et al.*, 2012). Cause mentioned is a higher production of secondary minerals with strong adsorption capacity of SOM for the Alps soils (Egli *et al.*, 2012). Moreover, the multilayer model was used to support the positive relationship of SOC content with poorly crystalline oxyhydroxides (Egli *et al.*, 2008), and the close relationship between clay content, accumulated OC and proteinaceous substances during SOC accumulation (Siewert & Kučerík, 2015). Apparently, these experimental results do not require the multilayer model for interpretation but can be explained by a variable availability of reactive mineral surfaces and by the fact that minerals offer different adsorption sites for the various components of OM. Unfortunately, most of the citing studies take the validity of the multilayer model for granted, despite it has never been soundly proven. This is astonishing because the fundamental principle of science, to test ideas first, is thus often violated.

2.2.3 Strong adsorption potential of N-containing compounds and enrichment of N in the stable SOM pool

The multilayer model proposes that an N-rich inner layer of OM exists and it is bound in a stable manner to specific mineral surfaces. This concept derived from the model is widely used to explain the lower C/N ratio of the subsoil than the topsoil (Favilli *et al.*, 2008), a marked decrease in the C/N ratios of the soil heavy fractions after sonication (Castanha *et al.*, 2008) and the enrichment of N in the stable SOC pool, i.e. H₂O₂-resistant fractions and the heavy density fractions (Barbera *et al.*, 2008; Sleutel *et al.*, 2011; Bonnard *et al.*, 2012; Dümig *et al.*, 2012; Zollinger *et al.*, 2013). However, all these studies ignored determining the fixed inorganic N (i.e. ammonium). Therefore, the soil N could be presented as fixed inorganic N too especially in deep mineral soils (Nieder *et al.*, 2011).

The stable binding of N-rich OM on mineral surfaces guarantees their strong resistance to decomposition. Therefore, Barbera *et al.* (2012) used the multilayer model to support the explanation that the stronger resistance of silt-clay associated OM to mineralization induced by agricultural practices was due to the higher total N concentration compared to the bulk soil. However, the high concentration of N should be the result of interactions between SOM and minerals rather than the trigger for the slow turnover of silt-clay associated OM.

Nitrogen depleted compounds can also form stable associations with minerals. Cusack *et al.* (2013) used the multilayer model to explain the higher abundance of proteinaceous C in the soils with agricultural disturbance. This was also attributed to the higher microbial activity in cultivated soils (Cusack *et al.*, 2013). Hobbie & Hobbie (2012) used the multilayer model to explain the stronger protection of native soil AAs from microbial uptake compared to the freshly added AAs. However, the native soil AAs could be hidden in microaggregates or located in pores inaccessible to microbes (Hobbie & Hobbie, 2012). Bimüller *et al.* (2014) compared N mineralization of particle size fractions and bulk soil and interpreted the smaller total N mineralization of different size fractions by an additional binding of N-rich compounds on the increased surfaces after fractionation. However, this conclusion is questionable because the loss of N during fractionation is unknown. With a high affinity between N-containing compounds and mineral surfaces, the multilayer model was adopted to explain the relative increase in amide+carboxyl functional groups adsorbed on Fe-containing precipitates in ground water over an eight-month aging and reductive transformation process (Cismasu *et al.*, 2016) and the possible long-term effects of N inputs on the increase of forest SOM storage by forming stable MOAs (Nave *et al.*, 2009). Although these studies focused on interaction of N-rich organic compounds with specific mineral surfaces, the role of N-rich OM in the formation of MOAs was not investigated.

2.3 Experimental evidence of the multilayer model?

2.3.1 Patchy distribution of adsorbed OM

In theory, a certain amount of OM must be clustered in small patches with a certain vertical extension if they are not evenly distributed on available mineral surfaces. This may support indirectly the multilayer model (Kleber *et al.*, 2007). In addition to the previous evidence for the patchy distribution of OM on mineral surfaces (Kleber *et al.*, 2007 and references cited therein), visual and direct evidence was obtained recently by state-of-the-art techniques, such as near-edge X-ray absorption fine structure spectroscopy (NEXAFS) and nano-scale secondary ion mass spectrometry (NanoSIMS) (Lehmann *et al.*, 2008; Solomon *et al.*, 2012; Vogel *et al.*, 2014; Hatton *et al.*, 2015). Vogel *et al.* (2014) observed that only 1–2% of the total area for the non-aggregated particles from clay-sized fractions was covered by OM, whereas 15–21% was covered by OM for the aggregated particles. Moreover, Hatton *et al.* (2015) reported that the particle area covered by OM across all density fractions was 42.4 and 8.3% on

average for aggregated and non-aggregated particles, respectively. To date, the evidence for the patchy distribution of associated OM cannot support the multilayer model on its own.

2.3.2 The role of proteinaceous compounds

Recently the enrichment of N-rich compounds on mineral surfaces was observed using NanoSIMS (Hatton *et al.*, 2012; Hatton *et al.*, 2015). However, NanoSIMS images also displayed C-rich organic compounds (C/N ratios > 80) in the densest soil fractions (> 2.65 g cm⁻³; Hatton *et al.*, 2015). Solomon *et al.* (2012) demonstrated numerous N-containing compounds located nearby mineral-organic interface by imaging N maps of the ultrathin section (approximately 150 µm diameter and 400 nm thick) of soil microaggregates using scanning transmission X-ray microscopy (STXM) coupled with NEXAFS spectroscopy. In fact, these interesting results showed different places with different N enrichment in microaggregates but cannot be used as an experimental proof of the multilayer model. No enrichment of N at natural soil mineral-organic interfaces was found by Mikutta *et al.* (2009), who observed a parallel decrease in C and N intensity during X-ray photoelectron spectroscopy (XPS) depth profiling analysis and an increasing portion of aromatic C. This finding was in line with other studies showing aromatic compounds possess a high affinity for metal oxides (Kaiser & Guggenberger, 2000; Chorover & Amistadi, 2001; Mikutta *et al.*, 2007). In contrast to the preferential adsorption of proteinaceous compounds from extracellular polymeric substances on goethite (Omoike & Chorover, 2006), the preferential adsorption of N was not observed on Al(OH)₃ (Mikutta *et al.*, 2011). Organic phosphorus containing compounds possibly play an important role in the formation of MOAs because these materials were adsorbed preferentially on both goethite and Al(OH)₃ (Omoike & Chorover, 2006; Mikutta *et al.*, 2011). Accordingly, the current evidence does not support the idea that N-rich organic compounds are generally enriched on mineral surfaces by preferential adsorption. The enrichment of N could be dependent on mineral surfaces as illustrated in the diagram of the multilayer model (Figure 1.1, **chapter 1**) that N-containing OM only serves as a surface conditioner on siloxane surfaces. Meanwhile, more attention should be paid on the application of surface analytical techniques to ensure the analysis of real mineral-organic interface. Furthermore, just the enrichment of N-rich organic compounds on mineral surfaces cannot be used as direct evidence of the multilayer model.

2.3.3 Multilayer structure

To date, it is still challenging to directly visualise the spatial organization of associated OM on mineral surfaces in a molecular scale and unravel the involved mechanisms as suggested in the multilayer model due to the heterogeneous SOC forms and mineral composition and the lack of suitable analytical techniques (Lehmann *et al.*, 2008; Liu *et al.*, 2013). However, some advanced techniques have showed potential to address these issues. A general increasing trend of aromatic C towards the mineral-organic interface was found via XPS depth profiling analysis (Mikutta *et al.*, 2009). This may indicate the vertical heterogeneity of the associated OM. Du *et al.* (2014) identified three different layers (ca. 100 μm thick) for the associated OM on soil particles using Fourier transform infrared photoacoustic spectroscopy (FTIR-PAS) with enrichment of heterocyclic N moieties in the inner layer (ca. 60 μm deep). But the spatial resolution in this study does not allow any conclusion about the validity of a molecular-based multilayer model. By integrating NanoSIMS with isotopic tracing, Vogel *et al.* (2014) and Hatton *et al.* (2015) observed new OM was preferentially attached to the OM-conditioned surface sites rather than bare mineral surfaces. However, any conclusion about a multilayer structure has to consider that thin coatings cannot be detected by NanoSIMS. A combination of laser desorption synchrotron postionization (synchrotron-LDPI) mass spectrometry and secondary ion mass spectrometry (SIMS) was adopted by Liu *et al.* (2013) to investigate the molecular properties of soil MOAs and they found lignin compounds was enriched in light soil fractions while aliphatic hydrocarbons was enriched in dense fractions. Moreover, the power of STXM, combined with NEXAFS, in identifying C functional groups in nanoscale was tested by Lehmann *et al.* (2008), Solomon *et al.* (2012) and Chen *et al.* (2014). They demonstrated complex C forms (aromatic, polysaccharides, aliphatic, amide and nucleic acids) in mineral-organic interface and correlate them to the surface Ca, Fe, Al and Si ions, Fe and Al hydr(oxides) and phyllosilicates. Furthermore, Remusat *et al.* (2012) showed the potential capabilities of NanoSIMS coupled with STXM-NEXAFS in analysing the chemical compositions of MOAs. It is clear that more research focussing on the molecular interactions of SOM and specific fractions thereof and soil minerals is needed to truly validate the multilayer model. Meanwhile, it is worthwhile to improve the feasibility and reliability of the applied techniques regarding the spatial resolution, sample preparation, control of radiation damage and spectral quantification (Lehmann & Solomon, 2010).

2.4 Conclusion

The conceptual multilayer model of MOAs has been widely used to underpin experimental observations and develop new theory in soil science and related fields across various spatial and temporal scales. However, to date, only very few studies have investigated directly its validity at a molecular level. This highlights a fundamental weakness of nowadays science in a way that popular, edge-cutting ideas become extensively used without profound testing beforehand. In particular the hypothesized multilayer structure and its coupled interaction between different types and classes of molecules that together constitute SOM still lacks rigorous testing. Many of the experimental findings can be explained by simpler explanations instead of the conceptual multilayer model, like aggregation effects for the storage of SOM and differences in the availability of different reactive mineral surfaces for the positive relationship between SOC content and the content of specific minerals. In other words, many studies violate the Occam's razor principle: the simplest explanation will be the most likely one. Nevertheless, given the success of the model in explaining important aspects of the dynamics of SOM, there is an urgent need for further validation of the model, particularly through studies that focus on specific classes of organic molecules and their interaction with well-defined soil mineral phases.

Chapter 3

Robust analysis of underivatized free amino acids in soil by hydrophilic interaction liquid chromatography coupled with electrospray tandem mass spectrometry

This chapter has been published as:

Gao, J., Helmus, R., Cerli, C., Jansen, B., Wang, X. & Kalbitz, K. 2016. Robust analysis of underivatized free amino acids in soil by hydrophilic interaction liquid chromatography coupled with electrospray tandem mass spectrometry. *Journal of Chromatography A*, **1449**, 78–88.

Abstract

Amino acids are an important and highly dynamic fraction of organic N in soils and their determination in soil without derivatization is challenging due to the difficulties in separation and detection of trace amounts of these polar analytes. In the present work, we developed an analytical method to quantify 20 free amino acids in aqueous soil extracts without derivatization. The method employed hydrophilic interaction liquid chromatography–tandem mass spectrometry (HILIC–MS/MS) technique combined with a cation exchange solid phase extraction (SPE). Four stable isotope labelled amino acids were used as internal standards to improve the method performance. Good separation of 20 underivatized amino acids was achieved within 12 min. The limit of detection (LODs) and limit of quantification (LOQs) were in the range of 13–384 ng g⁻¹ and 43–1267 ng g⁻¹ (dry soil basis), respectively. The results showed that overall recoveries with high precision were obtained for the extracted free amino acids from ten different soils. The overall recoveries of 18 amino acids were similar for the ten soils used, which differed substantially in organic C content and in other properties as soil texture and pH. For most of the amino acids, the average recoveries from soil extracts were between 74% and 117%, with the exception of Met (31%), Pro (52%) and Arg (68%). Variability was within acceptable limits (relative standard deviations were between 4% and 13%), with the exception of Met (relative standard deviation = 90%) and Arg (relative standard deviation = 53%). Thus the proposed method with high throughput and high analyte specificity shows great promise for consistent analysis of free amino acids extracted from soils and offers new horizons for the analysis of amino acids in terrestrial and aquatic ecosystem.

3.1 Introduction

Amino compounds (amino acids and amino sugars) play an important role in soil N cycling. These compounds account for 30–80% of total soil N and constitute the majority of soil organic N (Martens *et al.*, 2006; Olk, 2008; Olk *et al.*, 2008; Creamer *et al.*, 2012; Creamer *et al.*, 2013). Amino acids are the key component of soil dissolved organic nitrogen (DON) and they are closely related with the soil organic carbon (SOC) pool in terms of the dynamics and stabilization of dissolved organic carbon (Perakis & Hedin, 2002; Knicker, 2011). Amino acids not only represent a crucial N source for microorganism but also can be directly utilized by some plants (Näsholm *et al.*, 2000; Jones *et al.*, 2004). Additionally, these compounds can serve as biomarker to indicate their sources (e.g. microbial vs. plant residues) (Creamer *et al.*, 2013).

Amino acids are zwitterionic compounds, i.e. they can exist as an overall neutral form, a weak acid or a weak base. Due to the lack of specific chromophores for ultraviolet (UV) or fluorescence detection for most of amino acids (Kaspar *et al.*, 2009), derivatization is widely used to improve the separation and the sensitivity of detection for analysing amino acids in biological and environmental samples (Kielland, 1995; Callejón *et al.*, 2010; Inagaki *et al.*, 2010; Kvitvang *et al.*, 2011; Sarazin *et al.*, 2011; Sánchez-Hernández *et al.*, 2011). Overall these techniques can guarantee good separation, sensitive detection and high reproducibility but they have some drawbacks, such as being time-consuming and displaying instable derivatives, insufficient reproducibility of derivative yield, lack of analyte specificity and side effects of reagents (Langrock *et al.*, 2006; Kaspar *et al.*, 2009). Therefore, recently, the techniques for direct analysis of underivatized amino acids have gained more attention and several methodologies have been developed. Casella and Contursi (2003) measured 12 amino acids in milk using ion chromatography (IC) coupled to amperometric detection. High performance anion exchange chromatography combined with pulsed amperometric detection (HPAEC-PAD) was successfully applied to analyse soil amino acids (Martens & Loeffelmann, 2003; Olk *et al.*, 2008; Creamer *et al.*, 2012). Desiderio *et al.* (2010) demonstrated that capillary electrophoresis (CE) linked to mass spectrometry (MS) detection enabled analysis of amino acids without previous derivatization. Ion-pairing liquid chromatography (LC) coupled to MS detection is another alternative approach to analyse underivatized amino acids (Piraud *et al.*, 2005; Armstrong *et al.*, 2007; Liu *et al.*, 2008; Le *et al.*, 2014). However, there are still serious drawbacks connected to all described techniques, including low throughput, reagents-induced retention time shift and contamination of analytical system (Liu *et al.*, 2008; Kaspar *et al.*, 2009).

Most recently, hydrophilic interaction liquid chromatography (HILIC) has attracted considerable attention because of the many advantages over conventional normal phase LC and reverse phase LC (Buszewski & Noga, 2012). HILIC is capable of separating a broad range of polar compounds, including amino acids, peptides, carbohydrates, polar drugs, metabolites and biologically important compounds in proteomics, glycomics and clinical analysis (Dell'mour *et al.*, 2010; Jandera, 2011; Buszewski & Noga, 2012; Guo *et al.*, 2013). Guo *et al.* (2013) have demonstrated that HILIC is a reliable technique to analyse amino acids in food. The successful application of HILIC in detecting medicine and cellular metabolites was displayed as well (Preinerstorfer *et al.*, 2010; Zhou *et al.*, 2013). As part of these efforts, various HILIC columns have been tested for separation of amino acids, such as silica, amide, bridged ethyl hybrid (BEH) amide and zwitterion (Dell'mour *et al.*, 2010; Guo *et al.*, 2013; Gökmen *et al.*, 2012). While successfully applied in the before-mentioned matrices, the applicability of HILIC has yet to be tested for the analysis of amino acids from soils, which form a complex and difficult matrix because of the plethora of binding sites for various compounds including amino acids. In the mineral soil compartment, many interfering compounds can be co-extracted from soils together with the targeted amino acids (McDowell & Likens, 1988; Guggenberger & Zech, 1994; Kaiser *et al.*, 2001), and the free amino acid concentrations in soil solutions are generally low (Jones *et al.*, 2002). Therefore, in contrast to the application in matrices such as food, purification and concentration of soil extracts are most likely necessary prior to the analysis of soil amino acids. Solid phase extraction (SPE) has become a widely-used technique to clean up and concentrate extracted amino acids in complex samples through isolating analytes of interest from a wide variety of matrices, such as biological matrices (Armstrong *et al.*, 2007; Calderón-Santiago *et al.*, 2012; Tang *et al.*, 2014) and sediment (Yang *et al.*, 2011). However, only a few studies have reported the performance of the SPE technique in purifying and concentrating soil extracts prior to the measurement of free amino acids. Dell'mour *et al.* (2010) reported that the overall recoveries of 12 free amino acids in soil extracts through SPE procedure ranged between 13% and 70%.

Therefore, the aim of the present study was to develop and test a novel, robust and fast procedure to extract and analyse amino acids from soils through combining HILIC-HPLC-MS/MS and SPE technique. For this purpose, ten soils representing a broad range of compositions (pH, texture class, organic C content, etc.) were augmented with 20 amino acids that are common in soils. These were subsequently used to develop and test the new procedure.

3.2 Material and methods

3.2.1 Chemicals

Acetonitrile (ACN, LC/MS grade), methanol (MeOH, ULC/MS grade) and formic acid (FA, ULC/MS grade) were purchased from Biosolve B.V. (Valkenswaard, The Netherlands). Analytical grade ammonium formate (NH_4HCO_2) and ammonium acetate (NH_4OAc) were purchased from Sigma-Aldrich (Zwijndrecht, The Netherlands). Analytical grade hydrochloric acid (37%), ammonium hydroxide (25 wt%) and acetic acid (AcOH) were purchased from Merck KGaA (Darmstadt, Germany). Analytical grade sodium azide (NaN_3) was purchased from Janssen Chimica (Beerse, Belgium). All mobile phases and solutions were prepared using subboiled water (sub-boiling distilled water). Ultrapure deionized water produced by a Purelab Ultra system (MK2-Analytic, ELGA, High Wycombe, United Kingdom) was used to extract soil free amino acids.

Targeted amino acids and internal standards (IS) are listed in Table 3.1. Those amino acids were divided into three groups: acidic, basic and neutral amino acids. The purity of each compound was higher than 98%.

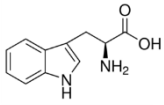
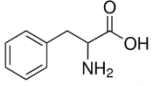
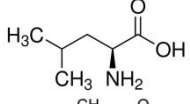
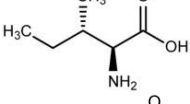
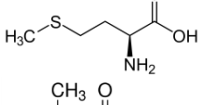
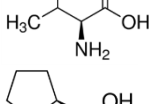
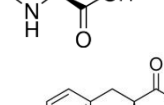
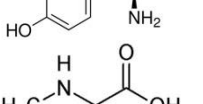
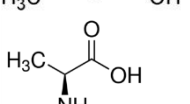
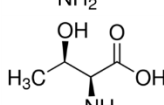
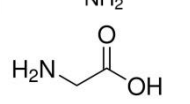

3.2.2 Instrumentation

The separation system employed a Prominence fast LC (Shimadzu, Kyoto, Japan), consisting of two LC-20AD XR pumps, a SIL-20AC XR auto-sampler and a CTO-20AC column oven. HILIC separation was performed on an ACQUITY UPLC BEH Amide separation column (2.1 mm \times 100 mm, 1.7 μm , Waters), together with an ACQUITY UPLC BEH Amide 1.7 μm VanGuard guard column. BEH amide column was selected because it can provide great retention and selectivity (Guo *et al.*, 2013; Kumar *et al.*, 2013). The injection volume was 20 μl . Sample was eluted at a flow rate of 0.4 ml min^{-1} . The column temperature was set at 35 $^\circ\text{C}$.

Mass spectrometry detection was carried out on a 4000 QTRAP LC-MS/MS System (AB SCIEX, MA, USA), coupled with an ESI interface. Multiple reaction monitoring (MRM) method was used to determine all the analytes. Data acquisition and analysis were performed with AB SCIEX Analyst software (ver. 1.5.1).

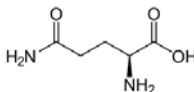
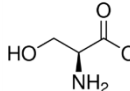
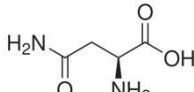
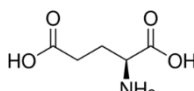
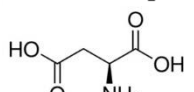
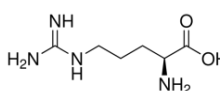
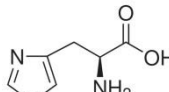
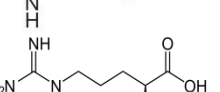
A bench-top freeze dryer (Scala Scientific, The Netherlands) was used to freeze-dry soil extracts.

Table 3.1 Properties and supplier of the targeted amino acids and internal standards.

Amino acids	Abb. ^a	Structure	MW	pI ^b	Supplier	
Neutral						
1	L-tryptophan	Trp		204.23	5.89	SA ^c
2	DL-phenylalanine	Phe		165.19	5.48	SA
3	L-leucine	Leu		131.18	5.98	SA
4	L-isoleucine	Ile		131.18	6.02	SA
5	L-methionine	Met		149.21	5.74	SA
6	L-valine	Val		117.15	5.96	SA
7	L-proline	Pro		115.13	6.30	SA
8	L-tyrosine	Tyr		181.19	5.66	SA
9	Sarcosine	Sar		89.09	6.20	SA
10	L-alanine	Ala		89.09	6.01	SA
11	L-threonine	Thr		119.12	6.16	SA
12	Glycine	Gly		75.07	5.97	SA

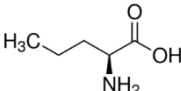
(Continued)

Table 3.1 Properties and supplier of the targeted amino acids and internal standards (continued).

Amino acids	Abb. ^a	Structure	MW	pI ^b	Supplier	
Neutral						
13	L-glutamine	Gln		146.15	5.65	SA ^c
14	L-serine	Ser		105.09	5.68	SA
15	L-asparagine	Asn		132.12	5.41	SA
Acid						
16	L-glutamic acid	Glu		147.13	3.24	SA
17	L-aspartic acid	Asp		133.1	2.77	SA
Basic						
18	L-arginine	Arg		174.2	10.76	SA
19	L-histidine	His		155.16	7.59	SA
20	L-lysine	Lys		146.19	9.82	SA

(Continued)

Table 3.1 Properties and supplier of the targeted amino acids and internal standards (continued).

Amino acids		Abb. ^a	Structure	MW	pI ^b	Supplier
Internal standards (IS)						
21	DL-norvaline	Nva		117.15		SA ^c
22	L-lysine HCl (4,4,5,5-D4)	Lys-D4		150.21		SA
23	L-alanine (2,3,3,3-D4)	Ala-D4		93.12		CIL ^d
24	Glycine (D5)	Gly-D5		80.1		CIL
25	L-glutamic acid (2,3,3,4,4-D5)	Glu-D5		152.16		CIL

^a Abbreviation; ^b Isoelectric point, from Barrett (1985) and Cernei *et al.* (2012); ^c Sigma-Aldrich (Zwijndrecht, the Netherlands); ^d Cambridge Isotope Laboratories (Andover, MA, USA).

3.2.3 Preparation of test solutions

Separate stock standard solutions of targeted amino acids (2000 $\mu\text{g ml}^{-1}$) were prepared by dissolving each compound in 0.1 M HCl. The concentration of Tyr was set at 500 $\mu\text{g ml}^{-1}$ because of its low solubility in water. Separate IS stock solutions (500 $\mu\text{g ml}^{-1}$) were also prepared in 0.1 M HCl. All the stock solutions were stored at $-20\text{ }^{\circ}\text{C}$ before use. Working solutions were prepared by mixing and diluting the stock standard solutions. According to our results, the stock standard solutions were stable for at least one month at $-20\text{ }^{\circ}\text{C}$ (data not shown).

3.2.4 Extraction of soil free amino acids

Table 3.2 shows the tested soil samples in this study. Ten different soils from around the world ranging from Podzols to Luvisols were selected to represent the broad range of complex matrices that could be encountered when extracting amino acids from soils. The effects of different pre-treatment of soil samples

were also considered in this study to cover the methods used by people in quantifying soil amino acids. Prior to the extraction some soils (1–6) were dried and ground, some soils (9 and 10) were only dried and sieved (< 2 mm), and soil 7 and 8 with field moisture were stored at 4 °C and directly extracted. Based on soil organic carbon (SOC) contents, different ratios of soil to water were used in extracting soil amino acids. A suspension of soil/ultrapure H₂O (1:20, w/v, for soil 1; 1:10, w/v, for soil 2–10) was horizontally shaken for 1 h (120 rpm) at ambient temperature, centrifuged (4000 g, 20 min) and filtrated through 0.2 µm mixed cellulose ester membrane filter (ME24, GE Healthcare Life Sciences, Whatman). The loss of the 20 AAs during the filtration was negligible (the filtration recovery for each of them was between 94% and 102%). To inhibit microbial activity NaN₃ (final concentration 1 mM) was added before shaking. The soil extracts were stored at 4 °C before use.

Another set of extracts was prepared using the same way as before but without addition of NaN₃ for the measurement of total organic carbon (TOC), total nitrogen (TN), dissolved organic nitrogen (DON) and solution pH. TOC and TN were determined by a TOC analyser (TOC-V_{CPH}, Shimadzu, Kyoto, Japan). Solution pH was measured with a multi-parameter analyser (CON-SORT C832, Abcoude, The Netherlands). The inorganic N in the extracts was analysed with a SAN⁺⁺ auto-analyser fitted with a 1074 auto-sampler (Skalar, Breda, The Netherlands). The DON was calculated as the difference between the TN and inorganic N contents. The C and N contents of bulk soils were determined using a C and N analyser (Elementar VarioEL, Hanau, Germany).

3.2.5 Sample concentration and clean up

Freeze-drying and an SPE technique were tested in this study to concentrate and clean up soil extracts. The three tested SPE cartridges (Waters Milford, MA, USA) and the corresponding extraction procedure are presented in Table 3.3. The initial SPE procedure was based on the suggestions of the supplier and reported methods (Yang *et al.*, 2011). All the eluted solutions were evaporated under N₂ gas flow on a water bath (50 °C) and reconstituted in ACN/H₂O (85:15, v/v).

After selecting the proper SPE sorbent, several wash steps, various eluent pH (1.25%, 3.75%, or 7.5% NH₄OH in methanol, v/v) and different final volumes (0.2 and 0.5 ml) were tested. Samples were filtered through a 0.2 µm

Table 3.2 Sources, classification, and properties of soil samples.

Code	Soil	Specification	Site	TC /%	TN /%	Texture (sand- silt-clay) %	Extraction ratio (W/W)	pH	DOC /mg C l ⁻¹	DON /mg N l ⁻¹
1	Fimic Anthrosol ^a	black humus layer (H)	Buunderkamp (The Netherlands)	12.65	0.62	NI	1:20	4.27	95.8	4.27
2	Fimic Anthrosol ^a	illuvial (Bs) horizon	Buunderkamp (The Netherlands)	0.65	0.03	NI	1:10	4.84	24.7	0.91
3	Haplic Luvisol ^b	Ap horizon (0–10 cm)	Southern Limburg (The Netherlands)	0.92	0.11	8.6-82.2-9.2	1:10	6.24	17.0	1.13
4	Endogleyic Stagnosol ^c	1000 years old Paddy soil, Alp (0–10 cm)	Cixi (China)	1.49	0.16	silt loam	1:10	6.25	35.7	2.32
5	Petric Calcisol ^d	eroded sediment	Alqueria (Spain)	1.05	0.07	43.2-47.3-9.5	1:10	8.34	33.7	2.60
6	Leptic dystric regosol	A horizon (0–10/12 cm)	Courmayeur - Aosta (Italy)	1.52	0.12	68.9-27.0-4.2	1:10	7.57	46.2	3.45
7	Dystric regosol ^e	Ap1 horizon (0–15 cm)	Parco del Ticino, Lombardia (Italy)	1.14	0.09	52-43-5	1:10	5.6	2.3	ND
8	Brunic dystric regosol ^e	A2 horizon (6–13 cm)	Bosco Siro Negri, Lombardia (Italy)	1.59	0.14	74-24-2	1:10	4.66	4.6	0.23
9	Haplic Luvisol ^f	A _p /A _h horizon (10–25 cm)	Speuld (The Netherlands)	1.04	0.03	NI	1:10	4.84	16.9	0.69
10	Haplic podzol ^g	E1 horizon (10–25 cm)	Klosterhede (Denmark)	2.72	0.10	NI	1:10	4.67	13.2	0.47

^a Jansen *et al.* (2005). ^b Wang *et al.* (2014). ^c Hanke *et al.* (2013). ^d Cammeraat (2004). ^e Cerli *et al.* (2009). ^f Koopmans *et al.* (1997). ^g Ingerslev (1997). ND: not detectable. NI: not included in the literature.

Table 3.3 Three different solid phase extraction (SPE) cartridges and the corresponding extraction procedure.

Cartridge	Size and properties	Extraction procedure			
		Equilibration	Loading	Washing	Elution
Oasis MCX	150 mg, 60 µm, strong cation exchange sorbent	Initial			
		a. 3 ml of MeOH b. 3 ml of acidified water (2% FA)	10 ml of acidified standard mixture (2% FA)	3 ml of MeOH	3 ml of basified MeOH (1.25% NH ₄ OH)
Oasis MAX	60 mg, 30 µm, strong anion exchange sorbent	Optimized			
		a. 3 ml of MeOH b. 3 ml of acidified water (2% FA)	10 ml of acidified standard mixture (2% FA)	a. 3 ml of MeOH b. 3 ml of acidified H ₂ O/MeOH (1:1, v/v, 0.1% FA)	3 ml of basified MeOH (7.5% NH ₄ OH)
Oasis WAX	60 mg, 30 µm, weak anion exchange sorbent	a. 1 ml of MeOH b. 1 ml of basified water (0.25% NH ₄ OH)	10 ml of basified standard mixture (1.25% NH ₄ OH)	1 ml of MeOH	1 ml of acidified MeOH (5% FA)
		a. 1 ml of MeOH b. 1 ml of acidified water (2% FA)	10 ml of standard mixture	1 ml of MeOH	1 ml of basified MeOH (1.25% NH ₄ OH)

hydrophilic polypropylene (GHP) syringe filter (Acrodisc, Pall Life Science, East Hills, NY) prior to injection.

3.2.6 Analytical method optimization

Both positive and negative ionization mode were tested for MS/MS detection. The optimal MS conditions for each analyte and IS were obtained by infusing the analytes according to the following steps: (1) isolation and selection of a precursor ion for each analyte and IS, (2) optimization of the declustering potential, (3) optimization of the collision energies and collision cell exit potential for the most abundant product ions. Afterwards, the source/gas parameters were optimized through flow injection analysis, including curtain gas (10 l h^{-1}), collision gas (6 l h^{-1}), ion-spray voltage (5500 V), temperature ($450 \text{ }^\circ\text{C}$), ion source gas 1 (40 l h^{-1}) and ion source gas 2 (60 l h^{-1}).

The HPLC gradient was based on the methodology reported by Guo *et al.* (2013). To improve separation, peak shape and intensity, the influences of buffer concentration (2–10 mM NH_4HCO_2 in both solvent A and B, see the composition of the mobile phase in Table A1 of appendix), mobile phase pH (3, 5, 7 and 9) and organic modifier (MeOH) were investigated under the optimal MS/MS condition. Modification of the HPLC gradient method was tested as well.

3.2.7 Method validation for amino acids in soil

The standard addition method was adopted to test the overall recovery of the SPE procedure, including extraction efficiency and matrix effects, with the 10 soil extracts and ultrapure H_2O . For this, 10 ml of the soil extracts or ultrapure H_2O were spiked with only IS or both IS and the amino acids standard mixture (the final concentration in the spiked extracts were $0.05 \mu\text{g ml}^{-1}$ Ala, Asp, Gln, Glu, Gly, Ile, Leu, Phe, Pro, Ser, Thr, Tyr, Val and $0.01 \mu\text{g ml}^{-1}$ Asn, His, Lys, Met, Sar, Trp). The entire samples were homogenised and purified using the optimized SPE technique described in the results section. All the experiments were performed in triplicate. Only the reconstituted sample of soil 6 was diluted 6 times in ACN/ H_2O (85:15, v/v) before measurement because the concentrations of some amino acids were outside the range of the calibration line. Both non-labelled (Nva) and stable isotope labelled IS (Ala-D4, Glu-D5, Lys-D4 and Gly-D5) were tested in this study to quantify free amino acids in soil

Table 3.4 Precursor/product ion pairs and optimal parameters for multiple reaction monitoring (MRM) of analytes and internal standards.

Code	Amino acids	Retention time /min	MRM transition (precursor/product)	DP ^d / V	CE ^e / V	CCEP ^f / V
1	Trp	2.5	205/188 ^a	49	15	11
			205/146 ^c	49	24	13
2	Phe	2.5	166/120 ^a	45	22	9
			166/120 ^b	45	35	9
			166/103 ^c	45	38	8
3	Leu	2.6	132/86 ^a	51	16	5
			132/86 ^b	51	25	5
4	Ile	2.8	132/86 ^a	54	14	3
			132/86 ^b	54	25	3
			132/69 ^c	54	26	5
5	Met	3.2	150/133 ^a	44	15	6
			150/61 ^c	44	33	1
6	Val	3.6	118/72 ^a	50	17	2
			118/72 ^b	50	27	2
			118/55 ^c	50	28	3
7	Pro	3.7	116/70 ^a	51	21	4
			116/70 ^b	51	47	4
			116/43 ^c	51	42	5
8	Tyr	3.7	182/165 ^a	44	13	8
			182/136 ^c	44	19	7
9	Sar	4.6	90/44 ^a	44	18	6
10	Ala	5.2	90/44 ^a	39	21	2
11	Thr	5.8	120/74 ^a	51	16	2
			120/102 ^c	51	13	4
12	Gly	6.1	76/48 ^a	44	10	8
			76/30 ^c	44	19	3
13	Gln	7	147/84 ^a	30	23	3
			147/130 ^c	30	11	4
14	Ser	7.1	106/60 ^a	20	14	2
			106/70 ^c	20	20	2

(Continued)

Table 3.4 Precursor/product ion pairs and optimal parameters for multiple reaction monitoring (MRM) of analytes and internal standards (continued).

Code	Amino acids	Retention time /min	MRM transition (precursor/product)	DP ^d / V	CE ^e / V	CCEP ^f / V
15	Asn	7.5	133/74 ^a	47	21	5
			133/87 ^c	47	14	6
16	Glu	7.8	148/84 ^a	54	23	6
			148/130 ^c	54	14	5
17	Asp	9.1	134/74 ^a	67	23	5
			134/88 ^c	67	11	4
18	Arg	9.3	175/70 ^a	54	33	5
			175/116 ^c	54	21	5
19	His	9.5	156/110 ^a	53	21	6
			156/83 ^c	53	35	6
20	Lys	9.5	147/84 ^a	30	23	3
			147/130 ^c	30	14	5
21	Nva	3.3	118/72 ^a	41	14	4
			118/55 ^c	41	32	8
22	Lys-D4	9.5	151/88 ^a	51	23	3
			151/134 ^c	51	14	6
23	Ala-D4	5.2	94/48 ^a	42	17	7
24	Gly-D5	6.1	78/32 ^a	44	19	3
			78/50 ^c	44	10	7
25	Glu-D5	7.8	153/88 ^a	44	25	3
			153/135 ^c	44	14	6

^a quantifier with optimal parameters. ^b quantifier (with less optimal parameters) used in quantifying soil amino acids. ^c quantifier. ^d declustering potential. ^e Collision energy. ^f Collision cell exit potential.

extracts. The concentration of Nva in the spiked soil extracts or ultrapure H₂O before loading was 0.025 µg ml⁻¹ and the concentrations of stable isotope labelled IS were 0.025 µg ml⁻¹ (Ala-D4, Glu-D5 and Lys-D4) or 0.125 µg ml⁻¹ (Gly-D5).

Intra-day precision of the method was examined by repeatedly measuring the SPE extraction samples of soil 3 for 5 times within a day and inter-day precision was examined by measure the same samples for three consecutive days.

3.2.8 Quality control

The standard mixture solution of 20 amino acids and IS for calibration were prepared in solvent B of the mobile phase. Calibration lines were made by plotting the ratio of analyte to IS concentration versus analyte to IS peak area. Quantification of all measurements was performed with a ten point calibration line. For each different level of analyte concentration, the IS concentration was kept the same. The concentration of Nva in the standard mixture solution for calibration was $0.2 \mu\text{g ml}^{-1}$ and the concentrations of the stable isotope labelled IS were $0.2 \mu\text{g ml}^{-1}$ (Ala-D4, Glu-D5 and Lys-D4) or $1 \mu\text{g ml}^{-1}$ (Gly-D5). Calibration lines only included the levels with accuracies lying between 70% and 130%. Meanwhile analogous transition ratios of quantifier to qualifier were guaranteed for different concentrations of each analyte except for Leu, Ala and Sar, which only had one sensitive transition.

The limit of quantification (LOQ) for each analyte equalled the lowest concentration of the calibration line and the limit of detection (LOD) was calculated by dividing the LOQ by 3.3. LOQs and LODs for free amino acids in a given soil were calculated assuming the extraction ratio of soil to water was 1:10 (v/v) and took into account the recoveries obtained in this study.

All tests were performed in triplicate.

3.3 Results and discussion

3.3.1 Optimization of MS/MS condition

The retention time, transitions and optimal MS conditions for all the targeted amino acids and IS are listed in Table 3.4. Positive ionization mode was selected in MRM detection in line with the study of Guo *et al.* (2013). For all amino acids except Gly-D5, the protonated molecular ion $[M+H]^+$ was selected as the precursor ion (Table 3.4). The precursor mass of Gly-D5 was based on the $[M-D_3+H_3+H]^+$ ion because its acidic deuterium atoms are exchanged with H upon aqueous dissolution (Štefanić *et al.*, 2009). The qualifier and quantifier ions of each analyte and IS were selected by direct infusion mode. The transition with higher intensity was selected as quantifier ion. Only one sensitive transition could be obtained for Leu, Ala, Sar and Ala-D4.

Almost all amino acids tested can generate several dominant product ions in MRM detection, especially those with relative high molecular weight (e.g. Trp,

Tyr and Arg). Among the dominant product ions, a neutral loss of the ion represented by m/z 46 was observed for the majority of the amino acids and attributed to the loss of formic acid (FA) (Langrock *et al.*, 2006). However, the product ion $[M+H-46]^+$ was not necessarily the most dominant for all these amino acids. Fragment ions $[M+H-17]^+$ and $[M+H-46-17]^+$ were the most intensive product ions for several amino acids, such as Trp, Met, Gln and Lys. Fragment ion $[M+H-17]^+$ was attributed to neutral loss of NH_3 (Liu *et al.*, 2008; Guo *et al.*, 2013). Because of the difficulty in detecting the above mentioned three fragment ions, the product ions of m/z 70 and 84 were selected to quantify Arg and Glu, respectively. Since the maximum MS detection limit was reached for Phe, Leu, Ile, Val and Pro in soils, no parameter optimization was necessary to quantify these amino acids.

3.3.2 Optimization of HPLC condition

The results revealed that raising the buffer concentration resulted in narrower and therefore higher peaks for Asn, Asp, Glu, Lys, Met and His, while it caused a loss in intensity (peak height) for other amino acids (Figure A1, Appendix). However, all amino acids showed slightly decreasing peak areas with increasing buffer concentration (Figure A2, Appendix), probably due to the ion suppression effect of the buffer (Annesley, 2003). In addition, increasing the buffer concentration from 2 to 10 mM resulted in relatively shorter retention time (shift 0.50–1.33 min) for a few late eluting basic or acidic amino acids (Arg, Asp, His and Lys), while small shifts (0.03–0.19 min) were observed for all other amino acids. Given the overall positive effects of higher buffer concentration, especially on Asp and His (Figure A3, Appendix), a concentration of 8 mM NH_4HCO_2 (0.12% FA) was selected as the optimum.

NH_4OAc , $AcOH$ and NH_4OH were used to prepare a mobile phase with different pH values for testing the influence of mobile phase pH (Table A2, Appendix). The best peak shapes for all the amino acids were observed at pH 3 as compared with pH 5, 7 and 9 (data not shown). Moreover, the retention time of all the tested amino acids increased when raising the pH from 3 to 5 and few differences were observed between pH 5 and 9 (data not shown). Specifically, basic (Arg, His and Lys), acidic (Asp and Glu) and some neutral amino acids (Ser, Thr, Asn and Gln) exhibited relatively large retention time shifts (0.91–2.53 min) over the pH range of 3–9, while other neutral amino acids had small retention time shifts (0.28–0.80 min). Because all the above mentioned amino acids have charged or polar uncharged side chains, stronger hydrophilic

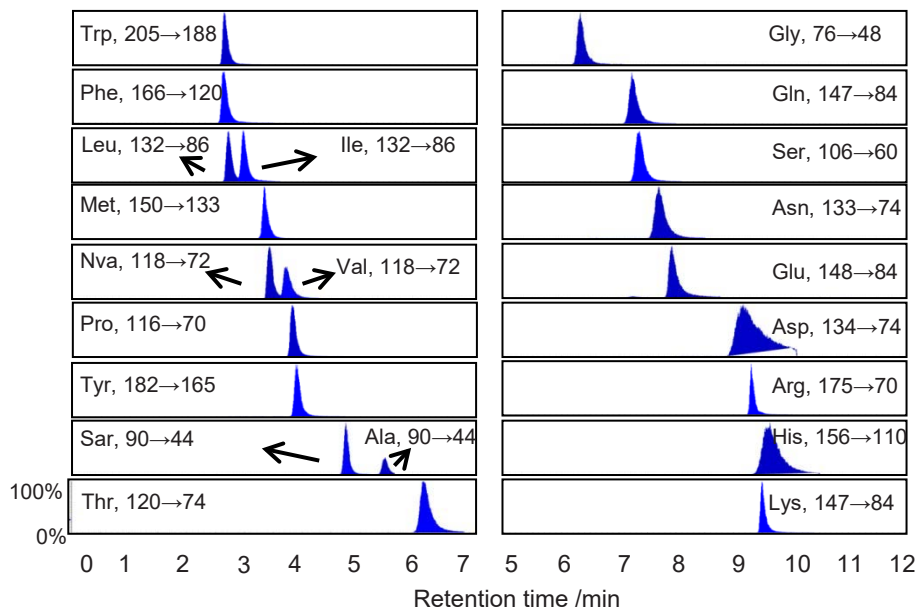


Figure 3.1 Typical chromatograms of the targeted amino acids (transitions of quantifier) obtained from standard mixture ($2.5 \mu\text{g ml}^{-1}$ for Asp and Gly, $0.5 \mu\text{g ml}^{-1}$ for the rest). The involved mobile phase included solvent A (90% H_2O , 10% ACN, 8 mM NH_4HCO_2 , 0.12% FA) and solvent B (90% ACN, 10% H_2O , 8 mM NH_4HCO_2 , 0.12% FA). The gradient method was 94–88% B from 0 to 6 min, 88–50% B from 6 to 11 min, constant 50% B from 11 to 12 min.

interactions could occur between these compounds and the column sorbent under neutral and basic condition. The remaining amino acids (Gly, Pro, Ala, Leu, Ile, Met, Phe, Sar, Trp, Tyr and Val) have no or only hydrophobic side chains, hence, little change of retention time occurred for them.

Overall, the mobile phase with pH 3 produced the best peak shape with shortest retention time (respecting dead volume) for all tested amino acids. In addition, at pH 3 clear separation of the isomer pairs, Leu/Ile and Val/Nva was obtained. Therefore, pH 3 was used as optimum pH in our study, also in line with previous results of Guo *et al.* (2013).

Compared with other amino acids, Asp and His still had relatively wide peaks under optimum buffer concentration and mobile phase pH. Thus, to improve their peak shape, modifications of solvent A or B with different concentration of MeOH (2.5–10%) were tested. The results illustrated that adding MeOH in

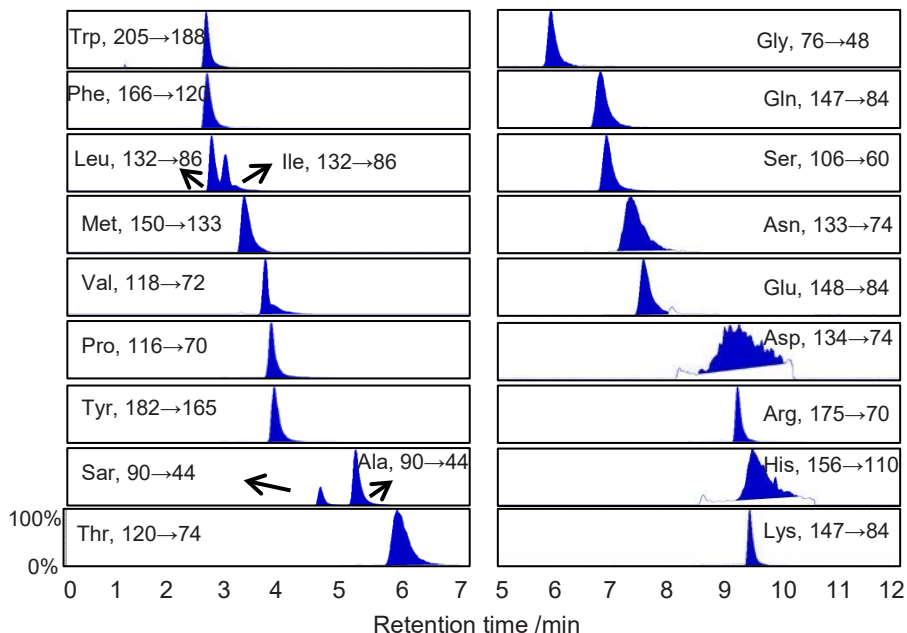


Figure 3.2 Typical chromatograms of the targeted amino acids (transitions of quantifier) obtained from purified soil extract. The involved mobile phase included solvent A (90% H₂O, 10% ACN, 8 mM NH₄HCO₂, 0.12% FA) and solvent B (90% ACN, 10% H₂O, 8 mM NH₄HCO₂, 0.12% FA). The gradient method was 94–88% B from 0 to 6 min, 88–50% B from 6 to 11 min, constant 50% B from 11 to 12 min.

solvent A or B not only impaired the separation of Leu/Ile and Val/Nva but also worsened the peak shape of several amino acids, i.e. Asp, Lys, His and Arg.

Further modification of the elution program showed that increasing the H₂O proportion from 40% to 50% over the period of 12–13 min produced narrower peaks for some amino acids (Asp, Glu, Lys, Gln, Arg and Ser) with reduced retention time (data not shown). Finally solvent A of mobile phase (100% H₂O, 8 mM NH₄HCO₂, 0.12% FA, v/v) was adjusted to contain 10% ACN to prevent growth of microorganism. Solvent B remained the same (90% ACN, 10% H₂O, 8 mM NH₄HCO₂, 0.12% FA, v/v). Following these adjustments, the finalized gradient method was 94–88% B from 0 to 6 min, 88–50% B from 6 to 11 min, constant 50% B from 11 to 12 min. The separation system was reconstituted to the start condition within 1 min and equilibrated for 10 min between injections. The typical chromatograms of targeted amino acids obtained from standard mixture are shown in Figure 3.1.

Table 3.5 Regression linear range, coefficients of determination (r^2), transition peak area ratios, limits of detection (LODs) and limits of quantification (LOQs) of the 20 targeted amino acids.

Code	Analyte	IS	Linear range / $\mu\text{g ml}^{-1}$	r^2	Transition ratio		LOD / ng ml^{-1}	LOD _{sqll} / ng g^{-1}	LOQ / ng ml^{-1}	LOQ _{sqll} / ng g^{-1}
					Average	(quantifier ^a /quantifier)				
1	Trp	Ala-D4	0.005–0.1 0.05–2	0.9986 0.9984	2.7	4.0	1.5	17	5	56
2	Phe	Ala-D4	0.005–2	0.9986	1.1	2.5	1.5	17	5	57
3	Leu	Ala-D4	0.005–1.0 0.1–2	0.9980 0.9930	NA		1.5	16	5	53
4	Ile	Ala-D4	0.005–0.1 0.02–2	0.9984 0.9980	2.9	5.2	1.5	17	5	56
5	Met	Ala-D4	0.005–0.1 0.2–2	0.9992 0.9978	1.8	4.0	1.5	49	5	163
6	Val	Ala-D4	0.005–0.1 0.02–2	0.9982 0.9980	1.9	4.8	1.5	20	5	67
7	Pro	Ala-D4	0.02–0.1 0.1–2	0.9956 0.9922	17.1	7.9	6.1	116	20	381
8	Tyr	Ala-D4	0.01–0.2 0.05–2	0.9996 0.9968	1.1	7.4	3.0	31	10	104

(Continued)

Table 3.5 Regression linear range, coefficients of determination (r^2), transition peak area ratios, limits of detection (LODs) and limits of quantification (LOQs) of the 20 targeted amino acids (continued).

Code	Analyte	IS	Linear range / $\mu\text{g ml}^{-1}$	r^2	Transition ratio		LOD / ng ml^{-1}	LOD _{soil} / ng g^{-1}	LOQ / ng ml^{-1}	LOQ _{soil} / ng g^{-1}
					Average	(quantifier ^a /quantifier)				
9	Sar	Ala-D4	0.005–0.5 0.02–2	0.9990 0.9984	NA		1.5	20	5	67
10	Ala	Ala-D4	0.005–0.5 0.1–2	0.9998 0.9990	NA		1.5	16	5	53
11	Thr	Gly-D5	0.005–0.1 0.05–2	0.9984 0.9988	2.2	5.7	1.5	13	5	43
12	Gly	Gly-D5	0.025–1 0.5–10	0.9926 0.9982	0.9	3.7	7.6	78	25	257
13	Gln	Ala-D4	0.005–0.1 0.05–2	0.9980 0.9972	1.3	7.0	1.5	19	5	64
14	Ser	Gly-D5	0.02–0.2 0.05–2	0.9932 0.9948	12.9	9.3	6.1	75	20	248
15	Asn	Gly-D5	0.01–0.1 0.02–2	0.9976 0.9958	1.1	5.3	3.0	35	10	114
16	Glu	Glu-D5	0.005–0.1 0.05–2	0.9992 0.9984	1.8	9.5	1.5	14	5	46

(Continued)

Table 3.5 Regression linear range, coefficients of determination (r^2), transition peak area ratios, limits of detection (LODs) and limits of quantification (LOQs) of the 20 targeted amino acids (continued).

Code	Analyte	IS	Linear range / $\mu\text{g ml}^{-1}$	r^2	Transition ratio		LOD /ng ml $^{-1}$	LOD $_{\text{spil}}$ /ng g	LOQ /ng ml $^{-1}$	LOQ $_{\text{spil}}$ /ng g
					Average	(quantifier ^a /quantifier)				
17	Asp	Glu-D5	0.1–2.5 1–10	0.9986 0.9954	1.6	7.5	30.3	384	100	1267
18	Arg	Lys-D4	0.005–0.2 0.02–2	0.9992 0.9952	2.4	6.3	1.5	22	5	73
19	His	Lys-D4	0.02–0.5 0.1–2	0.9992 0.9956	4.9	6.4	6.1	68	20	223
20	Lys	Lys-D4	0.005–2	0.9992	1.4	7.0	1.5	14	5	48

^aThe quantifier of Phe, Leu, Ile, Val and Pro were transitions with less optimal parameters (Table 3.4). NA: not applicable.

3.3.3 Optimization of SPE procedure

Most free amino acids in soil extracts were too low in concentration to be measured directly and pre-concentration was needed to enable their analysis. Therefore, an SPE technique was adopted to purify and concentrate free amino acids in the soil extracts. Comparison of various SPE cartridges indicated that the best recoveries were obtained on MCX cartridges for most of the amino acids (data not shown), therefore this sorbent was selected for further evaluation of the clean-up procedure.

Washing loaded cartridges once with neutral MeOH was found insufficient to purify soil extracts. The eluted solvent could have a slightly yellowish colour, probably derived from soil organic matter. Therefore, acidified MeOH/H₂O (1:1, 0.1% FA, v/v) was used to wash the cartridge, following neutral MeOH to wash away more polar compounds. Multiple elution experiments with varied eluent pH (1.25%, 3.75%, and 7.5% NH₄OH in MeOH for the first, second and third elution step, respectively) showed that for most of the amino acids, 1.25% NH₄OH was enough to yield nearly complete elution. However, increasing eluent pH with 7.5% NH₄OH would increase elution of His, Arg and Lys (Table A3, Appendix). Accordingly, the optimum was 7.5% NH₄OH in MeOH. Yang *et al.* (2011) also found poor recovery of Lys and Arg under 3% NH₄OH in MeOH and our results indicated increasing the eluent pH to 7.5% NH₄OH in MeOH would improve the recovery of Lys and Arg.

The absolute recovery of Nva was quite different from the majority of the targeted amino acids (data not shown) and thus deemed unsuitable for quantifying the targeted amino acids. Based on similarity of the absolute recoveries from the preliminary test (data not shown), the 20 amino acids could be divided into three groups, i.e. basic, acidic and neutral. Consequently, four stable isotope labelled amino acids, including one basic (Lys-D4), one acidic (Glu-D5) and two neutral amino acids (Ala-D4 and Gly-D5), were used as the IS to evaluate the SPE method.

When dried samples were reconstituted in a final volume of 0.2 ml, an aqueous layer and an organic layer were visually separated because of formation of an aqueous phase with a high concentration of buffer salts (i.e. NH₄HCO₂) produced during the SPE procedure. Increasing the final volume to 0.5 ml prevented this problem, and reduced other matrix effects. Hence, a volume of 0.5 ml was used to validate the SPE method.

3.3.4 Method performance

A separation of the linear range into two parts was necessary to build a reliable calibration line with a wide concentration range for most of the amino acids. The results are presented in Table 3.5. The coefficients of determination (r^2) were higher than 0.9922 for all the calibration lines (Table 3.5). The relative standard deviation (RSD) of the transition ratios were below 10% for all the amino acids with two sensitive transitions. The LODs ranged from 1.5 to 30.3 ng ml⁻¹ and the LOQs ranged from 5 to 100 ng ml⁻¹. These results indicated that the detection limits of the less sensitive amino acids, such as Thr, Glu and Lys, were clearly improved in comparison with the results of Guo *et al.* (2013). The corresponding LODs and LOQs for free amino acids in soil ranged from 13 to 384 ng g⁻¹ and from 43 to 1267 ng g⁻¹ (dry basis), respectively. In addition, for all the 10 different soils, the transition ratios of all the amino acids were similar to the standard results in pure H₂O (the differences were lower than 30%). The intra-day precision (RSD) was between 1% and 5%, and the inter-day precision (RSD) was between 1% and 14% (Table A4, Appendix).

3.3.5 Application to measurement of soil free amino acids

Table 3.6 shows the overall recoveries of spiked amino acids in ultrapure H₂O and soil extracts. Except for Val, Pro, Met and Arg the overall recoveries of the amino acids were similar for both the pure H₂O and soil extracts and ranged between 74% and 117% (Table 3.6). For Val and Pro, the overall recoveries were relatively consistent for soil extracts (74% for Val and 52% for Pro), and lower compared to pure H₂O (97% for Val and 94% for Pro). The overall recoveries of Met and Arg had large variation among pure H₂O and different soil extracts (Table 3.6). The overall recoveries of Val and Pro were normalized to the same IS of Ala-D4. The differences of the overall recoveries of Val or Pro between pure H₂O and soil extracts could be attributed to the weaker bonding of Val or Pro with the existence of other compounds extracted from soils. Conversely, some extracted compounds from soil probably enhanced the bonding of Met. Thus, the overall recoveries of Met for some soils were much higher than that for pure H₂O. Other soils did not contain the same compounds, therefore the overall recoveries of Met for these soils showed little change compared to pure H₂O. The large variation of the overall recoveries of Arg could be explained by the varied interaction between positively charged Arg and negatively charged organic compounds extracted from soil. These results indicated that the recovery process of some amino acids (Val, Pro, Met and Arg)

Table 3.6 Overall percent recoveries of spiked amino acids in ultrapure H₂O and soil extracts.

Analyte	H ₂ O	Soil 1	Soil 2	Soil 3	Soil 4	Soil 5	Soil 6	Soil 7	Soil 8	Soil 9	Soil 10	Mean
Trp	90±1	77±2	83±4	82±2	86±4	89±0	96±7	85±5	92±6	103±7	94±7	89±8
Phe	90±1	83±2	86±5	83±3	81±2	80±3	109±14	92±2	96±5	90±5	85±6	88±9
Leu	94±3	88±1	94±5	80±4	84±5	86±3	125±24	95±1	99±7	92±8	92±9	94±12
Ile	96±5	86±5	87±2	76±3	81±3	77±4	114±11	89±1	96±5	92±7	93±8	89±11
Met	4±4	71±4	66±2	5±0	26±4	4±1	30±21	0	5±2	63±5	36±6	31±28
Val	97±4	80±2	75±0	69±3	70±2	72±4	120±19*	71±2	75±3	79±8	79±8	74±4
Pro	94±5	60±1	54±1	57±1	47±3	51±2	49±4	50±1	51±3	53±4	51±6	52±4
Tyr	128±3	112±3	93±2	113±2	93±6	93±1	98±11	103±1	104±4	79±3	77±3	97±12
Sar	80±0	74±4	79±4	79±1	72±2	75±1	65±2	79±1	81±1	69±1	77±2	75±5
Ala	98±1	92±3	92±3	98±3	91±2	88±1	95±6	101±1	101±1	95±1	95±1	95±4

(Continued)

Table 3.6 Overall percent recoveries of spiked amino acids in ultrapure H₂O and soil extracts (continued).

Analyte	H ₂ O	Soil 1	Soil 2	Soil 3	Soil 4	Soil 5	Soil 6	Soil 7	Soil 8	Soil 9	Soil 10	Mean
Thr	120±2	119±6	117±3	127±2	108±5	111±4	108±6	121±2	123±2	113±4	121±1	117±7
Gly	98±2	99±3	97±6	100±4	94±6	93±3	91±2	98±4	97±1	100±6	103±12	97±4
Gln	83±1	77±2	81±5	85±1	77±5	83±1	70±3	77±2	82±2	72±10	78±2	78±5
Ser	80±0	79±2	84±4	83±2	79±2	79±5	85±8	82±1	85±3	73±4	79±0	81±4
Asn	83±2	93±7	94±10	77±4	87±12	77±9	113±3	85±2	89±3	79±14	85±5	88±11
Glu	117±4	105±1	107±1	108±5	124±17	103±6	99±68	114±2	115±4	109±1	108±1	109±7
Asp	80±7	88±11	79±5	77±4	76±20	83±8	111±12*	81±6	77±7	71±6	79±4	79±5
Arg	88±2	90±5	92±6	29±1	57±11	26±2	16±20	57±1	94±6	113±22	108±20	68±36
His	85±8	72±2	92±7	93±1	97±3	99±4	210±49*	87±10	98±3	89±12	81±4	90±9
Lys	100±2	102±3	104±4	108±1	107±4	107±13	115±13	99±4	107±2	104±4	96±4	105±5

Note: the results are presented as means with standard deviation (n=3). The values with an asterisk are taken as outliers. The data in the mean column are the averaged results of soil sample.

was highly dependent on the composition of soil extracts. More stable and accurate results could be obtained if stable isotope labelled analogues were used to quantify those amino acids. Typical chromatograms of the targeted amino acids obtained from purified soil extract are shown in Figure 3.2. The contents of soil free amino acids are presented in Table A5 (Appendix).

HPAEC-PAD has been widely used to analyse amino acids in soil digestions without derivatization and purification (Martens and Loeffelmann, 2003; Olk, 2008; Creamer *et al.*, 2012), but this method suffered from long runtime (35 min) and lack of analyte specificity. The HILIC method coupled with an SPE technique was first applied in rhizosphere samples by Dell'mour *et al.* (2010). However, in addition to a different matrix, Dell'mour *et al.* (2010) only tested 11 amino acids and their internal standard (^{13}C -tyrosine) was not suitable to quantify all the tested amino acids. In this study, good separation of 20 underivatized amino acids was achieved on a HILIC column within 12 min upon prior SPE extraction incorporating improvements in the technique as reported by Yang *et al.* (2011) but using more cost-efficient H-labelled instead of C/N labelled IS.

3.4 Conclusion

For the first time a reliable method for quantifying 20 common amino acids in 10 different soils spanning a wide range of matrix composition (texture, pH, organic C content etc.) was developed and validated. The method that consists of a combination of extraction and pre-concentration with SPE and subsequent analysis with HILIC-HPLC-MS/MS yielded good separation and accurate determination of the 20 amino acids without derivatization for all soils and all amino acids, with the exception of Arg and Met. With respect to extraction from the complex soil matrices, specifically, the cation exchange SPE technique was able to purify and concentrate amino acids in soil extracts, which are generally lower than the detection limit or not abundant enough for accurate analysis. For Arg and Met in spite of SPE extraction, significant differences in the recoveries between some of the soils were found that warrant further investigation. For all other amino acids, the newly developed method paves the way for broad routine application to analyse their presence and abundance in soils of varying composition. Added advantage is that the new methodology is cost-effective as only four deuterated internal standards were used for quantification of the targeted amino acids.

Chapter 4

Competition and surface conditioning alter the adsorption of phenolic and amino acids on soil minerals

This chapter has been published as:

Gao, J., Jansen, B., Cerli, C., Helmus, R., Mikutta R., Dultz S., Guggenberger, G. & Kalbitz, K. 2017. Competition and surface conditioning alter the adsorption of phenolic acids and amino acids on soil minerals. *European Journal of Soil Science*, **68**, 667–677.

Abstract

Adsorptive interactions of organic molecules with soil minerals often impair their bioavailability. However, little is known about the adsorption behaviour of phenolic and nitrogenous compounds on different minerals and their mutual interaction with respect to competition and surface conditioning, i.e. surface modification induced by preceding adsorption of the other class of compounds. Therefore, batch adsorption experiments were done to study the interaction between phenolic acids (PAs; salicylic acid, Sal; syringic acid, Syr; ferulic acid, Fer; vanillic acid, Van) and amino acids (AAs; lysine, Lys; glutamic acid, Glu, leucine, Leu; phenylalanine, Phe) during adsorption on goethite and Ca²⁺-montmorillonite at pH 6 by applying adsorbate concentrations of 0.01, 0.05 and 0.1 mM. Larger adsorption of PAs was observed on goethite than montmorillonite, whereas the phyllosilicate was a better adsorbent for AAs than the oxide. Among all tested PAs, Sal was preferentially adsorbed on both minerals. For the AAs, Glu was preferentially adsorbed on goethite and Lys on montmorillonite. The AAs were more competitive than PAs and partially suppressed the adsorption of PAs on both minerals. The adsorption of PAs or AAs on both minerals was enhanced by surface conditioning with the other group, with larger effects for goethite than montmorillonite. For goethite, surface conditioning by PAs enhanced the adsorption of AAs more (by 97–161%) than did AAs for PAs (9–48%). The results support the hypothesis that pre-adsorption of one class of organic compound can enhance the retention of another class. This suggests that adsorbed organic matter on soil mineral phases might be subject to a self-strengthening effect.

4.1 Introduction

Soil stores three to four times as much organic carbon (OC) as the atmosphere or plants (Lal, 2004), which represents an important role in global C cycling. Recently emerging concepts of soil organic matter (SOM) dynamics suggest that the long-term persistence of OC in soil depends on the complex interplay between SOM and environmental factors, e.g. accessibility to decomposer organisms, interaction with soil minerals and soil moisture (Schmidt *et al.*, 2011; Lehmann & Kleber, 2015). It has been shown that mineral–organic associations (MOAs) serve as an important reservoir of soil OC (Kögel-Knabner *et al.*, 2008) and the turnover of SOM is suppressed by its adsorption on mineral surfaces (Kalbitz *et al.*, 2005; Mikutta *et al.*, 2007).

Adsorptive interactions between soil minerals and organic compounds are governed by mineral surface structural and charge properties, chemical properties of the organic compounds, solution chemistry (pH, ionic strength and composition) and the presence of competing organic or inorganic compounds (Thomas & Kelley, 2010; Zhang *et al.*, 2012). Many studies have shown that soil minerals can preferentially bind aromatic compounds, thus increasing their turnover time in soil (Kaiser & Guggenberger, 2000; Kalbitz *et al.*, 2005). The primary sources of aromatic acids in soil are plant cell walls and lignin polymers of vascular plants, which can represent 20–30% of the C cycling in the biosphere (Croteau *et al.*, 2000). During the first step of lignin degradation (depolymerization) water-soluble aromatic degradation products are released into the soil solution and these compounds can be mineralized or adsorbed on mineral surfaces as a precondition for long-term stabilization (Kalbitz *et al.*, 2005; Hagedorn *et al.*, 2015).

This classical view of a preferential bonding of carboxylated phenolic compounds on many soil minerals (Kaiser & Guggenberger, 2000; Kalbitz *et al.*, 2005) has been challenged by the ‘onion’ or ‘multilayer’ model proposed by Kleber *et al.* (2007). This conceptual model suggests that the adsorbed organic compounds on mineral surfaces are self-organized into a multilayer structure with amphiphilic N-containing components enriched on the mineral surface, thereby forming the so called inner layer (Kleber *et al.*, 2007). However, experimental information about the adsorption of carboxylated phenolic and N-containing compounds on different mineral surfaces and their interaction with respect to competition and surface conditioning is lacking. There is no direct experimental support for the functioning of N-containing compounds for the development of a multilayer structure of organic compounds on mineral surfaces. This might be achieved with model compounds that represent

nitrogenous and lignin-derived SOM species.

Amino acids (AAs) are the most active pool of soil organic N and play an important role in soil N cycling (Schimel & Bennett, 2004). Although free AAs in soil are often quite limited, organic N retained in polymeric AA compounds can account for 30–40% of the total soil N pool (Martens & Loeffelmann, 2003). Interaction of AAs with soil mineral surfaces has been recognized as an important process that might affect the bioavailability of AAs in soil (Yeasmin *et al.*, 2014). Competitive interaction between AAs and other organic compounds (e.g. phenolic compounds) during adsorption on mineral surfaces, which are expected to occur frequently in natural environments, are still not well understood because previous studies examined interactions only between AAs and soil minerals in mono-component systems (Yeasmin *et al.*, 2014).

Phenolic acids (PAs), a natural constituent of soil solutions, are the simplest water-soluble products of lignin degradation. Numerous studies have shown that they have a strong affinity for soil or soil minerals (Celis *et al.*, 2005; Chefetz *et al.*, 2011). However, we do not know whether these monomeric aromatic acids are preferentially adsorbed with respect to N-containing compounds. Different soil mineral surfaces also have different charge properties, providing strongly different adsorption sites for PAs. Furthermore, experimental evidence is lacking for the notion that the proposed surface conditioning by AAs would increase the adsorption of aromatic moieties.

The main objective of this study was, therefore, to study the interaction between PAs and AAs during their adsorption on goethite (α -FeOOH) and montmorillonite. The latter are representatives of Fe oxides and 2:1 clay minerals respectively that are common in many soils and have different surface properties: goethite with variable charges and montmorillonite with permanent negatively charged silicate layers (Sposito, 2008). We aimed to test whether AAs were preferentially adsorbed compared with PAs and if surface conditioning of minerals by AAs affected the adsorption of PAs, and *vice versa*. We examined (i) the adsorption behaviour of different AAs representing acidic, neutral, basic and aromatic AAs (glutamic acid, leucine, lysine and phenylalanine) and PAs as model compounds for lignin degradation products (salicylic, syringic, ferulic and vanillic acid) on goethite and montmorillonite, (ii) the adsorption behaviour of PAs on soil minerals after surface conditioning by AAs, (iii) the adsorption behaviour of AAs on soil minerals following surface conditioning by PAs and (iv) the competitive adsorption of PAs and AAs by performing batch adsorption experiments.

4.2 Material and methods

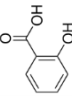
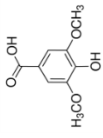
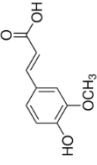
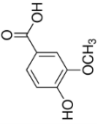
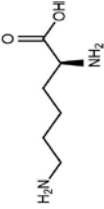
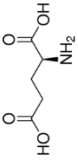
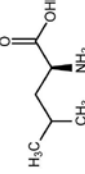
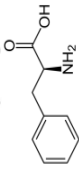
4.2.1 Minerals

Goethite was synthesized according to the method of Atkinson *et al.* (1967) by alkaline hydrolysis of 0.5 M FeCl₃ and freeze-dried at the end. Montmorillonite was obtained by separating the < 2- μ m fraction by sedimentation from Morocco bentonite. Exchange sites were saturated with Ca²⁺ by suspending the clay twice in 1 M CaCl₂ (1 g clay in 10 ml CaCl₂). Finally the montmorillonite was washed until salt free, freeze-dried and passed through a 200- μ m sieve. The X-ray diffraction patterns (Siemens, D500, Karlsruhe, Germany, Cu-K α radiation) indicated the presence of well-crystallized goethite and a high purity of the < 2- μ m fraction of the Morocco bentonite (Figure B1, Appendix). The specific surface area (SSA) and total pore volume (TPV) of minerals were derived from duplicate N₂ adsorption isotherms recorded with a Quantachrome Autosorb1-MP analyser (Quantachrome, Boynton Beach, FL, USA). An aliquot (20–200 mg) of sample was weighed into the sample cell and degassed at 40 °C until the pressure was < 0.12 Pa. The SSA was calculated from the linear Brunauer–Emmett–Teller (BET) plot from up to 10 adsorption points (Brunauer *et al.*, 1938). The TPV was taken at relative pressure P/P₀ ca. 0.995, where P and P₀ are the equilibrium and the saturation pressure respectively of N₂. The SSA of goethite and montmorillonite was 70 and 95 m² g⁻¹, and the TPV of goethite and montmorillonite was 0.73 and 0.19 cm³ g⁻¹, respectively. The anion exchange capacity (AEC) of goethite, calculated from the surface charge density at pH 6 in NaCl background electrolyte (Walsch & Dultz, 2010), was 13 mmol_c kg⁻¹. The cation exchange capacity (CEC) of montmorillonite determined with cobalt-hexamine trichloride was 888.2 mmol_c kg⁻¹ (Daou *et al.*, 2015).

4.2.2 Amino acids and phenolic acids

L-leucine (Leu), L-glutamic acid (Glu), L-lysine (Lys), DL-phenylalanine (Phe), DL-norvaline (Nva), salicylic acid (Sal), syringic acid (Syr), ferulic acid (Fer), vanillic acid (Van), and ethylvanillin (Eva) were purchased from Sigma-Aldrich (Zwijndrecht, The Netherlands). The purity was > 98%, except for Syr (\geq 95%) and Van (\geq 97%). The structures and properties are listed in Table 4.1. Nva and Eva were used as internal standards (ISs) in the measurement of AAs and PAs, respectively.

Table 4.1 Structure and properties of the selected low molecular weight (MW) phenolic acids and amino acids.

Compound	Abbreviation	Structure	MW	Water Solubility /g l ⁻¹ , 25 °C	Acidity constants			pI ^a
					pK _{a1}	pK _{a2}	pK _{a3}	
Salicylic acid	Sal		138.1	1.14 ^b	2.8	13.4 ^c		
Syringic acid	Syr		198.2	5.75 ^d	4.34	9.49 ^e		
Ferulic acid	Fer		194.2	0.78 ^b	4.56	9.39 ^e		
Vanillic acid	Van		168.1	1.53 ^d	4.42	9.39 ^e		
L-Lysine	Lys		146.2	> 1000 ^f	2.18	9.12	10.53	9.82 ^f
L-Glutamic acid	Glu		147.1	8.4 ^f	2.16	9.67	4.32	3.24 ^f
L-Leucine	Leu		131.2	23 ^f	2.36	9.60		5.98 ^f
DL-Phenylalanine	Phe		165.2	29.7 ^f	1.83	9.13		5.48 ^f

^a Isoelectric point; ^b Mota *et al.* (2008); ^c Yost *et al.* (1990); ^d Noubigh *et al.* (2007); ^e Ragnar *et al.* (2000); ^f Barrett (1985).

4.2.3 Preparation of PA and AA solutions

Separate stock standard solutions of each AA (2000 mg l^{-1}) were prepared in 0.1 M HCl and separate stock standard solutions of each PA were prepared in water at a concentration of 1000 mg l^{-1} for Sal, Syr and Van and 500 mg l^{-1} for Fer, respectively. A different concentration was used for Fer due to its low solubility in water. The stock solutions were stored at $4 \text{ }^{\circ}\text{C}$ for not longer than one month. Working mixture solutions with equal concentrations for individual PAs and AAs were freshly prepared by mixing and diluting the stock standard solutions.

4.2.4 Adsorption experiments with PAs and AAs

Adsorption of PAs (mixed solution of Sal, Syr, Fer and Van) and AAs (mixed solution of Leu, Glu, Lys and Phe) was done in triplicate with both goethite and montmorillonite at three different initial adsorbate concentrations of the individual compounds, i.e. 0.01 (small), 0.05 (intermediate) and 0.1 mM (large). The solutions were added to each mineral separately (control experiment), together (competition experiment) or after adsorption of the other mixture (conditioning experiment). For the latter, two conditioning experiments were carried out: adsorption of PAs on goethite or montmorillonite after adsorption of AAs (conditioning experiment I) and adsorption of AAs on the minerals after adsorption of PAs (conditioning experiment II). To our knowledge these experimental procedures were adopted for the first time.

Each 40 ml of adsorbate solution were added to a 50-ml Falcon tube containing either 200 mg goethite or 600 mg montmorillonite. A reliable measurement of AAs and PAs in the equilibrium solution could be achieved only with different mineral masses according to our pre-test, illustrating the different adsorption capacity of goethite and montmorillonite. The suspensions were shaken horizontally (1.58 s^{-1}) for 2 hours in the dark at $4 \text{ }^{\circ}\text{C}$, centrifuged (3500 g , 20 minutes) and filtered through $0.45\text{-}\mu\text{m}$ cellulose ester membranes (ME25, GE Healthcare Life Sciences, Whatman, Little Chalfont, UK). A short reaction time of 2 hours and a low temperature of $4 \text{ }^{\circ}\text{C}$ were chosen to minimize microbial effects. The filtered samples were stored at $4 \text{ }^{\circ}\text{C}$ before measurement. To inhibit microbial activity further and assure a constant electrolyte background, 10 mM NaN_3 was used as background electrolyte and the pH was adjusted to 6 before mixing with the minerals to simulate a common natural condition by the dropwise addition of 0.1 M NaOH or HCl . In the conditioning experiment, the

mineral remaining in the tube after centrifugation was re-suspended in 40 ml of the second adsorbate solution with a vortex mixer or glass rod before equilibration.

The pH of the filtrate after adsorption was measured with a multi-channel analyser (CONSORT C831, Abcoude, The Netherlands). In addition, the possible loss of mineral between the two adsorption steps after filtration was taken into account by calculating the weight difference of the membrane filter before and after filtration. The wet membrane filter was dried for ca. 16 hours at 80 °C before weighing. Loss of PAs or AAs during filtration was also calculated by comparing the concentration of the standard mixture before and after filtration. In brief, the maximum loss of minerals was ca. 1%, but there was a relatively large loss during filtration for Fer (12%) and Lys (11%). The adsorption of each adsorbate on the minerals was calculated as the difference between its concentration in the initial and equilibrium solution with compensation for the loss of mineral and adsorbate during filtration. During the conditioning experiments, desorption of previously adsorbed PAs or AAs was evaluated by measuring the concentration of PAs or AAs in the filtrates after the second adsorption step.

The adsorption of PAs on Fe³⁺-containing minerals could be accompanied by their oxidative transformation including the formation of Fe²⁺ (Polubesova *et al.*, 2010), and soil minerals can also catalyse the reaction of AAs and the formation of peptides (Zaia, 2004). Since these transformation reactions would bias the adsorption results, they were tested under anoxic conditions. For PAs that reacted with goethite, no Fe²⁺ was detected in either liquid or solid samples to indicate phenol transformation by oxidation. Furthermore, concentrations of total organic carbon (TOC) in equilibrium solutions were no larger than those derived from compound-specific concentrations measured by high performance liquid chromatography (HPLC; see below), which also indicated that PAs and AAs remained unaltered during the experiments.

4.2.5 Measurement of PAs and AAs

Liquid chromatography/mass spectroscopy grade acetonitrile (ACN), methanol (MeOH), formic acid (FA) and analytical NH₄HCO₂ were used in the measurement of PAs and AAs. For the HPLC measurement, the mobile phase, AAs and PAs solutions were prepared using sterile ultrapure water.

The PAs in the filtrates were directly analysed with a Prominence HPLC system equipped with a diode array detector (Shimadzu, Kyoto, Japan). Separation was done with a LiChrospher/Superspher RP-18 100-Å column (125 mm × 2 mm, 4 µm; Phenomenex, Torrance, CA, USA) and an RP-18 4-µm guard column. The mobile phase was solvent A (MeOH, 0.1% FA, v/v%) and solvent B (ultrapure H₂O, 0.1% FA, v/v%) with an isocratic elution of 27% solvent A for 15 minutes. Solvent A (90%) was used to wash the column between injections for 5 minutes followed by a 15 minutes equilibration period. The flow rate of the mobile phase was 0.3 ml minute⁻¹. The injection volume was 10 µl and the oven temperature was 35 °C. Sal, Van, Syr, Fer, and Eva were detected at 240, 260, 270, 320 and 280 nm, respectively. The IS (Eva, final concentration 5 mg l⁻¹) was added to the aqueous sample before the injection.

Prior to measurement, the AAs in the filtrates were diluted 10 or 20 times (90% ACN, 10% H₂O, 8 mM NH₄HCO₂, 0.12% FA, v/v%) and spiked with Nva (IS) at a final concentration of 0.1 mg l⁻¹. Hydrophilic interaction LC (Shimadzu, Kyoto, Japan) coupled with electrospray mass spectrometry was used to analyse the AAs without derivatization (Gao *et al.*, 2016). Separation was with an ACQUITY UPLC BEH Amide column (100 mm × 2.1 mm, 1.7 µm, Waters, Milford, MA, USA), together with an ACQUITY UPLC BEH Amide 1.7-µm VanGuard guard column. The MS detection was carried out with a 4000 QTRAP LC–MS/MS System (AB SCIEX, Milford, MA, USA), coupled with an ESI interface. The mobile phase was solvent A (90% H₂O, 10% ACN, 8 mM NH₄HCO₂, 0.12% FA, v/v%) and solvent B (90% ACN, 10% H₂O, 8 mM NH₄HCO₂, 0.12% FA, v/v%). Gradient elution was used: 94–88% B from 0 to 6 minute, 88–50% B from 6 to 11 minute, constant 50% B from 11 to 12 minute. The separation system was reconstituted to the start condition within 1 minute and equilibrated for 10 minutes between injections. The injection volume was 20 µl; samples were eluted at 0.4 ml minute⁻¹. The column temperature was set at 35 °C.

4.2.6 Zeta potential measurement of pure and surface conditioned minerals

Zeta (ζ) potential measurements were carried out with phase-analysis light scattering (ZetaPALS, Brookhaven Instruments Corp., Holtsville, NY, USA). The ζ potential was calculated from electrophoretic mobility by the Smoluchowski equation. Following the adsorption experiment, moist mineral pastes were used to prepare mineral suspensions of 100 mg l⁻¹ in ultrapure water in 25 ml flasks without pH adjustment, except for the pure goethite suspension for which the

pH was adjusted to the same value as the suspension of surface-conditioned goethite. After gentle shaking, 1.6 ml were sampled with a pipette, transferred to a cuvette and measured at 20 °C. Each sample was measured five times and each of the five replicates (runs) consisted of 20 single measurements (cycles). The electrical conductivity of the suspensions was determined simultaneously and used to control electrolyte concentration. The pH was determined in the cuvette by a miniaturized electrode (BlueLine 16pH, Si Analytics, Mainz, Germany).

4.2.7 Statistics

Statistical analysis was performed with SigmaPlot (version 13.0). A two way analysis of variance (ANOVA) was used to evaluate the effect of mineral types, adsorbate concentration, competition and surface conditioning on the adsorption of PAs and AAs. Data were transformed if necessary to meet both the normality (Shapiro–Wilk) and homogeneity of variance (Brown–Forsythe) tests (see Appendix, Tables B1, B2, B5–B12). Fisher's least significant difference (LSD) was used for multiple comparisons of the means. The significance level of the difference was set at $P < 0.05$.

We introduced the relative adsorbed amount in the competition and conditioning experiments because this approach showed the effects of competition and conditioning more clearly on the adsorption of PAs and AAs. The relative adsorbed amount is the percentage value from the adsorption results relative to that obtained from the control experiment. The same mean values from the control experiments were used for each of the three replicates in calculating the relative values of adsorbed amounts.

4.3 Results

4.3.1 Control experiment – Adsorption of PAs and AAs on minerals

Both the mineral type and adsorbate concentration had significant effects ($P < 0.001$) on the adsorption of PAs and AAs, and the effects of them were interdependent (Tables B1 and B2, Appendix). The adsorption of PAs and AAs on goethite and montmorillonite at slightly acidic conditions increased with increasing initial concentrations from 0.01 to 0.1 mM (Table 4.2). The increased adsorption of PAs was, however, less than the increase in adsorbate

Table 4.2 Mean values of total adsorption of PAs and AAs on goethite and montmorillonite, respectively, in the control experiment.

Compounds	Mineral	Initial concentration /mM	Mean ^a / $\mu\text{mol g}^{-1}$	SEM ^b	LSD ^c
PAs	G ^d	0.01	1.07 (1.92)	0.01	0.02
		0.05	1.82 (5.18)		
		0.10	2.05 (6.75)		
	M ^e	0.01	0.33 (0.39)		
		0.05	0.73 (1.06)		
		0.10	0.86 (1.37)		
AAs	G	0.01	0.03 (0.34)	0.03	0.08
		0.05	0.12 (1.03)		
		0.10	0.19 (1.61)		
	M	0.01	0.05 (0.49)		
		0.05	0.31 (2.36)		
		0.10	0.86 (4.63)		

^a The data are transformed mean values with original values in parentheses; ^b Standard error of the transformed mean determined using the residual mean square (12 d.f.); ^c Least significant difference, $P < 0.05$; ^d Goethite; ^e Montmorillonite.

concentration, indicating a limited number of adsorption sites. Although it was difficult to plot an adsorption isotherm for PAs or AAs on soil minerals because of the limited adsorption points, goethite appeared to have a larger adsorption capacity for PAs than AAs. In contrast, montmorillonite was a much better adsorbent for AAs than for PAs (Table 4.2). Salicylic acid was the predominantly adsorbed PA for both minerals (contribution of Sal to adsorbed PAs: 70–75% for goethite and 96–100% for montmorillonite). However, its adsorption on goethite was much greater than on montmorillonite (Figure B2, Appendix). Adsorption of other PAs (Syr, Fer and Van) on goethite was rather limited and no or negligible adsorption occurred on montmorillonite (Figure B2, Appendix). Among the different AAs, goethite adsorbed only Glu (acidic AA), whereas montmorillonite adsorbed only Lys (basic AA).

The net surface charge of goethite (positive) was opposite to that of montmorillonite (negative, Table 4.3). The ζ potential of montmorillonite decreased considerably by surface conditioning of PAs or AAs, whereas it tended to increase for goethite (Table 4.3). For both of the minerals, minor

Table 4.3 Effect of surface conditioning by PAs or AAs on the zeta (ζ) potential of goethite and montmorillonite.

Mineral	Initial concentration /mM	ζ potential /mV		EC ^a / μ S cm ⁻¹		pH	
		Mean	SEM ^b	Mean	SEM	Mean	SEM
G-PAs ^c	Blank ^g	33.9	1.6	14.3	0.83	5.7	0.10
	0.01	36.5		5.0		5.8	
	0.05	38.6		5.0		5.9	
	0.10	38.3		4.7		5.8	
M-PAs ^d	Blank	-22.9		4.3		6.2	
	0.01	-51.6		4.3		6.1	
	0.05	-56.1		5.0		6.2	
	0.10	-53.8		4.0		6.3	
G-AAs ^e	Blank	33.9	2.1	14.3	0.86	5.7	0.03
	0.01	35.5		7.0		5.7	
	0.05	37.5		5.3		5.6	
	0.10	45.6		4.7		5.8	
M-AAs ^f	Blank	-22.9		4.3		6.2	
	0.01	-48.6		4.0		6.1	
	0.05	-45.6		4.3		6.2	
	0.10	-49.6		4.0		6.2	

^a Electrical conductivity of mineral suspension; ^b Standard error of the mean determined using the residual mean square (16 d.f.); ^c Goethite surface-conditioned by PAs; ^d Montmorillonite surface-conditioned by PAs; ^e Goethite surface-conditioned by AAs; ^f Montmorillonite surface-conditioned by AAs; ^g Pure mineral.

differences in ζ potential were observed among different initial concentrations (Table 4.3). The solution pH increased after adsorption of PAs and AAs (Table B3, Appendix). This increase was larger for goethite than montmorillonite and differed only slightly between the treatments including the blanks.

4.3.2 Competition experiment – Adsorption of PAs and AAs on minerals

Competition between PAs and AAs at slightly acidic conditions decreased the adsorption of PAs on goethite and montmorillonite by 8 and 12%, respectively, for the intermediate initial concentration, and by 29 and 15%, respectively, for the large initial concentration (Figure 4.1a and Table B4). All these differences

were statistically significant ($P < 0.05$). There were small changes at the small initial concentration for both minerals. The general patterns of individual PA uptake on goethite and montmorillonite were affected little by AAs. Salicylic acid remained the predominantly adsorbed PA on both minerals. Competition with AAs resulted in reduced adsorption for all the PAs on goethite except for Fer, for which the adsorption increased markedly by 419 and 255% at intermediate and large initial concentrations, respectively (Figure B3a, Appendix). Despite this huge relative increase, the absolute amount of adsorbed Fer remained small (0.87 and $0.99 \mu\text{mol g}^{-1}$). For montmorillonite there was also a reduction in the adsorption of Sal, especially for the intermediate and large initial concentrations (Figure B3b, Appendix). Negligible or no adsorption of Syr, Fer and Van occurred on montmorillonite even in the absence of AAs.

Adsorption behaviour of the individual AAs was similar to that observed without the presence of PAs, i.e. goethite adsorbed only Glu, whereas montmorillonite adsorbed only Lys. The presence of PAs resulted in significantly increased adsorption of AAs on montmorillonite by 25, 21 and 25% for the small, intermediate and large initial concentrations, respectively ($P < 0.05$; Figure 4.1b and Table B4). We also observed a significant increase in the adsorption of AAs ($P < 0.05$) on goethite for the large initial concentration. However, there were no significant changes for the small and intermediate concentrations (Figure 4.1b and Table B4). The large variation in the adsorption of AAs could be attributed to the relatively small amounts adsorbed, which caused a small reduction only in the equilibrium concentrations ($< 10\%$).

4.3.3 Conditioning experiment I – Adsorption of PAs following adsorption of AAs

The adsorption of PAs on goethite after adsorption of AAs increased significantly compared with the control experiment by 41 and 48% for the intermediate and large initial concentrations, respectively ($P < 0.05$; Figure 4.1c and Table B4). An increase of 9% was also observed for the small initial concentration, but with no significant difference. Similarly, the adsorption of PAs on montmorillonite after preceding adsorption of AAs was significantly enhanced by 18 and 30% at the intermediate and large concentrations, respectively ($P < 0.05$; Figure 4.1c and Table B4). Although the adsorption of PAs on montmorillonite was reduced significantly at the small initial

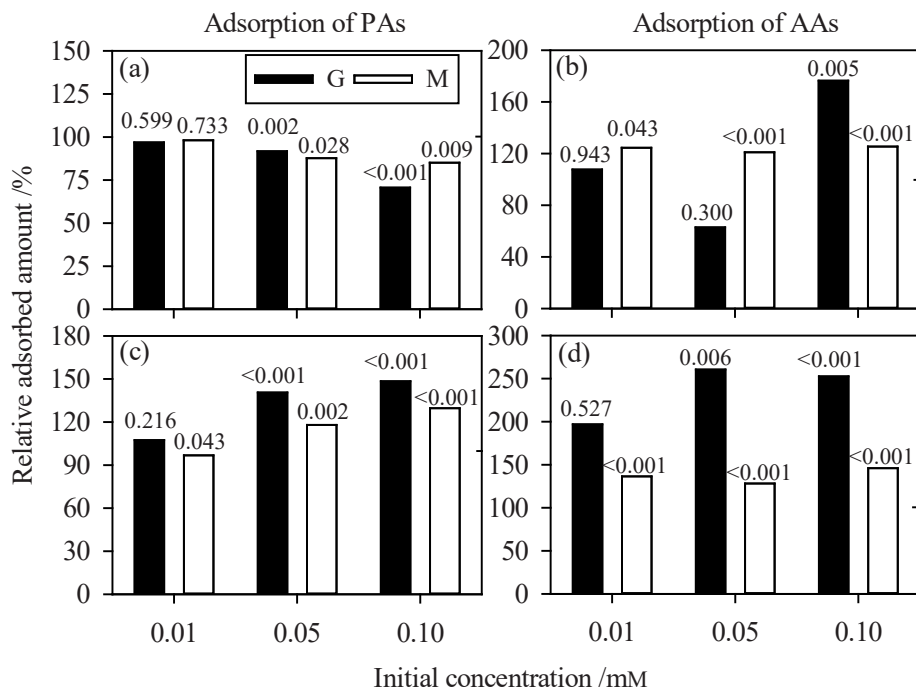


Figure 4.1 Relative effects of: (a) competition on the adsorption of PAs, (b) competition on the adsorption of AAs, (c) surface conditioning by AAs on the adsorption of PAs and (d) surface conditioning by PAs on the adsorption of AAs on goethite (G) and montmorillonite (M). Dotted lines refer to the reference values (control experiment). The results are presented as mean values ($n = 3$). P value above each column is from the analysis of variance of the absolute adsorption results and it indicates the significance of the difference compared with the corresponding reference.

concentration, the change was small ($0.01 \mu\text{mol g}^{-1}$). The adsorption of PAs on goethite was much greater than on montmorillonite (Table B4, Appendix) as for the control experiment. The retention of all individual PAs was generally greater on goethite after adsorption of AAs than on pure goethite (Figure B4a, Appendix). Salicylic acid remained the predominantly adsorbed PA and its adsorption was ca. 18% greater than on pure goethite for the different initial concentrations (Figure B4a, Appendix). Although the adsorption of PAs on montmorillonite increased after adsorption of AAs, the uptake of Sal on the AA-coated montmorillonite was 8–9% less than on pure montmorillonite for all initial concentration values (Figure B4b, Appendix). This also means that the adsorption of Syr, Fer and Van was particularly promoted by surface

conditioning with AAs. Nevertheless, the adsorption of Syr, Fer and Van remained small ($< 0.27 \mu\text{mol g}^{-1}$; Figure B4b, Appendix). Depending on the initial concentration, 52–78% of the previously adsorbed AAs on goethite were desorbed or displaced by PAs during their adsorption. This proportion was much smaller for montmorillonite, with 14–19% only of the previously adsorbed AAs mobilized on interaction with PAs (Table 4.4).

4.3.4 Conditioning experiment II – Adsorption of AAs following adsorption of PAs

The adsorption of AAs on goethite and montmorillonite after conditioning with PAs increased by 97–161% and 28–46%, respectively, for different initial concentrations (Figure 4.1d and Table B4). All the differences were significant ($P < 0.05$) except for goethite at the small initial concentration. The differences in the adsorption of AAs between goethite and montmorillonite after surface conditioning with PAs tended to increase with increasing initial concentration (Figure B5, Appendix). For individual AAs, the adsorption of Glu on goethite after conditioning with PAs increased significantly by 97–114% compared with pure goethite at all initial concentrations ($P < 0.05$; Figure B6, Appendix). A small amount of Leu ($< 0.62 \mu\text{mol g}^{-1}$) was also adsorbed on surface-conditioned goethite, but no retention occurred for Lys and Phe. Although a small amount of Glu, Leu and Phe was adsorbed on montmorillonite after adsorption of PAs, it was much less than Lys with an increase in adsorption of 15–19% ($P < 0.05$; Figure B6, Appendix). Addition of AAs resulted in a similar desorption of previously adsorbed PAs from montmorillonite (29–41%) and goethite (17–39%; Table 4.4).

4.4 Discussion

4.4.1 Adsorption of specific PAs and AAs to pure soil minerals

4.4.1.1 Phenolic acids

Adsorption of Sal on both goethite and montmorillonite was much stronger than Syr, Fer and Van (Figure B2, Appendix). This could be ascribed to the adjacent position of the carboxyl and hydroxyl group of Sal, which resulted in the formation of bidentate inner-sphere complexes with the mineral (Yost *et al.*, 1990; Kubicki *et al.*, 1997). Chefetz *et al.* (2011) also found relatively little

adsorption of Syr, Van and Fer on Fe^{3+} - and Ca^{2+} -montmorillonite at pH 6. The larger adsorption of Sal on goethite than montmorillonite can be attributed to the opposite charge of PAs to the goethite at pH 6. The carboxyl groups of the PAs are deprotonated and negatively charged at pH 6, whereas the goethite is positively charged (pH_{PZC} of goethite, 7.6; Mikutta *et al.*, 2007); this was supported by the positive ζ potential (Table 4.3). By contrast, montmorillonite is negatively charged overall at pH 6 (Table 4.3), like Sal and the other PAs. In addition to the permanent negative charges, pH-dependent charges exist at the broken edges of the montmorillonite and become positively charged at pH 6 (Tombácz *et al.*, 2004). Thus, a small amount of Sal can be attracted by the montmorillonite, resulting in the formation of outer- and inner-sphere complexes (Yeasmin *et al.*, 2014). Moreover, since the montmorillonite was saturated with Ca^{2+} , cation bridges possibly also contributed to the retention of Sal (Mikutta *et al.*, 2007). A similar desorption of Sal from goethite and montmorillonite might support a similar bonding mechanism of PAs. Nevertheless, the different charge characteristics of goethite and montmorillonite are probably responsible for the greater adsorption capacity of PAs on goethite than on montmorillonite.

4.4.1.2 Amino acids

Glutamic acid (acidic AA) was preferentially adsorbed on goethite and Lys (basic) on montmorillonite. The negatively charged Glu was probably selectively bound by positively charged goethite and the positively charged Lys by negatively charged montmorillonite at pH 6 through electrostatic attraction. These results corroborated those of Yeasmin *et al.* (2014), who reported a stronger affinity of Lys to phyllosilicates than to goethite and *vice versa* for Glu. Neither a single carboxyl group nor a single amino group is sufficient for efficient binding of AAs on positively and negatively charged minerals, respectively. This means that the net charge of AAs (acidic or basic) arising from extra carboxyl or amino groups was decisive for their electrostatic bonding. The greater desorption of Glu from goethite (52–78%; Table 4.4) than Lys from montmorillonite (14–19%; Table 4.4) after addition of PAs indicates a stronger binding of AAs on negatively charged minerals by amino groups than on positively charged mineral surfaces by carboxylic groups in outer-sphere coordination.

Table 4.4 Desorption of previously adsorbed PAs and AAs after addition of AAs and PAs, respectively, in the conditioning experiments.

Compounds	Mineral	Initial concentration for adsorption /mM	Desorption / $\mu\text{mol g}^{-1}$		Desorbed proportion /%	
			Mean	SEM ^a	Mean	SEM
PAs	G ^b	0.01	0.33	0.03	17	0.9
		0.05	2.00		39	
		0.10	2.64		39	
	M ^c	0.01	0.11		29	
		0.05	0.44		41	
		0.10	0.52		38	
AAs	G	0.01	0.17	0.03	52	8.5
		0.05	0.79		71	
		0.10	1.41		78	
	M	0.01	0.07		14	
		0.05	0.42		18	
		0.10	0.88		19	

^a Standard error of the mean determined using the residual mean square (12 d.f.); ^b Goethite; ^c Montmorillonite.

4.4.2 Competitive adsorption of PAs and AAs on pure soil minerals

The adsorption of PAs (i.e. mainly Sal) on goethite and montmorillonite under slightly acidic conditions was partially suppressed in presence of AAs at intermediate and large initial concentrations. These results demonstrate a larger competitiveness of AAs than PAs. At small initial concentrations, competition was negligible probably because of the sufficient and large number of adsorption sites, whereas at intermediate and large initial concentrations the adsorption sites became limited and competition became evident. The predominant adsorption of Sal among different PAs did not change in the presence of AAs. The formation of bidentate complexes between Sal and mineral surfaces requires two adjacent adsorption sites (Yost *et al.*, 1990; Kubicki *et al.*, 1997), whereas any of the AAs used probably needs only one binding site (Kitadai *et al.*, 2009; Yang *et al.*, 2016). Therefore, it is more likely that one binding site required by AAs is available than two adjacent ones for PAs (i.e. mainly Sal), particularly at large concentrations. Furthermore, the Glu can displace some weakly bound PAs (Gu *et al.*, 1996), e.g. Syr, Fer and Van.

The adsorption of AAs on montmorillonite and goethite was enhanced by PAs, and the effect on montmorillonite was stronger than on goethite (i.e. at large initial concentrations only). Taking the competitiveness of AAs into account, we can assume a surface conditioning effect of PAs that enhances the adsorption of AAs.

4.4.3 Effect of surface conditioning on adsorption of PAs and AAs – evidence for multilayer adsorption?

At present there is little conclusive evidence for the multilayer model in the formation of natural soil MOAs. Mikutta *et al.* (2009) investigated the vertical structure of MOAs along a mineralogical soil gradient and found no evidence of enrichment of organic N compounds at mineral surfaces. Du *et al.* (2014) used depth-profiling Fourier transform infrared photo-acoustic spectroscopy and identified three different layers (ca. 100 μm thick) for the associated OM on soil particles, with enrichment of N moieties in the inner layer (ca. 60 μm deep). The spatial resolution of this study, however, does not enable any conclusion about the validity of a molecular-based multilayer adsorption model.

Our model experiments showed clearly that the adsorption of organic monomers on minerals modified their surface properties and subsequently altered their adsorption behaviour for other organic compounds. The adsorption of AAs on goethite and montmorillonite was enhanced by surface conditioning with PAs, despite partial desorption or displacement of PAs during adsorption of AAs. Therefore a fraction of the adsorbed components (the strongly bound one) was responsible for the enhanced adsorption of AAs. Preceding adsorption of PAs increased the positive charges on the goethite surface and negative ones on montmorillonite indicated by the more positive and negative ζ potentials for goethite and montmorillonite, respectively, after adsorption of PAs (Table 4.3), and therefore the number of binding sites for Glu on goethite and Lys on montmorillonite. This effect was not expected for goethite and might be caused primarily by dispersion of aggregates during the batch adsorption procedure (Mikutta *et al.*, 2014). Light scattering measurements revealed a decrease in the average particle diameter of goethite from 220 nm of the untreated mineral to 40 nm after adsorption (tested for 0.1 mM AAs). In addition, the ζ potential of goethite became more positive with the adsorption of PAs and AAs. Thus, dispersion of goethite possibly occurred during the batch experiments. Walsch & Dultz (2010) also reported that dispersion of goethite occurred at $\text{pH} \leq 6.5$ in batch adsorption experiments. Furthermore, the negative charges added by

adsorption of organic acids (Table 4.2) were much smaller than the surface charge density of goethite (e.g. $48.8 \mu\text{mol}_c \text{g}^{-1}$ at a specific surface area of $70 \text{m}^2 \text{g}^{-1}$ and assuming a charge density of $0.7 \mu\text{mol}_c \text{m}^{-2}$; Walsch & Dultz (2010)). Both factors might be responsible for the adsorption of organic acids on goethite that resulted in slightly increased positive charges (Table 4.3). The dispersion-induced increase in number of adsorption sites might explain why surface conditioning by PAs did not change the character of the adsorbed AAs, i.e. it increased mainly the adsorption of AAs with the opposite charge.

In addition to the effects of dispersion, aromatic rings of PAs might be important for increased adsorption of AAs. Once PAs (predominantly Sal) were adsorbed on mineral surfaces primarily by their carboxyl (and hydroxyl) groups (Guan *et al.*, 2006), the aromatic ring of PAs probably offered some additional binding sites for AAs. Although no additional charged sites could be created by Sal, molecular interactions of aromatic rings with ionizable AAs through polar- π interaction could occur (Keiluweit & Kleber, 2009). In turn, surface conditioning by Sal increased the adsorption of negatively and positively charged AAs on goethite (Glu) and montmorillonite (Lys), respectively. The negligible adsorption of Phe (aromatic AA) suggests weak π - π interaction. Moreover, the smaller effect of surface conditioning by PAs for montmorillonite on the immobilization of AAs relative to goethite corresponded to the much smaller adsorption of PAs (Table 4.2). Therefore, the additional retention of AAs appears to depend on the abundance of aromatic rings, but this hypothesis remains to be tested in a forthcoming study. The larger effect of surface conditioning for goethite than montmorillonite can be explained by the dispersion of aggregates, which probably occurred for goethite only.

Although the stimulating effect of surface conditioning by PAs on the adsorption of AAs was quite unexpected, we anticipated an enhanced adsorption of PAs on montmorillonite after adsorption of AAs. The enhanced retention of PAs might provide an example of a more general mechanism through which the adsorption of one class of SOM components enhances the uptake of another. Such enhanced adsorption might be interpreted as an indirect experimental indication of the multilayer model (Kleber *et al.*, 2007), where preferential adsorption of N-containing compounds modify the binding environments on mineral surfaces in a way that renders them more attractive for other compound classes. These effects might be observed theoretically for both the negatively and positively charged mineral. Interestingly, the stimulating effect of surface conditioning by AAs on the binding of PAs was less than the effects of conditioning by PAs on the adsorption of AAs (Figure 4.1 and Table B4). The

effect of surface conditioning by AAs on montmorillonite was less than that for goethite, despite stronger adsorption of AAs on montmorillonite and less desorption after the addition of PAs. This suggested that the larger accessible surface induced by the dispersion of goethite aggregates was a potential mechanism. The minor effect of surface conditioning by AAs for montmorillonite might be explained by the partial intercalation of Lys into the interlayer spaces (Parbhakar *et al.*, 2007; Kitadai *et al.*, 2009). The intercalation probably prevented desorption and crosslinking to other compounds. Because PAs were negatively charged at pH 6, the amino groups of attached AAs could provide additional binding sites to retain more PAs. Aromatic AAs (Phe) did not result in an additional effect on the adsorption of PAs compared with Glu (goethite) or Lys (montmorillonite), which further supported the role of amino groups as additional binding sites for PAs.

4.5 Conclusions

Our results demonstrate clearly that at slightly acidic conditions the adsorption of PAs and AAs depend strongly on the type of mineral, adsorbate properties and concentrations. Amino acids, although the more labile carbon source, are more competitive than PAs in binding on mineral surfaces such as goethite and montmorillonite. Furthermore, surface conditioning with AAs enhanced the adsorption of PAs. These results illustrate the important role of free acidic and basic AAs for surface conditioning in relation to adsorption and probably stabilization of SOM by soil minerals, irrespective of the surface charges of the mineral. Our results also showed the potential contribution of PAs (i.e. lignin degradation products) in the formation of mineral–organic associations. Aromatic structures in PAs can enhance the adsorption of AAs and probably of other organic components, independently of net charge characteristics. The PAs resulted in a larger increase in the adsorption of AAs than AAs did for PAs. From our results we can conclude that adsorption of one class of SOM components might alter the adsorption, and potential preservation, of other classes. Nevertheless, we still lack understanding of the true molecular-scale arrangements of individual compounds which requires a combination of molecular spectroscopy (e.g. synchrotron-based mass spectrometry or X-ray photoelectron spectroscopy) and quantum chemical modelling approaches. We recommend further batch experiments to assess possible altered adsorption site availabilities induced by mineral dispersion.

Chapter 5

Organic matter coatings of soil minerals affect adsorptive interactions with phenolic and amino acids

This chapter has been submitted as:

Gao, J., Jansen, B., Cerli, C., Helmus, R., Mikutta R., Dultz S., Guggenberger, G., Vogel C. & Kalbitz, K. 2017. Organic matter coatings of soil minerals affect adsorptive interactions with phenolic and amino acids. *European Journal of Soil Science*.

Abstract

Phenolic acids (PAs) and amino acids (AAs) potentially contribute to the formation of mineral-organic associations (MOAs) resulting in the stabilization of organic matter (OM) in soils. However, little is known about how natural OM coating affects the subsequent adsorption of these compounds and their mutual interaction upon adsorption. Therefore, batch adsorption experiments were conducted to study how the coating of mineral surfaces with dissolved OM (DOM; derived from forest leaf litter (L-DOM) and O horizon (O-DOM)) affects adsorptive interactions of PAs (salicylic, syringic, ferulic and vanillic acid) and AAs (lysine, Lys; glutamic acid, Glu; leucine; phenylalanine) on goethite, kaolinite, and montmorillonite at pH 6. Adsorption of DOM depended on the mineral (goethite >> kaolinite > montmorillonite) and DOM sources (O-DOM > L-DOM for goethite). Coating of all minerals with both DOM sources reduced the adsorption of PAs and acidic AA (Glu), but enhanced the adsorption of basic AA (Lys). The effect of organic coatings was strongly dependent on the amount of adsorbed OM. The strong bonds between AAs and OM-coated minerals resulted in generally enhanced adsorption of PAs with surface conditioning by AAs, which possibly indirectly evidences a multilayer model of MOAs. However, adsorption of AAs was rarely influenced by surface conditioning with PAs. Competition between AAs and PAs generally suppressed the adsorption of AAs on coated minerals, whereas it had little influence on the adsorption of PAs. These results emphasize that the amount and composition of OM coatings affect the adsorption of PAs and AAs.

5.1 Introduction

Substantial efforts have been dedicated to understanding the formation of mineral-organic associations (MOAs) by adsorptive interaction between soil minerals and natural organic compounds (Schmidt *et al.*, 2011; Lehmann & Kleber, 2015). These interactions are decisive for the protection of organic matter in soils against microbial decay (Schneider *et al.*, 2010; Mikutta *et al.*, 2007). At new mineral surfaces and low C loading organic matter (OM) is very strongly adsorbed through multidentate bonding, while at larger C loading less functional groups of the organic molecules are involved (Kaiser & Guggenberger, 2007), thus rendering OM more susceptible to desorption and vulnerable to microbial decomposition.

Currently, there is no consensus on the processes and involved organic substances in the formation of MOAs. The classical view of a preferential bonding of lignin-derived components such as phenolic acids (PAs) to many soil minerals (Kaiser & Guggenberger, 2000; Kalbitz *et al.*, 2005; Kothawala *et al.*, 2012; Kramer *et al.*, 2012) is in contrast to the "onion" or "multilayer" model (Sollins *et al.*, 2006; Kleber *et al.*, 2007) assuming that amphiphilic, N-rich molecules (e.g. amino acids; AAs) build up an inner layer directly linked to the charged aluminosilicates surfaces and an outer layer of more loosely bound organic substances, probably including PAs. Thus, exploring competitive adsorption processes of AAs versus PAs could advance our current understanding which class of compounds might be more relevant in the formation of MOAs.

As degradation products of lignin and proteins, respectively, AAs and PAs are very active components in the cycling of N and C in soils. So far, the knowledge about the adsorption patterns of nitrogenous and aromatic components including AAs and PAs to soils or soil minerals has been obtained either in mono-component systems or by the changes in the composition of dissolved organic matter (DOM) following adsorption (Kaiser *et al.*, 1997; Kalbitz *et al.*, 2005; Chefetz *et al.*, 2011; Yeasmin *et al.*, 2014). However, consequences of interactions between AAs and PAs during and upon adsorption for the formation of MOAs were rarely studied, yet are crucial to assess the validity of conceptual adsorption models. It can be expected that these interactions between AAs and PAs might not only be affected by the nature of the mineral surface (e.g. variable charged oxides vs. uncharged and hydrophobic 1:1 clay minerals vs. permanently charged 2:1 clay minerals) but also by the coverage of these surfaces by adsorbed OM. Adsorption of DOM depends on its composition, with usually higher adsorption of DOM derived from decomposed OM than from

fresh litter (Schneider *et al.*, 2010), and modifies the surface properties of soil minerals, such as specific surface area (SSA), surface charge and hydrophilicity. Such changes in surface properties are important for DOM cycling as they govern the remaining adsorption and stabilization capacity of the mineral phase (Sanderman *et al.*, 2008; Kaiser & Kalbitz, 2012). However, effects of these changes in surface properties on the adsorption of AAs and PAs are not well understood, besides the above mentioned decrease in chemical bonds of organic compounds on mineral surfaces with increasing C loading.

Recently we have shown that a preceding adsorption of both AAs and PAs on soil minerals enhanced the adsorption of the other group of compounds (Gao *et al.*, 2017). In other studies, the retention of non-polar organic compounds was greatly enhanced on minerals after coating with OM (Murphy *et al.*, 1990; Wang *et al.*, 2008; Polubesova *et al.*, 2009). However, whether that holds true for polar compounds such as PAs and AAs is unknown.

Therefore, the main objective of our study was to clarify how the coating of mineral surfaces with DOM affects adsorptive interactions between AAs and PAs. Goethite (α -FeOOH), kaolinite, and montmorillonite were chosen as test minerals, representing the most important minerals in many soils (Fe oxides, 1:1 and 2:1 clay minerals) and exhibiting different surface properties (goethite: variable charge, kaolinite: little isomorphous substitution and wide hydrophobic region, montmorillonite: rich isomorphous substitution and permanent negative charge; Sposito, 2008). We studied (i) the adsorption behavior of different AAs (glutamic acid, leucine, lysine and phenylalanine; representing acidic, neutral, basic and aromatic AAs) and PAs (salicylic, syringic, ferulic and vanillic acid; representing lignin degradation products) to these minerals coated with DOM; (ii) changes in the adsorption behavior of PAs on DOM-coated minerals after surface conditioning by AAs; (iii) changes in the adsorption behavior of AAs on DOM-coated minerals after surface conditioning by PAs, and (iv) competition effects between PAs and AAs on their adsorption on DOM-coated minerals. Herein, “coating” and its derivatives refer to the adsorption of DOM, “conditioning” and its derivatives refer to the adsorption of PAs and AAs.

5.2 Material and methods

5.2.1 Minerals

Goethite was synthesized according to the method of Atkinson *et al.* (1967) by

alkaline hydrolysis of 0.5 M FeCl_3 and freeze-dried at the end. Montmorillonite was obtained by separating the $< 2\text{-}\mu\text{m}$ fraction via sedimentation from Morocco bentonite (Ddani *et al.*, 2005). Exchange sites were saturated with Ca^{2+} by suspending the clay twice in 1 M CaCl_2 (1:10; w:v). Kaolinite (KGa-2) was purchased from the Clay Mineral Society (Warren County, Georgia, USA). A suspension of kaolinite in deionised H_2O (1:15; w:v) was sonicated for 8 minutes (120 W) to break the aggregates. Afterwards, exchange sites were also saturated with Ca^{2+} by suspending the clay thrice in 1 M CaCl_2 (1:5; w:v). Finally the montmorillonite and kaolinite were washed until salt-free, freeze-dried, and passed through a 200- μm sieve. The X-ray diffraction patterns (Siemens, D500, Cu-K α radiation, Karlsruhe, Germany) indicated the presence of well-crystalline goethite and a high purity of the $< 2\text{-}\mu\text{m}$ fraction of the Morocco bentonite and kaolinite (Figures B1 and C1, Appendix). The specific surface area (SSA) and total pore volume (TPV) of minerals were derived from duplicate N_2 gas adsorption isotherms recorded with a Quantachrome Autosorb1-MP analyzer (Quantachrome, Boynton Beach, FL, USA). For this purpose, 20–200 mg of each sample was weighed into the sample cell and degassed at 40 °C until the pressure was < 0.12 Pa. The SSA was calculated from the linear Brunauer–Emmett–Teller (BET) plot (Brunauer *et al.*, 1938) by using up to 10 adsorption points. The TPV was taken at P/P_0 ca. 0.995, where P and P_0 are the equilibrium and the saturation pressure, respectively of N_2 . The results and other properties are listed in Table 5.1.

5.2.2 Amino acids and phenolic acids

L-leucine (Leu), L-glutamic acid (Glu), L-lysine (Lys), DL-phenylalanine (Phe), DL-norvaline (Nva), salicylic acid (Sal), syringic acid (Syr), ferulic acid (Fer), vanillic acid (Van) and ethylvanillin (Eva) were purchased from Sigma-Aldrich (Zwijndrecht, The Netherlands). The purity was $> 98\%$, except for Syr ($\geq 95\%$) and Van ($\geq 97\%$). The chemical structure and properties of these compounds are listed in Table 4.1 (**chapter 4**). Nva and Eva were used as the internal standards (ISs) for the measurement of AAs and PAs, respectively.

5.2.3 Preparation of PA and AA solutions

Stock standard solutions of each AA (2000 mg l^{-1}) were prepared in 0.1 M HCl while those of PAs were prepared in water at concentration of 1000 mg l^{-1} for

Sal, Syr and Van and 500 mg l^{-1} for Fer, respectively. A lower concentration was used for Fer due to its low solubility in water (Table 4.1, **chapter 4**). The stock solutions were stored at $4 \text{ }^{\circ}\text{C}$ for not longer than one month. Working mixture solutions with equal concentration for individual PAs and AAs were freshly prepared by mixing and diluting the stock standard solutions.

5.2.4 Dissolved organic matter

Dissolved OM was extracted from litter (Oi horizon) and the Oe+Oa horizon of a beech forest (Grinderwald, Germany; Leinemann *et al.*, 2016) to represent DOM from the two most important sources percolating into the mineral soil. The leaf litter from Oi horizon was dried and ground into small pieces. The field moist samples from Oe+Oa horizon was sieved to $< 4.8 \text{ mm}$ and stored at $4 \text{ }^{\circ}\text{C}$. Suspensions of leaf litter in deionized H_2O (1:10; w/v) or of Oe+Oa horizon sample (1:5; w:v) were stirred with a glass rod first and left at $20 \text{ }^{\circ}\text{C}$ for 16 hours. The supernatant of the suspension was centrifuged (3500 g , 20 minutes) and filtered under vacuum through $0.45\text{-}\mu\text{m}$ mixed cellulose ester membrane (ME25, GE Healthcare Life Sciences, Whatman, Little Chalfont, UK). The DOM stock solution was stored at $4 \text{ }^{\circ}\text{C}$ before use. The dissolved organic carbon (DOC) concentration and pH of the extracts derived from leaf litter (L-DOM) and Oe+Oa horizon (O-DOM) were 1107 and 138 mg l^{-1} , 5.1 and 4.4 , respectively. More properties of the DOM were measured and showed in another study (Kalbitz *et al.*, 2003).

5.2.5 Preparation of OM-coated minerals

In order to verify a similar coating efficiency for all minerals, adsorption isotherms for the two DOM types (L-DOM and O-DOM) and three minerals were first constructed in a batch adsorption experiment in duplicate at pH 6 (Schneider *et al.*, 2010). To inhibit microbial activity and assure a constant electrolyte background, NaN_3 was added to the solutions with a final concentration of 10 mM and the pH was adjusted to 6 before mixing with minerals by dropwise addition of 0.1 M NaOH or HCl . Based on the adsorption isotherms, we selected the solid-to-solution conditions under which 50% of the maximum DOM adsorption capacity of the minerals was achieved. Fifty percent coverage was selected to ensure that the unsaturated minerals had sufficient remaining adsorption sites to interact with PAs and AAs. Briefly, goethite (20–

Table 5.1 Cation exchange capacity (CEC), specific surface area (SSA), total pore volume (TPV), average pore radius (APR), C content, OC loading, and ζ potential of pure and OM-coated minerals^a.

Mineral	CEC /mmol _c kg ⁻¹	SSA /m ² g ⁻¹	TPV /mm ³ g ⁻¹	APR /nm	C content /mg g ⁻¹	OC loading ^b /%	ζ potential measurement		
							ζ potential /mV	EC ^c /μS cm ⁻¹	pH
G ^d	13 ^m	69.7 (1.1)	730 (3)	21.0 (0.2)	1.4 (0.1)		40.4 (1.7)	4.0 (0.0)	6.2 (0.1)
L-G ^e	-	63.0 (2.4)	647 (36)	20.5 (0.4)	9.1 (0.0)	54	-6.8 (0.5)	5.3 (0.6)	6.0 (0.1)
O-G ^f	-	69.3 (3.5)	702 (66)	20.2 (0.9)	17.9 (0.0)	53	-27.5 (2.1)	7.3 (0.6)	6.3 (0.1)
K ^g	37 ⁿ	25.0 (0.9)	315 (51)	25.2 (3.2)	0.5 (0.0)		-23.2 (1.3)	4.0 (0.0)	6.0 (0.1)
L-K ^h	-	23.4 (1.1)	379 (6)	32.4 (1.0)	1.5 (0.0)	59	-37.9 (1.8)	4.0 (0.0)	6.1 (0.0)
O-K ⁱ	-	23.6 (0.5)	403 (84)	34.1 (6.4)	1.6 (0.0)	54	-42.7 (0.3)	4.0 (0.0)	6.0 (0.1)
M ^l	888 ^o	94.7 (6.0)	187 (6)	4.4 (1.0)	1.1 (0.0)		-29.5 (3.5)	5.0 (0.0)	6.3 (0.1)
L-M ^k	-	51.8 (0.2)	112 (4)	4.3 (0.2)	2.0 (0.0)	59	-49.3 (1.6)	6.0 (0.0)	6.2 (0.1)
O-M ^l	-	48.6 (0.1)	110 (2)	4.5 (0.1)	2.2 (0.0)	74	-54.1 (2.8)	5.0 (0.0)	6.2 (0.1)

^a the results are presented as mean values with standard deviation except for the OC loading. All the measurement had three replicates except for the C content, which had two replicates; ^b proportion of the maximum adsorption capacity for the respective DOM; ^c electrical conductivity; ^d goethite; ^e goethite coated with L-DOM; ^f goethite coated with O-DOM; ^g kaolinite; ^h kaolinite coated with L-DOM; ⁱ kaolinite coated with O-DOM; ^j montmorillonite; ^k montmorillonite coated with L-DOM; ^l montmorillonite coated with O-DOM; ^m calculated from the negative surface charge density at pH 6 in NaCl background electrolyte Walsch & Dultz (2010); ⁿ Borden & Giese (2001); ^o Daou et al. (2015).

700 mg), kaolinite (50–1200 mg), or montmorillonite (40–1500 mg) were suspended in 40 ml L-DOM or O-DOM solution adjusted to pH 6 (ca. 120 mg OC l⁻¹ for goethite and ca. 50 mg OC l⁻¹ for kaolinite and montmorillonite) and shaken horizontally (95 rpm) for 16 h in the dark at 4 °C to achieve equilibrium, then centrifuged (3500 g, 20 min), and filtrated through 0.45-µm mixed cellulose ester membranes. The UV absorbance of the filtrates at 280 nm was measured using a Spectroquant Pharo 300 spectrometer (Merck KGaA, darmstadt, Germany). The pH of the filtrate was measured using a multi-channel analyser (CONSORT C831, Abcoude, The Netherlands). The DOC concentrations of the filtrates were measured by a TOC analyser (TOC-V CPH Shimadzu, Kyoto, Japan). Adsorbed OC was calculated as the difference between the TOC in the initial and equilibrium solutions.

The OM-coated minerals (L-DOM-coated goethite, L-goethite; L-DOM-coated kaolinite, L-kaolinite; L-DOM-coated montmorillonite, L-montmorillonite; O-DOM-coated goethite, O-goethite; O-DOM-coated kaolinite, O-kaolinite; O-DOM-coated montmorillonite, O-montmorillonite) were freeze-dried, ground with agate mortar and pestle, sieved to < 200 µm. The C contents (Table 5.1) were measured by a CN analyser (Elementar Vario EL, Hanau, Germany). The C loadings of the three minerals were between 45–67%, which is close to the desired 50% of the maximum adsorption capacity.

5.2.6 Adsorption experiments with PAs and AAs

Adsorption of PAs (mixed solution of Sal, Syr, Fer and Van) and AAs (mixed solution of Leu, Glu, Lys and Phe) were conducted with pure goethite, kaolinite, and montmorillonite and minerals coated with L-DOM and O-DOM. Experiments were conducted in triplicate and at three different initial concentrations of the individual adsorbates: 0.01 (small), 0.05 (intermediate), and 0.1 mM (large). The solutions were added to each OM-coated mineral separately (control experiment), together (competition experiment), and after pre-conditioning of the other mix (conditioning experiment). For the latter, two conditioning experiments were conducted: PAs adsorption on OM-coated minerals after adsorption of AAs (conditioning experiment I) and AAs adsorption on the OM-coated minerals after adsorption of PAs (conditioning experiment II). The initial pH conditions were set at 6 for all the experiments and they rose to 6.2–6.7 after adsorption. Details of the adsorption procedure and results of PAs and AAs adsorption on pure goethite and montmorillonite are given in Gao *et al.*

(2017). Adsorption results of PAs and AAs on pure kaolinite are presented in the Appendix (Figures C2 and C3).

5.2.7 Measurement of PAs and AAs

The PAs in the filtrates were analysed directly by a Prominence high performance liquid chromatography (HPLC) system equipped with a diode array detector (Shimadzu, Kyoto, Japan). The details are given in Appendix (C) and Table C1. Prior to measurement, the AAs in the filtrates were diluted 10 or 20 times in organic solvent (90% acetonitrile, 10% H₂O, 8 mM ammonium formate, 0.12% formic acid, v/v%) and spiked with Nva (IS) at a final concentration of 0.1 mg l⁻¹. Hydrophilic interaction LC (Shimadzu, Kyoto, Japan) coupled with a 4000 QTRAP LC-MS/MS System (AB SCIEX, MA, USA) was used to analyse the AAs (Gao *et al.*, 2016; Gao *et al.*, 2017). High accuracies of the analytical methods of PAs and AAs were obtained by comparing the measured concentrations of the mixture with the calculated values (Table C2, Appendix). These results indicated the measurement of PAs and AAs were not affected by each other. The typical chromatograms of PAs and AAs were showed in Figures C4 and C5 (Appendix).

5.2.8 Desorption experiments and potential flocculation of PAs or AAs with desorbed OM

The adsorption reversibility of OM and the potential contribution of DOM-derived PAs and AAs was assessed by a desorption experiment using 10 mM NaN₃ (pH 6) as the same electrolyte background in the adsorption experiment. Suspensions of OM-coated minerals in 40 ml NaN₃ solution (200 mg goethite, 600 mg kaolinite or montmorillonite) were shaken horizontally (95 rpm) for 2 hours in the dark at 4 °C, then centrifuged (3500 g, 20 minutes) and filtered through 0.45-µm mixed cellulose ester membranes. The minerals were re-suspended by vortex before carrying out a second cycle. The DOC concentrations in the filtrates were analysed by a TOC analyser (TOC-V CPH Shimadzu, Kyoto, Japan). Desorption was generally small for kaolinite and goethite (Table C3, Appendix). Strong mechanical force was needed to grind the OM-coated montmorillonite, this may result in the relatively higher desorption of OM (22.2–26.7%). The PAs and AAs in the solutions of the first desorption cycle were generally undetectable except for little AAs for the L-

goethite (Table C4, Appendix). This indicates that the PAs and AAs measured in the adsorption experiments almost exclusively derive from the added compounds.

The filtrate after the first desorption cycle was further used to test potential flocculation of PAs or AAs by possible desorbed OM, as flocculation would result in decreasing concentrations of PAs and AAs in filtrates after adsorption and therefore in overestimation of their adsorption. Therefore, 5 ml desorption solution was spiked with mixture solution of PAs or AAs with final concentration of 1, 4, 10 and 20 mg l⁻¹ (the concentration was the same for individual compound in each mixture). The high recoveries of the spiked PAs and AAs (91–93% and 86–101%, respectively; Table C5, Appendix) implies the negligible effects of flocculation.

5.2.9 Potential exchange of PAs or AAs with adsorbed OM

The PAs and AAs solutions (intermediate initial concentration) in the control experiments were analysed for TOC concentration as well. The differences between the measured TOC concentration and the calculated results from HPLC analysis were similar to the desorbed OC that obtained from the desorption experiments (data not shown). In addition, the desorption results showed that the majority of the adsorbed OM was irreversible. Thus, the exchange of PAs or AAs with adsorbed OM was supposed to be negligible in this study.

5.2.10 Zeta potential measurement of OM-coated minerals

Zeta (ζ) potential measurements were carried out using phase-analysis light scattering (ZetaPALS, Brookhaven Instruments Corp., Holtsville, NY, USA). Mineral suspensions of 100 mg l⁻¹ were prepared in ultrapure water in 25-ml flasks without further pH adjustment. After gentle shaking, 1.6 ml was sampled with a pipette, transferred into a cuvette and measured at 20 °C. Each sample was measured five times and each of the five replicates consisted of 20 single measurements. The ζ potential was calculated from electrophoretic mobility using the Smoluchowski equation (Hunter, 1981). The electrical conductivity of the suspensions was determined simultaneously and used to reflect electrolyte concentration. The pH was determined in the cuvette using a miniaturized electrode (BlueLine 16pH, Si Analytics, Mainz, Germany).

5.2.11 Statistics

Statistical analysis was performed with SigmaPlot (version 13.0). Two way ANOVA was used to evaluate the influences of mineral types, OM coating, adsorbate concentration, competition and surface conditioning on the adsorption of PAs and AAs. Data were transformed if necessary to meet both the normality (Shapiro-Wilk) and homogeneity of variance (Brown-Forsythe) tests using appropriate methods. Fisher's least significant difference (LSD) was used for multiple comparisons of means. The significant level of difference was set at $P < 0.05$.

We introduced the relative adsorbed amount because this approach more clearly showed the effects of OM coating, competition and surface conditioning on the adsorption of PAs and AAs. The references referred to the adsorption results obtained from control experiment and the same reference mean values were used for each of the three replicates in calculating the relative values of adsorbed amounts.

5.3 Results

5.3.1 Adsorption of natural DOM on pure minerals

The adsorption of L-DOM and O-DOM on soil minerals followed the same order of goethite >> kaolinite > montmorillonite on both mass and surface area basis under nearly neutral conditions (Figure 5.1 and Table C6). Goethite retained more O-DOM than L-DOM, while a similar adsorption of both DOM solutions was observed for kaolinite and montmorillonite. The experiments with L-DOM showed a preferential adsorption of aromatic compounds to all minerals revealed by decreasing specific UV absorbance at 280 nm (Figure C6, Appendix). For O-DOM, such a preferential adsorption could only be observed to montmorillonite. The SSA of different minerals followed the order of montmorillonite > goethite > kaolinite, while a different order of goethite > kaolinite > montmorillonite was observed for the TPV (Table 5.1) and this was in line with the adsorption results. The SSA of montmorillonite was remarkably reduced by both types of DOM, while the effects on goethite and kaolinite were small (Table 5.1). In addition, the equilibrium pH after adsorption increased with the reduction of OC in solution (Figure C7, Appendix), which depended on the mineral and the type of DOM. The ζ potential of goethite was reversed to negative by adsorption of DOM with a stronger effect for O-DOM (Table 5.1).

Organic matter coatings led to more negative ζ potentials of kaolinite and montmorillonite with similar effect for L-DOM and O-DOM. The increase in negative surface charge upon DOM coating increased with the amount of C adsorbed (Figure C8, Appendix). These changes were largest for goethite and differed between the two types of DOM, as more O-DOM was adsorbed on goethite than L-DOM (Figure 5.1).

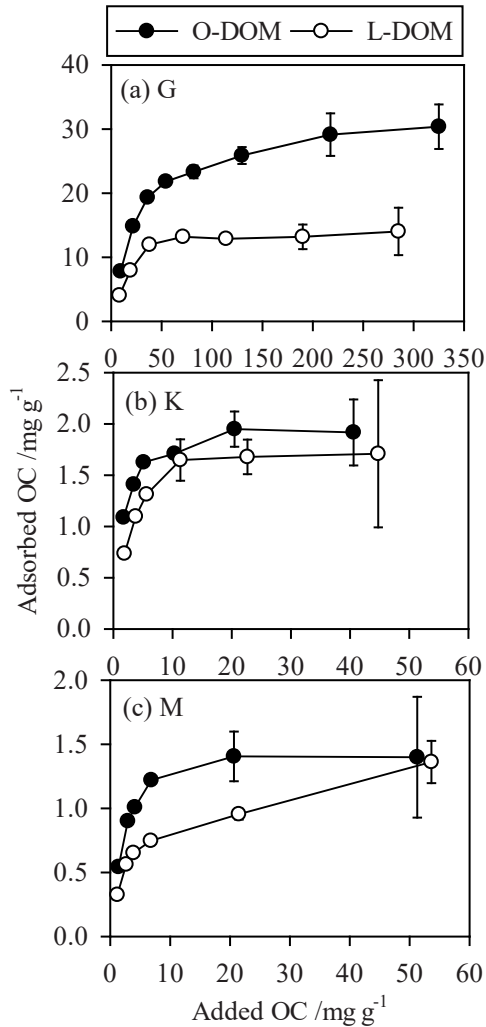


Figure 5.1 Adsorption isotherms of O-DOM and L-DOM on different minerals. The results are presented as mean values with standard deviation ($n = 2$). G, goethite; K, kaolinite; M, montmorillonite.

5.3.2 Control experiment – adsorption of PAs or AAs on OM-coated minerals

5.3.2.1 Phenolic acids

The adsorption of PAs on pure minerals followed the order: goethite >> kaolinite > montmorillonite under slightly acidic conditions (Figure C2a, Appendix) and was suppressed by the OM coating irrespective of the mineral and the type of DOM (Figure 5.2a and b). For both DOM types, the suppressing effect increased with increasing adsorption of DOM. The reduction of PAs adsorption on the OM-coated mineral as compared to the pure mineral was largest for goethite, which had the highest OM loading (Figure 5.2a and b). As a result of this effect, the final adsorption sequence of PAs on the O-DOM-coated minerals was in the following order: montmorillonite > kaolinite > goethite (Figure C2c, Appendix). That means the adsorption order of PAs was completely reversed by O-DOM coating compared to pure minerals. When differentiating between L-DOM and O-DOM, the O-DOM-coated minerals suppressed the adsorption of PAs to a larger extent, except for coated montmorillonite where both types of DOM had a similar effect. Coating of goethite with O-DOM was so large that it completely suppressed adsorption of all PAs. For the other minerals, Sal was the only adsorbed PA on their O-DOM coated forms, while adsorption of the other PAs (Syr, Fer and Van) was completely blocked by the O-DOM coating. Desorption of PAs from OM-coated minerals was larger than that from pure minerals (Gao *et al.*, 2017) and larger from minerals coated with L-DOM than O-DOM (Table C4, Appendix).

5.3.2.2 Amino acids

On pure minerals, adsorption of AAs followed the order: montmorillonite \geq kaolinite > goethite under slight acidic conditions (Figure C3, Appendix). Among the different AAs, goethite adsorbed only Glu, whereas montmorillonite adsorbed only Lys (Gao *et al.*, 2017). Both Glu and Lys were adsorbed on kaolinite with a dominating role for Lys (Figure C9, Appendix). No adsorption of Leu and Phe was observed on kaolinite either. The adsorption of AAs responded very differently to the OM coating compared to PAs. If effects occurred they were mostly positive, i.e. increasing adsorption of AAs by OM coating (Figure 5.2c and d). Adsorption of AAs on L-goethite and L-montmorillonite increased by 56–145% and 24–40%, respectively, for different initial concentrations. All the differences were significant ($P < 0.05$) except for goethite at the small initial concentration (Figure 5.2c). Specifically, Lys, Leu

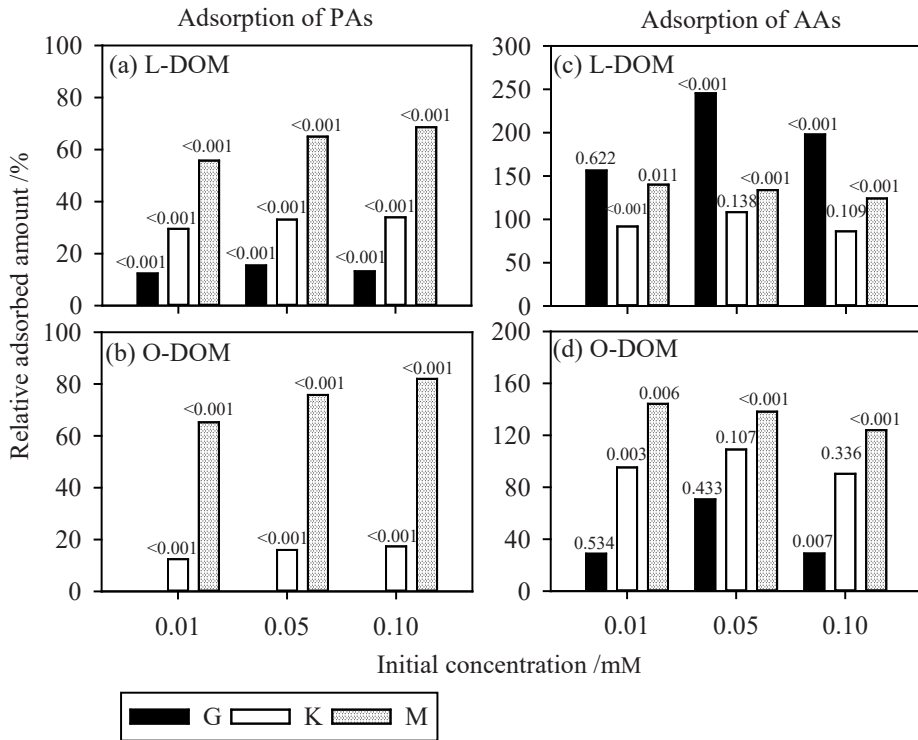


Figure 5.2 Relative adsorption of: (a) PAs on coated minerals with L-DOM, (b) PAs on coated minerals with O-DOM, (c) AAs on coated minerals with L-DOM and (d) AAs on coated minerals with O-DOM in the control experiment. Dotted lines refer to the reference values (absolute adsorption results on pure minerals). The results are presented as mean values ($n = 3$). P value above each column is from the analysis of variance of the absolute adsorption results and it indicates the significance of the difference compared with the corresponding reference. G, goethite; K, kaolinite; M, montmorillonite.

and Phe, which did not show adsorption on pure goethite, were adsorbed on L-goethite besides Glu (Figure C10a, Appendix). There were no significant differences between the adsorption of Glu on pure goethite and L-goethite (Figure C11a, Appendix). The adsorption of Lys on L-kaolinite significantly increased by 18–36% for different initial concentrations ($P < 0.05$; Figure C12a, Appendix), although the sum of various AAs did not change. Conversely, the adsorption of Glu on L-kaolinite significantly decreased by 74% or 60% for the small or intermediate initial concentration ($P < 0.05$) and it was entirely suppressed for the large initial concentration (Figure C11b, Appendix).

Coating of goethite with O-DOM did reduce the adsorption of AAs (Figure 5.2d) and changed the type of adsorbed AA, i.e. Glu replaced by Lys. Nevertheless, the adsorption of Lys on O-goethite ($0.10\text{--}0.96 \mu\text{mol g}^{-1}$) was much lower than that on O-kaolinite ($0.57\text{--}3.29 \mu\text{mol g}^{-1}$) and O-montmorillonite ($0.71\text{--}5.74 \mu\text{mol g}^{-1}$). Similar to goethite, coating of kaolinite with O-DOM resulted in entirely suppressed adsorption of Glu and increased adsorption of Lys (increase by 24–54%), thus resulting in no changes of total adsorption of AAs to O-kaolinite (Figure 5.2d). Moreover, the adsorption of Lys, the only adsorbed AA on both pure montmorillonite and O-montmorillonite, was significantly increased by 24–44% on O-montmorillonite ($P < 0.05$; Figure C12b, Appendix).

In contrast to PAs, the presence of OM coatings reduced desorption of AAs from minerals. Percentages of desorbed AAs from OM-coated minerals were even lower than those of PAs (Table C4, Appendix).

5.3.3 Competition experiment – adsorption of PAs and AAs on OM-coated minerals

5.3.3.1 Phenolic acids

Competition with AAs was minor and resulted mostly in a slightly decreased PAs adsorption to OM-coated minerals ($< 0.32 \mu\text{mol g}^{-1}$; Figure 5.3a and b). Sal was the only adsorbed PA. There was a tendency of increasing adsorption of PAs on O-kaolinite (significant for the intermediate and large initial concentrations) as compared to the situation without AAs (Figure 5.3b).

5.3.3.2 Amino acids

The presence of PAs resulted in significantly decreased adsorption of AAs on all L-DOM-coated minerals ($P < 0.05$; Figure 5.3c). Glu was the only adsorbed AA on L-goethite, and Lys on L-kaolinite and L-montmorillonite under competition with PAs. The strongest reduction in adsorption was for L-goethite, with a decrease by 66–76% ($0.40\text{--}2.24 \mu\text{mol g}^{-1}$; Figure 5.3c).

The adsorption of AAs on O-goethite was significantly increased by 130% ($0.95 \mu\text{mol g}^{-1}$) or 556% ($2.58 \mu\text{mol g}^{-1}$) for the intermediate or large initial concentration ($P < 0.05$; Figure 5.3d). Little change ($0.02 \mu\text{mol g}^{-1}$) was observed for the small initial concentration. Both Glu and Lys were adsorbed on

O-goethite and O-kaolinite, while only Lys was adsorbed on O-montmorillonite under competition with PAs. There were no consistent effects of competition on the adsorption of AAs on O-kaolinite. However, adsorption of Glu became detectable ($0.02\text{--}0.41\ \mu\text{mol g}^{-1}$) besides Lys. Competition resulted in reduced adsorption of AAs on O-montmorillonite by 9–30% ($0.21\text{--}0.54\ \mu\text{mol g}^{-1}$) for different initial concentrations ($P < 0.05$, Figure 5.3d).

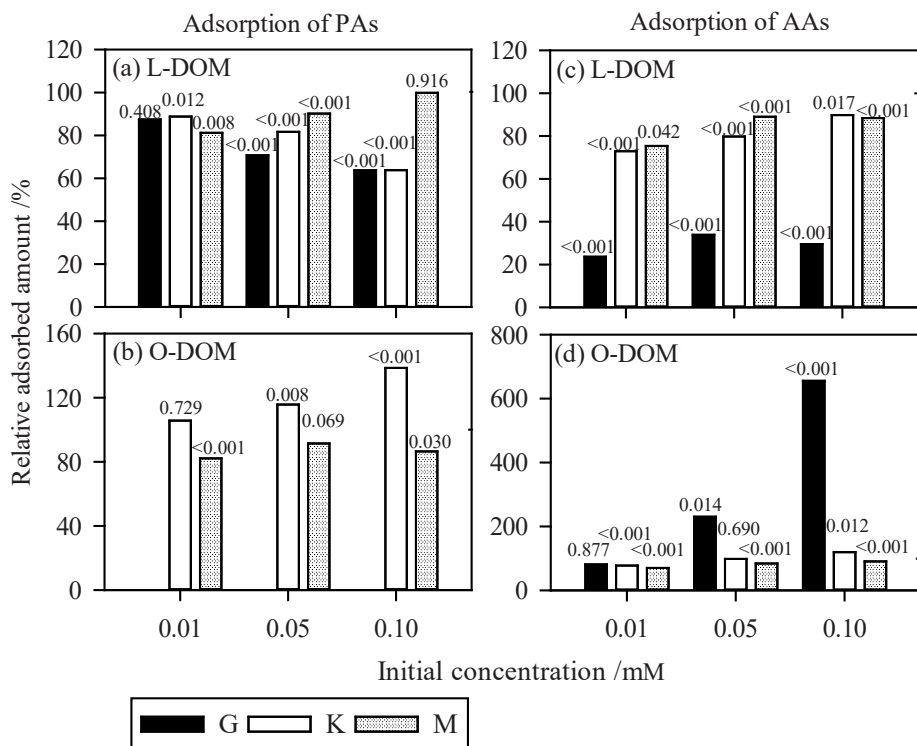


Figure 5.3 Effects of competition on the adsorption of: (a) PAs on coated minerals with L-DOM, (b) PAs on coated minerals with O-DOM, (c) AAs on coated minerals with L-DOM and (d) AAs on coated minerals with O-DOM. Dotted lines refer to the reference values (control experiments). The results are presented as mean values ($n = 3$). P value above each column is from the analysis of variance of the absolute adsorption results and it indicates the significance of the difference compared with the corresponding reference. The adsorption of PAs on O-goethite (b) is not displayed because the values of the reference are zero. G, goethite; K, kaolinite; M, montmorillonite.

5.3.4 Conditioning experiment I – adsorption of PAs on OM-coated minerals after adsorption of AAs

Preceding adsorption of AAs on OM-coated minerals resulted mostly in significantly increased adsorption of PAs (Figure 5.4a and b). The largest effect was observed for L-montmorillonite (increase by 25–86%) but little changes were observed for both L-goethite and L-kaolinite ($< 0.13 \mu\text{mol g}^{-1}$). Surface conditioning by AAs on O-goethite resulted in an increased adsorption of PAs from 0 to $0.20\text{--}1.22 \mu\text{mol g}^{-1}$ at different initial concentrations (Figure C13, Appendix), whereas for both O-montmorillonite and O-kaolinite PAs increased by 24–70% ($P < 0.05$). Sal was the only adsorbed PA on L-goethite, L-kaolinite, and O-kaolinite with or without surface conditioning of AAs. Despite little adsorption of Syr, Fer and Van was observed for L- and O-montmorillonite following surface conditioning, Sal remained the predominantly adsorbed PA.

5.3.5 Conditioning experiment II – adsorption of AAs on OM-coated minerals after adsorption of PAs

In general, preceding adsorption of PAs on OM-coated minerals did not result in significant changes in the adsorption of AAs (Figure 5.4c and d). The large relative increase of adsorbed AAs on O-goethite at the small initial concentration was very small in absolute numbers ($0.2 \mu\text{mol g}^{-1}$). Lys remained the predominantly adsorbed AA on OM-coated kaolinite and montmorillonite after adsorption of PAs.

5.4 Discussion

5.4.1 Adsorption of natural DOM on pure minerals

The observed stronger adsorption capacity of goethite for the two types of DOM relative to kaolinite and montmorillonite (Figure 5.1) was in agreement with the results of Mikutta *et al.* (2007) and Meier *et al.* (1999). They reported larger amounts of adsorbed DOM for goethite in comparison to 2:1 phyllosilicates (pyrophyllite and vermiculite) or 1:1 phyllosilicates (kaolinite). This is mainly driven by the positive charge of the goethite in nearly neutral conditions, while kaolinite and montmorillonite are overall negatively charged (Table 5.1). The more negative ζ potential upon DOM adsorption illustrates the predominant negative charge provided by both types of DOM at pH 6. For kaolinite and

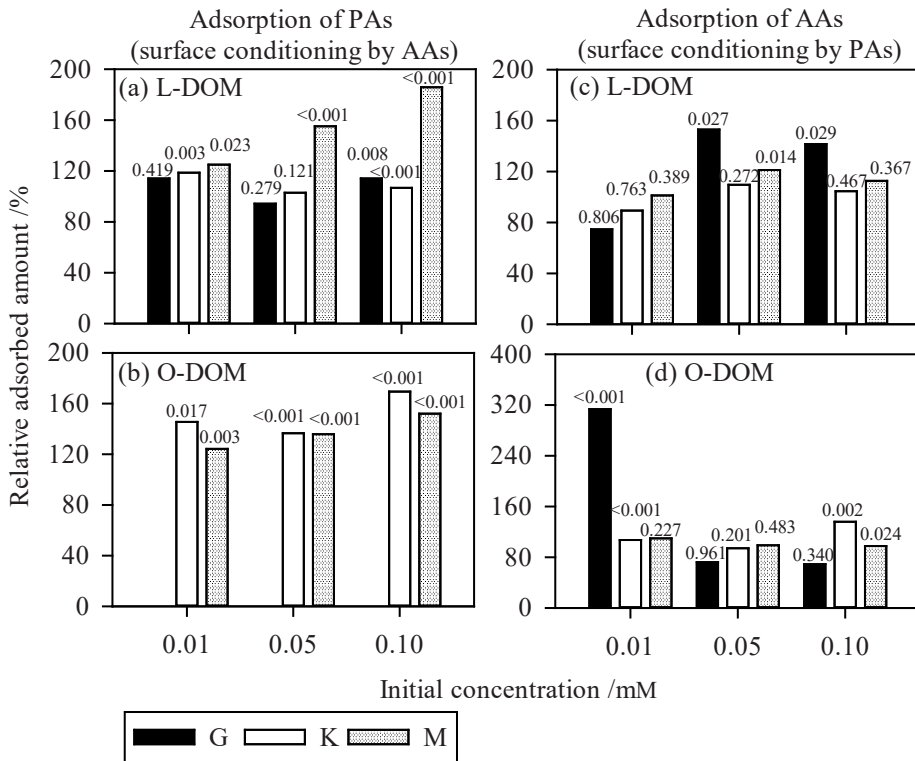


Figure 5.4 Effects of surface conditioning on the adsorption of: (a) PAs on coated minerals with L-DOM, (b) PAs on coated minerals with O-DOM, (c) AAs on coated minerals with L-DOM and (d) AAs on coated minerals with O-DOM. Dotted lines refer to the reference values (control experiments). The results are presented as mean values ($n = 3$). P value above each column is from the analysis of variance of the absolute adsorption results and it indicates the significance of the difference compared with the corresponding reference. The adsorption of PAs on O-goethite (b) is not displayed because the values of the reference are zero. G, goethite; K, kaolinite; M, montmorillonite.

montmorillonite less DOM can be bound due to the limited number of positively charged sites (protonated hydroxyls) existing on the edges of phyllosilicates in slightly acidic conditions (Tombácz *et al.*, 2004; Zhao *et al.*, 2008; Barré *et al.*, 2014). Furthermore, the positively charged functional groups (e.g. protonation of amino groups) of DOM allow binding to negatively charged sites of the minerals. However, these compounds are scarce in natural DOM solution (Kalbitz *et al.*, 2003). The relatively higher adsorption of DOM on kaolinite than on

montmorillonite (Figure 5.1) could be attributed to larger pore volume and size (Table 5.1). A positive relationship between the associated OC with Fe oxide and the average pore radius was proved by Mikutta *et al.* (2014). Another reason was possibly the massive uncharged and hydrophobic regions on kaolinite surface, which attract strongly hydrophobic moieties of DOM (Sposito, 2008). A consistent increase of equilibrium solution pH after DOM adsorption was observed for all combinations of DOM and minerals (Figure C7, Appendix), hinting to ligand exchange of DOM with hydroxyl groups of mineral surface as an important binding mechanism (Murphy *et al.*, 1990; Chorover & Amistadi, 2001; Polubesova *et al.*, 2008; Zhang *et al.*, 2012).

The SSA was a poor predictor of DOM adsorption to different minerals. Montmorillonite had the highest SSA, but the lowest degree of adsorption for both types of DOM, and kaolinite adsorbed more DOM than montmorillonite in spite of its smaller SSA (Figure 5.1 and Table 5.1). These observations possibly further highlighted the significance of pore and hydrophobic interactions for kaolinite. The literature does not give a consistent picture related to differences in adsorption of DOM on different phyllosilicates (Feng *et al.*, 2005; Saidy, *et al.*, 2013; Wang & Xing, 2005; Saidy *et al.*, 2013). The same increasing order of TPV and DOM adsorption for the different minerals (Table 5.1) highlights the potential role of TPV in predicting adsorption potential of DOM on minerals.

Higher adsorption of O-DOM relative to L-DOM was observed for goethite (Figure 5.1 and Table C6). Extracts from the forest floor litter (O-DOM) typically contain more aromatic compounds in comparison to leaf litter (Kalbitz *et al.*, 2003; Hansson *et al.*, 2010; Klotzbücher *et al.*, 2013), as also confirmed by the specific UV absorbance at 280 nm (Figure C6, Appendix). Many studies have shown the preferential adsorption of aromatic compounds to mineral surfaces (Kaiser & Guggenberger, 2000; Kalbitz *et al.*, 2005; Kothawala *et al.*, 2012). Dissolved OM from O horizon is expected to have higher negative charges than that from leaf litter due to oxidative changes during litter decomposition, as reflected by the more acidic water extract for the former (pH 4.4). This enrichment of negative charge promotes their binding on positively charged surfaces (e.g. goethite) and thus underpins the observed stronger decrease in the ζ potential after adsorption of O-DOM on goethite in comparison to L-DOM (Table 5.1). However, changes in the specific UV absorbance do not confirm a preferential adsorption of aromatic compounds for the adsorption cases of O-DOM on goethite and kaolinite (Figure C6, Appendix). Aliphatic fractions and nitrogenous components might adsorb preferentially as well according to Wang & Xing (2005) and Aufdenkampe *et al.* (2001).

5.4.2 Effects of OM coatings on the adsorption of PAs and AAs on minerals

The binding of OM reversed the surface charge of goethite from positive to negative and increased the negative charge of the phyllosilicates (Table 5.1). This is in agreement with findings from other studies (Davis, 1982; Ramos & McBride, 1996; Zhuang & Yu, 2002; Tombácz *et al.*, 2004). The development towards larger negative charges upon DOM adsorption can result in more homogeneous adsorption behaviour of the different soil minerals towards PAs and AAs (Davis, 1982; Sposito, 2008).

5.4.2.1 Phenolic acids

The increase in negative surface charge by OM coating is likely to be the most important reason for the observed reduced adsorption of the negatively charged PAs via enhancing the repulsion effects. This is supported by the fact that the strongest changes in surface charge coincided with the largest decrease in PAs adsorption (goethite) and that the O-DOM with a larger negative charge had a stronger effect than L-DOM with a smaller negative charge (Table 5.1 and Figure 5.2). The combination of both, a more negative charge of DOM (O-DOM) and a strong increase in surface negative charge for goethite deriving from coating by O-DOM, even resulted in a complete suppression of PAs adsorption (Figure 5.2b). This was unexpected as the OM loading of the mineral surface was just about 50% of the adsorption capacity (Table 5.1). On the other hand, when DOM molecular is adsorbed on mineral surfaces, the hydrophilic portions associate directly with mineral surface and the hydrophobic portions are exposed outwards (Kleber *et al.*, 2007). This would result in mineral surfaces with strong hydrophobicity thus preventing adsorption of polar organic compounds. These results suggest that the overall charge characteristics are more important for adsorption of PAs than the theoretical number of available adsorption sites. We can only speculate whether new mineral surfaces are still available after saturation of 50% of the adsorption capacity. Our results most likely indicate that PAs were still primarily attached to the adsorption sites of the mineral surface not yet occupied by DOM, but the bonds were weaker as indicated by a larger desorption in comparison to pure minerals (Gao *et al.*, 2017 and Table C4). The association of PAs with adsorbed OM might occur through polar- π interactions (Keiluweit & Kleber, 2009), but its contribution should be negligible. Therefore, metal (hydr)oxides play a dominant role in the adsorption of PAs rather than organic components (Huang *et al.*, 1977; Cecchi

et al., 2004). Regardless of the exact mechanism involved, our results clearly show that OM coatings have a distinctly different effect on the adsorption of PAs on mineral surfaces than for non-polar organic compounds of which the adsorption is proposed to be enhanced by such coatings (Murphy *et al.*, 1990; Wang *et al.*, 2008; Polubesova *et al.*, 2009).

5.4.2.2 Amino acids

The effects of OM coatings on the adsorption of AAs were found to mainly depend on the changes in surface charges of the minerals and the charge characteristics of the AAs. This explains why we found opposite effects on adsorption for the basic Lys and the acidic Glu. Increasing negative charge by the OM coating is most likely responsible for the increased adsorption of Lys on all minerals (Figure C12, Appendix) and decreased adsorption or no adsorption at all of Glu on L- and O-kaolinite and O-goethite (Figure C11, Appendix). The large negative charge of montmorillonite most likely caused the lack of any adsorption of Glu on this mineral independent of adsorbed OM. The small changes in adsorption of Glu on L-goethite might be related to low adsorption of this type of DOM (i.e., low surface coverage) having a lower negative charge than O-DOM (Table 5.1 and Figure 5.1). The slightly increased adsorption of neutral AAs (Leu and Phe) on L-goethite which were not adsorbed to pure and O-DOM-coated goethite illustrates the importance of surface charge which was closest to zero at the surface of the L-goethite (Table 5.1). Our results thus underline the importance of soil OM for the adsorption of AAs, especially for basic and neutral ones. Many studies also reported natural soil and sediments possessed much higher adsorption capacity for basic AAs (Lys) than acidic (Glu) and neutral ones, e.g. leucine, glycine and alanine (Henrichs & Sugai, 1993; Wang & Lee, 1993; Jones & Hodge, 1999; Liu & Lee, 2007). Mikutta *et al.* (2010) showed stronger association (higher abundance) of acidic AAs with metal-organic precipitates and variable-charge minerals obtained via separating bulk soil samples. Based on these results, we propose that soil OM and negatively charged minerals contribute to the immobilization of basic AAs, while the retention of acidic AAs is primarily controlled by soil minerals with positive charges, i.e. oxides and hydroxides. This rationale would underpin the varied dynamics and distribution pattern of PAs and AAs across soil profiles characterized by large differences in soil OM contents between top and sub soil horizons. The low desorbability of AAs bound to OM-coated mineral surfaces (Table C4, Appendix) possibly hints to the formation of stable inner sphere complexes particularly between Lys and adsorbed OM via interaction between

protonated amino groups of AAs and carboxyl or hydroxyl groups of adsorbed OM rather than electrostatic interaction and outer sphere complexes. This need to be verified by further study considering the relatively short period of time (2 hours) for the desorption process.

5.4.3 Competitive adsorption of PAs and AAs on OM-coated minerals

According to the results of Gao *et al.* (2017), PAs and AAs compete for adsorption sites on mineral surface with larger competitiveness of AAs compared to PAs resulting in smaller adsorption of PAs under competitive conditions (in slightly acidic condition). The authors explained the larger competitiveness of AAs than PAs (mainly Sal as the predominant adsorbed PA) by the different number of bonds between the organic acid and the mineral surface. Bidentate complexes between Sal and mineral surfaces require two adjacent adsorption sites (Yost *et al.*, 1990; Kubicki *et al.*, 1997), while the tested AAs probably need only one binding site at the mineral surface (Kitadai *et al.*, 2009; Yang *et al.*, 2016). Taking into account the less favourable conditions for adsorption of PAs on organically coated mineral surfaces (Figure 5.2a and b), the slightly decreased adsorption of PAs under competitive conditions (Figure 5.3a and b) seems to be reasonable. The enhanced adsorption of PAs on O-kaolinite in the presence of AAs contradicts the trend of decreased adsorption observed for PAs alone, and could be attributed to the surface conditioning by AAs, which promoted the adsorption of PAs (Figure 5.4b).

However, the hypothesized larger competitiveness of AAs than PAs on OM-coated minerals must be refuted based on our results. In contrast to pure minerals (Gao *et al.*, 2017), competition between PAs and AAs resulted in a reduced adsorption of AAs to mineral surfaces coated with OM, except for O-goethite and O-kaolinite (Figure 5.3). The reduction in adsorption was even larger for AAs than for PAs. The strongest decrease in the adsorption of AAs (i.e. Glu) under competition with PAs (i.e., Sal) was observed for L-goethite, where we found the strongest increase in adsorption of AAs induced by the OM coating in absence of PAs (Figure 5.2c). In turn, the largest increase in adsorption of AAs under competition with PAs coincided with high abundance of O-DOM coatings (O-goethite; Figure 5.2d). Therefore, we can conclude that coating the mineral surfaces with DOM changes the competition between different organic components for adsorption sites and the competitive strength of AAs disappears. It seems that the coating of the mineral surface is

quantitatively more important for adsorption than competition between single molecules.

5.4.4 Adsorption of PAs and AAs on OM-coated minerals with surface conditioning by AAs and PAs

Surface conditioning by AAs generally enhanced the adsorption of PAs on all OM-coated minerals, except partly (some concentrations) for L-goethite and L-kaolinite (Figure 5.4a and b). This is in accordance with the results for pure minerals (Gao *et al.*, 2017) and supports the conceptual model of Kleber *et al.* (2007) proposing that N-rich organic material bound on mineral surfaces may offer more reactive binding sites for other organic compounds (e.g. PAs). The strength of the effects seems to be related to the amount of adsorbed AAs, and is larger for phyllosilicates than for Fe oxides. Since PAs are negatively charged in slightly acidic condition, the amino groups of attached AAs could provide additional binding sites for PAs explaining an increased adsorption of PAs (mainly Sal) on O-goethite and O-kaolinite as well (Figure 5.4). Earlier we showed Lys was selectively adsorbed on OM-coated minerals, thus only basic AAs possibly could perform this bridging function.

Surface conditioning by PAs generally had little influence on the adsorption of AAs on OM-coated minerals (Figure 5.4c and d). Obviously, the largely reduced adsorption of PAs on OM-coated minerals in comparison to the pure ones prevented any effect of adsorbed PAs on the subsequent adsorption of AAs.

5.5 Conclusion

This study shows that the adsorption of natural DOM on soil minerals depended highly on both the charge characteristics of mineral surfaces and the composition of natural DOM. DOM adsorption was more strongly related to the total pore volume of soil minerals than to the SSA, to which the link was weak. Organic matter coating on mineral surfaces had remarkable influence on the surface charge properties and the adsorption of PAs and AAs. Coating of various mineral surfaces (goethite, kaolinite and montmorillonite) by natural DOM consistently increased their negative charges and consequently altered the adsorption of PAs and AAs, i.e. promoting adsorption of basic AAs and suppressing the PAs and acidic AAs under slightly acidic conditions. Binding sites on metal oxides not yet occupied by OM (positive charges) were

particularly important for adsorption of PAs and acidic AAs, while the retention of basic AAs was strongly dependent on negative charges of clay minerals and can be further increased by adsorption of DOM. The binding of basic AAs as Lys was particularly strong on OM-coated mineral surfaces. These stable bonds of adsorbed Lys on OM-coated mineral surface resulted in an enhanced adsorption of PAs thus providing indirect evidence for the multilayer model. The amount and composition of the OM coatings on mineral surfaces were quantitatively more important for adsorption of PAs and AAs than the competition between single molecules or effects of surface conditioning by the other class of compounds. Future studies should focus on direct evidence of the formation of a multilayer structure and the functions of specific compound classes using molecular spectroscopy (e.g. infrared or X-ray photoelectron spectroscopy) and modelling approaches.

Chapter 6

Synthesis

In this synthesis the findings of the overall research are compiled and interpreted within the context of the adsorptive interaction between soil minerals and natural organic compounds. In addition, efforts are devoted to linking the findings of this study to the multilayer conceptual model of mineral–organic associations (MOAs; Kleber *et al.*, 2007).

6.1 Analytical methods to measure free amino acids from soils

To test the conceptual multilayer model of MOAs using well defined phenolic acids (PAs) and amino acids (AAs), a first step was to obtain reliable analytical methods. For PAs, the quantification can be readily achieved by traditional HPLC coupled with ultraviolet (UV) detector. The situation is more complicated for AAs. Amino acids are zwitterionic compounds and lack specific chromophores for UV or fluorescence detection, thus derivatization is required in the traditional approaches to achieve clear separation of individual AAs and a high sensitivity (Kielland, 1995; Inagaki *et al.*, 2010; Sarazin *et al.*, 2011). However, these approaches suffer from low efficiency, poor reproducibility and lack of analyte specificity (Langrock *et al.*, 2006; Kaspar *et al.*, 2009). Although, direct analysis of underivatized AAs has been achieved by using capillary electrophoresis (CE) coupled with mass spectrometry (MS; Desiderio *et al.*, 2010) and ion-pairing liquid chromatography (LC) coupled with MS (Armstrong *et al.*, 2007; Le *et al.*, 2014), clear drawbacks still affect their application such as low throughput, reagents-induced retention time shift and contamination of reagents (Liu *et al.*, 2008; Kaspar *et al.*, 2009).

Previous research has demonstrated that hydrophilic interaction liquid chromatography (HILIC) coupled with MS is a reliable technique in measuring AAs without derivatization in various materials (Dell'mour *et al.*, 2010; Jandera, 2011; Buszewski & Noga, 2012; Guo *et al.*, 2013). However, the applicability of this technique in detecting free AAs from soils was unknown. Purification is often compulsory to eliminate the strong matrix effects. Moreover, the free AAs in soil extracts are generally present in concentrations lower than the detection limit. To overcome these issues, we developed a HILIC technique coupled with solid phase extraction (SPE) to quantify 20 free AAs extracted from soils (**chapter 3**). The method yielded good separation and accurate determination of 20 AAs without derivatization. Its applicability was validated by analysing the AAs extracted from 10 different soils spanning a wide range of matrix composition. The varied adsorption and desorption behaviour of AAs on SPE cartridge indicated the adsorptive immobilization of AAs in soils is controlled by

their specific properties. It is reasonable to separate the common soil AAs into three groups, i.e. acidic, basic and neutral, due to the analogous SPE recovery for each group. These laid the foundation for the rest of this study.

Our work greatly improved the previous SPE approach of Dell'mour *et al.* (2010) by including more natural AAs and increased the accuracies in quantifying free AAs from soils by using multiple H-labelled internal standards. Furthermore, this cost-efficient technique has promising application for the routine analysis of complex samples in soil and aquatic science. Apparently, more research is needed to address the difficulties in quantifying cysteine, Arg and Met. Cysteine was excluded in this study due to the poor peak shape. We observed the recovery of Arg and Met was affected strongly by the composition of soil, which blocks the application of the technique. More research is needed to address these issues. Finally, the method we developed also has potential to analyse amino sugars together with AAs.

6.2 Adsorption of PAs and AAs on pure minerals

With respect to the adsorption of AAs and PAs on soil minerals in the context of the multilayer model, until now the effects of interaction between these two groups of compounds were unclear. Some studies found a high affinity of carboxylated phenolic compounds to bulk soils and minerals (Kaiser & Guggenberger, 2000; Kalbitz *et al.*, 2005; Chefetz *et al.*, 2011), whereas other evidence supports a preferential retention of N-containing compounds (Kleber *et al.*, 2007). It was thus unclear whether PAs are preferentially adsorbed with respect to AAs or *vice versa*. In **chapters 4 and 5**, our results showed preferential adsorption of specific PAs and AAs on soil minerals. Compared with Syr, Fer and Van, Sal was adsorbed preferentially on mineral surfaces irrespective of the types of minerals. For AAs (Glu, Lys, Leu and Phe), acidic AA (Glu) was adsorbed preferentially on goethite while basic AA (Lys) on phyllosilicates (kaolinite and montmorillonite). For different minerals, larger total adsorption of PAs was observed on goethite than phyllosilicates, while the phyllosilicates were better adsorbent for AAs than goethite. This pattern remained the same when the PAs and AAs were present together. However, the adsorption of PAs (i.e. mainly Sal) on goethite and montmorillonite was partially suppressed in presence of AAs at intermediate and high initial concentrations. These results indicate the overall adsorption pattern of PAs and AAs depends strongly on the type of mineral and adsorbate properties, which is not affected by the competition between PAs and AAs.

Moreover, we observed AAs were more competitive than PAs in binding on mineral surfaces such as goethite and montmorillonite, and surface conditioning with AAs enhanced the adsorption of PAs. These results illustrate the important role of free acidic and basic AAs for surface conditioning in relation to adsorption and probably stabilization of SOM by soil minerals, irrespective of the surface charges of the mineral. Our results also showed that aromatic structures in PAs can enhance the adsorption of AAs and probably of other organic components, independently of net charge characteristics. The PAs resulted in a larger increase in the adsorption of AAs than AAs did for PAs. These findings improved our understanding of the adsorptive process of natural organic compounds on mineral surfaces by mimicking the complex composition of the organic material and the mineral phase. The adsorption of one class of SOM components might alter the adsorption, and potential preservation, of other classes. Thus, we assume that the cycling of different components of SOM possibly affect each other. Nevertheless, the true molecular-scale arrangements of individual compounds on mineral surfaces are still unknown. Elucidation of such arrangements could be achieved by nanoscale spectroscopy (e.g. synchrotron-based mass spectrometry or X-ray photoelectron spectroscopy) and quantum chemical modelling approaches. We also recommend further batch adsorption experiments to assess possible altered adsorption site availabilities induced by mineral dispersion.

6.3 Adsorption of PAs and AAs on OM-coated minerals

Organic matter coating on mineral surfaces can alter the surface properties and thus the remaining adsorption and stabilization capacity of the mineral phase (Sanderman *et al.*, 2008; Kaiser & Kalbitz, 2012). However, the effects of these changes induced by OM coating on the adsorption of AAs and PAs were not well understood. In **chapter 5**, we observed the coating of OM reversed the surface charge of goethite from positive to negative and increased the negative charge of the phyllosilicates. Moreover, the O-DOM (from the O horizon) with a larger negative charge had a stronger effect than L-DOM (from forest leaf litter) with a smaller negative charge. These results support the observations that natural DOM coating reduced the adsorption of PAs and the acidic AA (Glu), but enhanced the adsorption of the basic AA (Lys). This trend proved consistent for all minerals (goethite, kaolinite and montmorillonite). These results further support the observation that the strongest changes in surface charge coincided with the largest decrease in PAs adsorption (goethite). Thus, we proposed that

the effect of DOM coating on the adsorption of PAs and AAs is strongly dependent on the amount and composition of adsorbed OM. Our results support the conclusion that metal (hydr)oxides play a dominant role in the adsorption of PAs rather than organic components (Huang *et al.*, 1977; Cecchi *et al.*, 2004). By contrast, soil OM and negatively charged minerals contribute to the immobilization of basic AAs, while the retention of acidic AAs is primarily controlled by soil minerals with positive charges, i.e. oxides and hydroxides.

Furthermore, we found DOM coating changed the adsorption behaviour of PAs and AAs under competition. Competition between AAs and PAs generally suppressed the adsorption of AAs on OM-coated minerals, while it had little influence on the adsorption of PAs. The strong bonds between AAs and DOM-coated minerals resulted in generally enhanced adsorption of PAs with surface conditioning by AAs. This is in accordance with the results for pure minerals. These results indicate that N-rich organic material bound on mineral surfaces may offer more reactive binding sites for other organic compounds. We found Lys was selectively adsorbed on OM-coated minerals, thus only basic AAs possibly could perform this bridging function. This provides indirect evidence for the multilayer model of MOAs (Kleber *et al.*, 2007). These results demonstrated that the amount and composition of the OM coating on mineral surfaces were more important for adsorption of PAs and AAs than the competition between single molecules. They also support the strong influence of OM coating on the properties of mineral phase and the cycling of fresh SOM. The turnover of carboxylated aromatic compounds and acidic AAs in OM-rich soils could be faster than that in mineral soils. Conversely, the accumulation of OM can enhance the residence time of basic AAs in soils. These results highlight the controlling role of surface adsorbed OM in the cycling of fresh SOM and indicate that labile organic compounds can also possess long residence time. Future studies should focus on clarifying the mechanisms involved in the adsorptive interaction between organic compounds and mineral phase, and between free and bound organic compounds on mineral surfaces. More research is needed to visualize the spatial structure of associated OM using molecular spectroscopy techniques.

6.4 Implication for and assessment of the multilayer model

In **chapter 2**, we summarized the applicability and validity of the conceptual multilayer model of Kleber *et al.* (2007). This model suggests that the associated OM on mineral surfaces is arranged in a discrete zonal structure

(Figure 1.1, **chapter 1**) consisting of the following three zones: (1) the polar functional groups of organic compounds interact with mineral hydroxyls via ligand exchange to form the contact zone, or form association via electrostatic force; (2) an entropically driven membrane-like bilayer structure is developed via hydrophobic interacting with other amphiphilic compounds, forming the so-called hydrophobic zone and exposing the hydrophilic portions towards aqueous solution, and (3) more organic compounds possibly interact with the hydrophilic moieties in the hydrophobic zone via cation bridging, hydrogen bonding and other interactions to form an outer region (kinetic zone).

The multilayer model has been extensively used to underpin experimental observations and develop new theory in soil science and related fields across various spatial and temporal scales. However, to date, the hypothesized multilayer structure and its coupled interaction between different types and classes of molecules that together constitute SOM still lack rigorous testing. In fact, many of the experimental findings can be explained by simpler explanations instead of the multilayer model, like aggregation effects for the storage of SOM and differences in the availability of reactive mineral surfaces for the positive relationship between SOC content and the content of specific minerals.

Although a patchy distribution of associated OM on mineral surfaces was proved recently by analysing the surface elemental composition of soil particle (Vogel *et al.*, 2014; Hatton *et al.*, 2015), its existence cannot be treated as direct evidence for the multilayer model. The significance of proteinaceous compounds has often been overestimated and misused in literature. The current evidence does not support the idea that N-rich organic compounds are generally enriched on mineral surfaces by preferential adsorption. The enrichment of N could depend on mineral surfaces. To date, it is still challenging to directly visualise the spatial organization of associated OM on mineral surfaces at the molecular scale and unravel the mechanisms involved due to the heterogeneous SOC forms and mineral composition and the lack of suitable analytical techniques (Lehmann *et al.*, 2008; Liu *et al.*, 2013). Some state-of-the-art techniques have great potential to address these issues, including XPS depth profiling, NanoSIMS and STXM-NEXAFS. However, many challenges still affect their performance. Thus, more work is needed to improve the feasibility and reliability of these techniques regarding the spatial resolution, sample preparation, control of radiation damage and spectral quantification (Lehmann & Solomon, 2010). Our results as described in **chapter 5**, provide indirect evidence for the multilayer structure of the associated organic compounds, i.e.

that the adsorption of basic AAs can be enhanced by OM coating on mineral surfaces and OM-coated minerals generally resulted in enhanced adsorption of PAs with surface conditioning by AAs. Integrating nanoscale spectroscopy into batch adsorption experiments is required in the future research to clarify the adsorption mechanisms and spatial organization of well-defined organic compounds on mineral surfaces.

6.5 Conclusions

This thesis provides an analytical method to quantify free AAs in soils and increased our understanding of the adsorptive protection and cycling of PAs and AAs in soils. Our findings highlight the controlling role of surface adsorbed OM in the cycling of fresh SOM and indicate that labile organic compounds can also possess long residence time. Thus it provides new, direct evidence that adsorptive interaction with mineral phase should be perceived as an important factor in the cycling of SOM. Moreover, our results demonstrated that the cycling of different components of SOM can affect each other via competitive or sequential adsorption on mineral phase. The direct and reliable experimental evidence for the multilayer conceptual model is still missing. Indirect evidence was showed in this research. The role of proteinaceous compounds in the formation of MOAs was generally overestimated and misused. The enrichment of N-rich OM on mineral surfaces possibly depends on types of minerals. The patchy distribution of adsorbed OM and enrichment of N-rich organic compounds on mineral surfaces cannot be used as direct evidence of the multilayer model. Therefore, we suggest being more cautious in applying this multilayer model.

Appendices

Appendix (A) to Chapter 3

Table A1 Composition of mobile phase with different buffer concentration.

Buffer concentration (mM)	Solvent A	Solvent B
2 (3.05) ^a	100% H ₂ O, 2 mM NH ₄ HCO ₂ , 0.03% FA	90% ACN, 10% H ₂ O, 2 mM NH ₄ HCO ₂ , 0.03% FA
4 (3.02)	100% H ₂ O, 4 mM NH ₄ HCO ₂ , 0.06% FA	90% ACN, 10% H ₂ O, 4 mM NH ₄ HCO ₂ , 0.06% FA
6 (3.04)	100% H ₂ O, 6 mM NH ₄ HCO ₂ , 0.09% FA	90% ACN, 10% H ₂ O, 6 mM NH ₄ HCO ₂ , 0.09% FA
8 (3.03)	100% H ₂ O, 8 mM NH ₄ HCO ₂ , 0.12% FA	90% ACN, 10% H ₂ O, 8 mM NH ₄ HCO ₂ , 0.12% FA
10 (3.00)	100% H ₂ O, 10 mM NH ₄ HCO ₂ , 0.15% FA	90% ACN, 10% H ₂ O, 10 mM NH ₄ HCO ₂ , 0.15% FA

^a Measured pH value of the solvent A was in the parenthesis.

Table A2 Composition of mobile phase with different pH.

pH value	Solvent A	Solvent B
3 (3.00) ^a	100% H ₂ O, 10 mM NH ₄ HCO ₂ , 0.15% FA	90% ACN, 10% H ₂ O, 10 mM NH ₄ HCO ₂ , 0.15% FA
5 (4.92)	100% H ₂ O, 10 mM NH ₄ OAc, 0.02% AcOH	90% ACN, 10% H ₂ O, 10 mM NH ₄ OAc, 0.02% AcOH
7 (6.60)	100% H ₂ O, 10 mM NH ₄ OAc	90% ACN, 10% H ₂ O, 10 mM NH ₄ OAc
9 (8.92)	100% H ₂ O, 10 mM NH ₄ OAc, 0.04% NH ₄ OH	90% ACN, 10% H ₂ O, 10 mM NH ₄ OAc, 0.04% NH ₄ OH

^a Measured pH value of the solvent A was in the parenthesis.

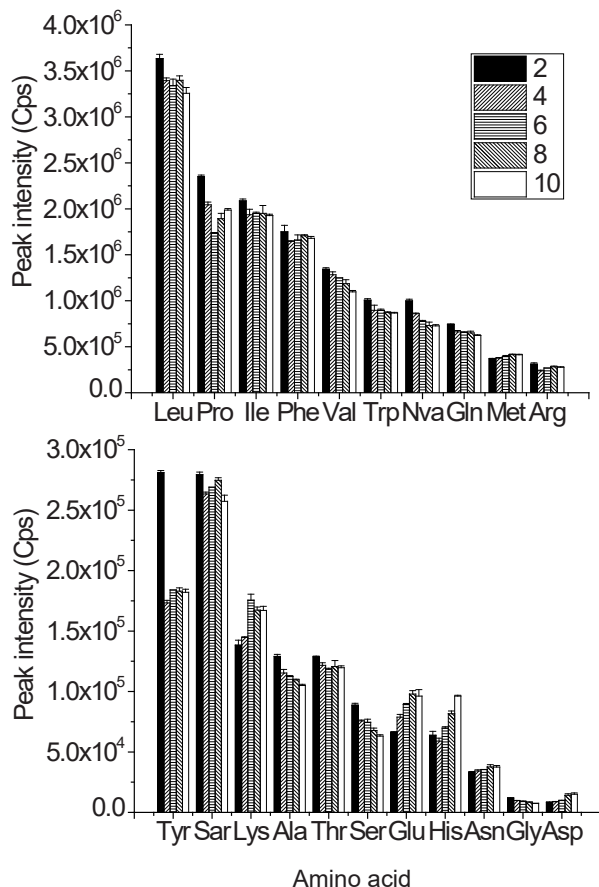


Figure A1 Influence of buffer concentration (mM) on peak intensity of the targeted amino acids. A standard mixture ($2.5 \mu\text{g ml}^{-1}$ for Asp and Gly, $0.5 \mu\text{g ml}^{-1}$ for the rest) was repeatedly injected under different mobile phase within around 10 hours to obtain the chromatograms. The composition of the mobile phase was presented in Table A1. The gradient method was 94–89% B from 0 to 6 minutes, 89–78% B from 6 to 10 minutes, 78–67% B from 10 to 12 minutes, constant 67% B from 12 to 13 minutes. The results are showed as average with standard deviation ($n = 3$).

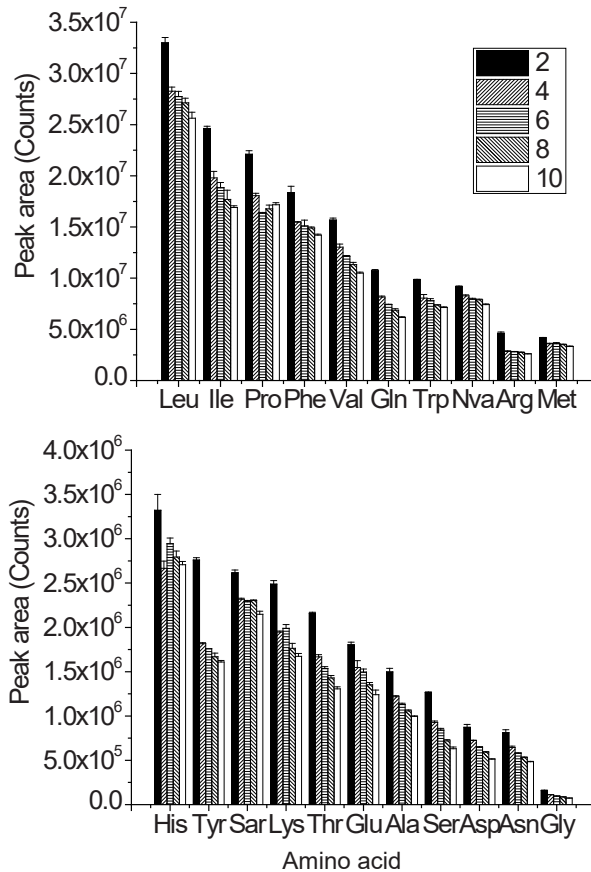


Figure A2 Influence of buffer concentration (mM) on peak area of the targeted amino acids. A standard mixture ($2.5 \mu\text{g ml}^{-1}$ for Asp and Gly, $0.5 \mu\text{g ml}^{-1}$ for the rest) was repeatedly injected under different mobile phase within around 10 hours to obtain the chromatograms. The composition of the mobile phase was presented in Table A1. The gradient method was 94–89% B from 0 to 6 minutes, 89–78% B from 6 to 10 minutes, 78–67% B from 10 to 12 minutes, constant 67% B from 12 to 13 minutes. The results are showed as average with standard deviation ($n = 3$).

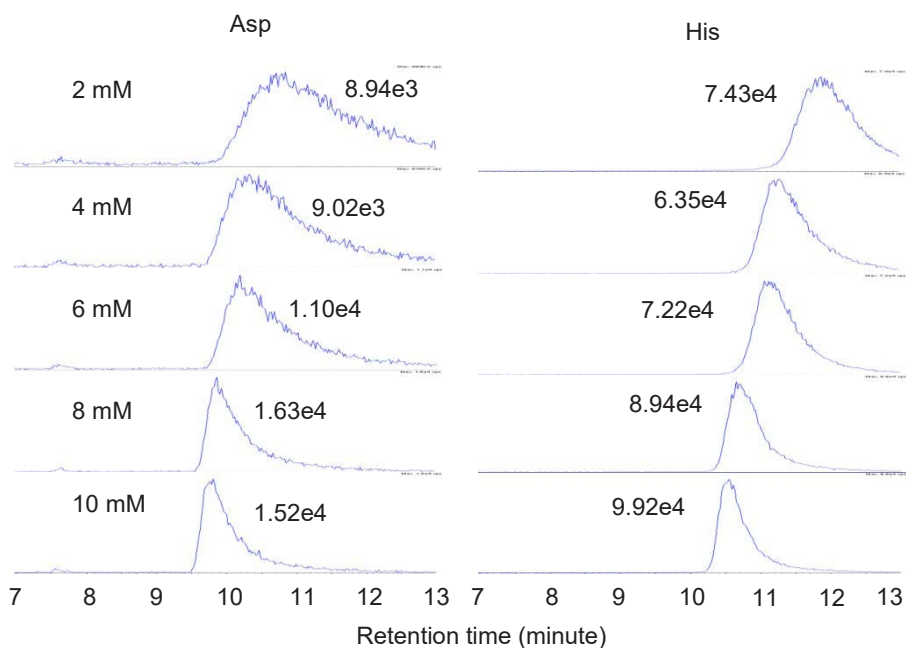


Figure A3 Extracted chromatograms of Asp and His (labelled with peak intensity in cps) under different buffer concentration in mobile phase obtained from standard mixture ($0.5 \mu\text{g ml}^{-1}$ for His and $2.5 \mu\text{g ml}^{-1}$ for Asp). The composition of the mobile phase were presented in Table A1. The gradient method was 94–89% B from 0 to 6 minutes, 89–78% B from 6 to 10 minutes, 78–67% B from 10 to 12 minutes, constant 67% B from 12 to 13 minutes.

Table A3 Eluted percentage of 20 amino acids in pure water and soil extracts for three consecutive elution steps with varied eluent pH through SPE procedure ($n = 3$).

Analyte	Eluent pH (%NH ₄ OH) ^a	H ₂ O	Soil 1	Soil 2	Soil 3
Trp	1.25	99	94	87	92
	3.75	1	5	11	6
	7.5	0	1	2	2
Phe	1.25	99	97	94	96
	3.75	1	2	4	3
	7.5	0	1	1	1
Leu	1.25	99	98	96	98
	3.75	1	1	3	2
	7.5	0	1	1	1
Ile	1.25	99	98	96	97
	3.75	1	2	3	2
	7.5	0	1	1	1
Met	1.25	100	100	100	100
	3.75	0	0	0	0
	7.5	0	0	0	0
Val	1.25	99	98	98	98
	3.75	0	1	2	1
	7.5	0	0	0	1
Pro	1.25	100	98	98	99
	3.75	0	1	2	1
	7.5	0	0	1	1
Tyr	1.25	100	97	97	98
	3.75	0	2	3	2
	7.5	0	1	0	0
Sar	1.25	98	97	98	98
	3.75	1	1	1	1
	7.5	1	1	1	1
Ala	1.25	100	99	98	99
	3.75	0	1	1	0
	7.5	0	0	1	0

(continued)

Table A3 Eluted percentage of 20 amino acids in pure water and soil extracts for three consecutive elution steps with varied eluent pH through SPE procedure ($n = 3$) (continued).

Analyte	Eluent pH (%NH ₄ OH) ^a	H ₂ O	Soil 1	Soil 2	Soil 3
Thr	1.25	100	98	97	99
	3.75	0	1	2	1
	7.5	0	0	1	0
Gly	1.25	100	100	100	100
	3.75	0	0	0	0
	7.5	0	0	0	0
Gln	1.25	100	99	98	99
	3.75	0	1	2	1
	7.5	0	0	0	0
Ser	1.25	100	96	94	97
	3.75	0	2	3	1
	7.5	0	2	2	1
Asn	1.25	100	100	100	100
	3.75	0	0	0	0
	7.5	0	0	0	0
Glu	1.25	100	100	95	95
	3.75	0	0	5	4
	7.5	0	0	0	1
Asp	1.25	100	100	100	100
	3.75	0	0	0	0
	7.5	0	0	0	0
Arg	1.25	1	10	2	2
	3.75	29	14	3	4
	7.5	70	76	95	94
His	1.25	92	83	68	84
	3.75	8	17	32	16
	7.5	0	0	0	0
Lys	1.25	94	91	76	56
	3.75	6	8	24	37
	7.5	0	2	0	7

^a The percentage of NH₄OH in MeOH.

Table A4 Intra-day and inter-day precision of amino acids overall recoveries for soil 3.

Analyte	Intra-day (% , <i>n</i> = 5)			Inter-day (% , <i>n</i> = 3)		
	Mean	STD	RSD	Mean	STD	RSD
Trp	82	2	3	85	3	3
Phe	83	3	3	86	5	6
Leu	80	4	5	85	6	7
Ile	76	3	5	83	9	10
Met	5	0	2	6	1	14
Val	69	3	5	74	7	10
Pro	57	1	1	57	2	4
Tyr	113	2	2	97	14	14
Sar	79	1	2	81	2	2
Ala	98	3	3	96	3	3
Thr	127	2	2	121	6	5
Gly	100	4	4	100	2	2
Gln	85	1	1	86	2	2
Ser	83	2	2	83	1	1
Asn	77	4	5	81	5	6
Glu	108	5	4	112	4	4
Asp	77	4	5	80	3	4
Arg	29	1	3	30	1	3
His	93	1	1	92	4	5
Lys	108	1	1	104	4	4

Table A5 Free amino acids content extracted from soil ($\mu\text{g g}^{-1}$).

Analyte	Soil 1	Soil 2	Soil 3	Soil 4	Soil 5	Soil 6	Soil 7	Soil 8	Soil 9	Soil 10
Trp	19 ± 1	4.6 ± 0.3	34 ± 1	60 ± 4	33 ± 1	244 ± 10	2 ± 0.1	ND	12 ± 1	15 ± 1
Phe	520 ± 15	64 ± 2	453 ± 15	357 ± 16	250 ± 5	1955 ± 64	12.4 ± 0.3	6 ± 0.3	51 ± 2	127 ± 9
Leu	679 ± 22	116 ± 3	934 ± 40	625 ± 17	349 ± 3	2946 ± 97	17.7 ± 0.4	7.9 ± 0.3	84 ± 4	186 ± 13
Ile	360 ± 8	73 ± 4	429 ± 19	290 ± 11	267 ± 6	1208 ± 32	8.8 ± 0.4	4.2 ± 0.2	35 ± 2	107 ± 7
Met	2.1 ± 0.2	1.1 ± 0.1	ND	80 ± 17	22 ± 7	820 ± 23	ND	ND	1.2 ± 0.4	1.2 ± 0.1
Val	374 ± 16	112 ± 2	683 ± 48	433 ± 23	463 ± 8	1528 ± 74	11.9 ± 0.6	3 ± 0.2	60 ± 1	189 ± 13
Pro	526 ± 16	64 ± 6	89 ± 4	197 ± 16	113 ± 8	349 ± 13	ND	ND	24 ± 1	73 ± 7
Tyr	588 ± 26	38 ± 2	155 ± 3	228 ± 16	200 ± 4	944 ± 11	5.3 ± 0.8	ND	54 ± 1	84 ± 1
Sar	93 ± 1	6.8 ± 0.4	13 ± 0	13 ± 0	7.8 ± 0.2	10 ± 0	1.9 ± 0.1	1.6 ± 0.1	3.5 ± 0.2	2.7 ± 0.1
Ala	924 ± 2	288 ± 1	885 ± 38	1005 ± 21	747 ± 6	3106 ± 53	17.4 ± 0.4	10.2 ± 0.3	150 ± 2	304 ± 0

(continued)

Table A5 Free amino acids content extracted from soil^a ($\mu\text{g g}^{-1}$, continued).

Analyte	Soil 1	Soil 2	Soil 3	Soil 4	Soil 5	Soil 6	Soil 7	Soil 8	Soil 9	Soil 10
Thr	512 ± 12	138 ± 2	582 ± 12	541 ± 20	537 ± 8	1832 ± 68	9.7 ± 0.4	5.5 ± 0.4	74 ± 8	139 ± 1
Gly	566 ± 22	293 ± 3	556 ± 25	652 ± 14	1000 ± 11	1193 ± 29	21 ± 2.2	19.2 ± 2.3	147 ± 10	136 ± 10
Gln	103 ± 1	108 ± 6	137 ± 5	296 ± 11	89 ± 4	1735 ± 52	7 ± 0.1	4.9 ± 0.2	436 ± 21	259 ± 7
Ser	597 ± 11	139 ± 5	388 ± 12	483 ± 2	356 ± 5	1470 ± 61	ND	ND	88 ± 17	125 ± 3
Asn	136 ± 9	59 ± 1	171 ± 8	138 ± 4	256 ± 4	1434 ± 94	ND	ND	197 ± 27	150 ± 5
Glu	569 ± 17	205 ± 8	2024 ± 95	3240 ± 63	1405 ± 20	12987 ± 198	53.4 ± 2.6	45.5 ± 2.2	321 ± 3	136 ± 1
Asp	1581 ± 130	193 ± 20	464 ± 43	1068 ± 36	1239 ± 10	1556 ± 97	ND	ND	160 ± 15	109 ± 1
Arg	187 ± 2	77 ± 5	124 ± 2	180 ± 6	264 ± 15	10832 ± 125	6.8 ± 0.2	6.9 ± 0.4	62 ± 3	72 ± 3
His	46 ± 2	ND	16 ± 0	38 ± 2	96 ± 2	227 ± 8	ND	ND	4.6 ± 0.5	4.8 ± 0.5
Lys	252 ± 1	16 ± 1	53 ± 1	55 ± 1	345 ± 4	673 ± 15	5.6 ± 0.8	1.6 ± 0.1	13 ± 1	27 ± 3
sum	8636	1996	8189	9979	8039	47049	181	116	1977	2245

^a The data are presented as means with standard deviation ($n = 3$). ND: not detectable.

Appendix (B) to Chapter 4

Table B1 Summary results of two way analysis of variance (ANOVA) for the adsorption of PAs on different minerals (goethite and montmorillonite) in the control experiment.

Source of variation	Degrees of freedom	Mean square	F ratio	P
Mineral	1	4.568	31503.7	<0.001
Concentration	2	0.926	6386.2	<0.001
Interaction	2	0.084	582.1	<0.001
Residual	12	0.000145		
Total	17	0.388		

Note: the data were transformed using function $Y = \ln(X + 1)$ prior to analysis, X and Y represent the initial and transformed value, respectively.

Table B2 Summary results of two way ANOVA for the adsorption of AAs on different minerals (goethite and montmorillonite) in the control experiment.

Source of Variation	Degrees of freedom	Mean square	F ratio	P
Mineral	1	0.382	176.0	<0.001
Concentration	2	0.363	167.0	<0.001
Interaction	2	0.170	78.5	<0.001
Residual	12	0.00217		
Total	17	0.0867		

Note: the data were transformed using the function $Y = X / (10 - X)$ prior to analysis, X and Y represent the initial and transformed value, respectively.

Table B3 Increase in solution pH after adsorption of PAs and AAs on goethite (G) and montmorillonite (M).

Mineral	Initial concentration /mM	Increase in pH			
		Control	PAs	AAs	PAs & AAs
G	0	0.80 (0.08)	NA	NA	NA
	0.01	NA	0.68 (0.05)	0.64 (0.02)	0.72 (0.04)
	0.05	NA	0.72 (0.02)	0.66 (0.02)	0.75 (0.03)
	0.10	NA	0.73 (0.01)	0.67 (0.01)	0.76 (0.01)
M	0	0.52 (0.02)	NA	NA	NA
	0.01	NA	0.42 (0.02)	0.40 (0.01)	0.42 (0.03)
	0.05	NA	0.44 (0.01)	0.41 (0.02)	0.42 (0.02)
	0.10	NA	0.43 (0.01)	0.40 (0.01)	0.44 (0.01)

Note: the results are presented as mean values with standard deviation ($n = 3$). Control: 10 mM NaN_3 solution. NA: not applicable.

Table B4 Mean values of total adsorption of PAs and AAs on goethite and montmorillonite, respectively, with competition and surface conditioning.

Compounds	Effects	Mineral	IC ^a /mM	Mean ^b / $\mu\text{mol g}^{-1}$	SEM ^c	LSD ^d	
PAs	Comp. ^e	G ^g	0.01	1.86		0.08	0.24
			0.05	4.76			
			0.10	4.77			
		M ^h	0.01	0.28	(0.39)	0.01	0.03
			0.05	0.48	(0.93)		
			0.10	0.54	(1.16)		
	Surf. ^f	G	0.01	2.08		0.09	0.27
			0.05	7.29			
			0.10	10.0			
		M	0.01	2.62	(0.38)	0.03	0.08
			0.05	0.80	(1.26)		
			0.10	0.57	(1.77)		
AAs	Comp.	G	0.01	0.36		0.25	0.77
			0.05	0.65			
			0.10	2.83			
		M	0.01	0.61		0.04	0.12
			0.05	2.86			
			0.10	5.81			
	Surf.	G	0.01	0.66		0.35	1.09
			0.05	2.69			
			0.10	4.05			
		M	0.01	0.40	(0.67)	0.00	0.01
			0.05	0.75	(3.03)		
			0.10	0.87	(6.76)		

^a Initial concentration; ^b Original mean values are presented in the bracket if transformed data are used for ANOVA; ^c Standard error of the transformed mean determined using the residual MS (12 d.f.); ^d Least significant difference, $P < 0.05$; ^e Competition; ^f Surface conditioning; ^g Goethite; ^h Montmorillonite.

Table B5 Summary results of two way ANOVA for effects of competition on the adsorption of PAs on goethite in the competition experiment.

Source of Variation	Degrees of freedom	Mean square	F ratio	P
Competition	1	3.056	164.7	<0.001
Concentration	2	25.11	1353.0	<0.001
Interaction	2	1.561	84.1	<0.001
Residual	12	0.0186		
Total	17	3.330		

Table B6 Summary results of two way ANOVA for effects of competition on the adsorption of AAs on goethite in the competition experiment.

Source of Variation	Degrees of freedom	Mean square	F ratio	P
Competition	1	0.379	2.02	0.181
Concentration	2	5.641	30.09	<0.001
Interaction	2	1.051	5.61	0.019
Residual	12	0.187		
Total	17	0.942		

Table B7 Summary results of two way ANOVA for effects of competition on the adsorption of PAs on montmorillonite in the competition experiment.

Source of Variation	Degrees of freedom	Mean square	F ratio	P
Competition	1	0.0030	11.9	0.005
Concentration	2	0.1280	498.4	<0.001
Interaction	2	0.000542	2.1	0.163
Residual	12	0.000256		
Total	17	0.0154		

Note: the data were transformed using the function $Y = X / (1 + X)$ prior to analysis, X and Y represent the initial and transformed value, respectively.

Table B8 Summary results of two way ANOVA for effects of competition on the adsorption of AAs on montmorillonite in the competition experiment.

Source of Variation	Degrees of freedom	Mean square	<i>F</i> ratio	<i>P</i>
Competition	1	1.611	378.3	<0.001
Concentration	2	32.80	7703.8	<0.001
Interaction	2	0.430	101.1	<0.001
Residual	12	0.00426		
Total	17	4.007		

Table B9 Summary results of two way ANOVA for effects of conditioning by AAs on the adsorption of PAs on goethite in the conditioning experiment.

Source of Variation	Degrees of freedom	Mean square	<i>F</i> ratio	<i>P</i>
Conditioning	1	15.31	644.8	<0.001
Concentration	2	63.31	2666.3	<0.001
Interaction	2	3.685	155.2	<0.001
Residual	12	0.0237		
Total	17	8.799		

Table B10 Summary results of two way ANOVA for effects of conditioning by PAs on the adsorption of AAs on goethite in the conditioning experiment.

Source of Variation	Degrees of freedom	Mean square	<i>F</i> ratio	<i>P</i>
Conditioning	1	9.814	26.16	<0.001
Concentration	2	8.225	21.93	<0.001
Interaction	2	1.727	4.60	0.033
Residual	12	0.375		
Total	17	2.013		

Table B11 Summary results of two way ANOVA for effects of conditioning by AAs on the adsorption of PAs on montmorillonite in the conditioning experiment.

Source of Variation	Degrees of freedom	Mean square	F ratio	P
Conditioning	1	0.024	11.7	0.005
Concentration	2	6.687	3278.7	<0.001
Interaction	2	0.028	13.5	<0.001
Residual	12	0.00204		
Total	17	0.793		

Note: the data were transformed using the reciprocal function prior to analysis.

Table B12 Summary results of two way ANOVA for effects of conditioning by PAs on the adsorption of AAs on montmorillonite in the conditioning experiment.

Source of Variation	Degrees of freedom	Mean square	F ratio	P
Conditioning	1	0.0143	397.0	<0.001
Concentration	2	0.377	10463.2	<0.001
Interaction	2	0.000265	7.3	0.008
Residual	12	0.0000360		
Total	17	0.0453		

Note: the data were transformed using the function $Y = X / (1 + X)$ prior to analysis, X and Y represent the initial and transformed value, respectively.

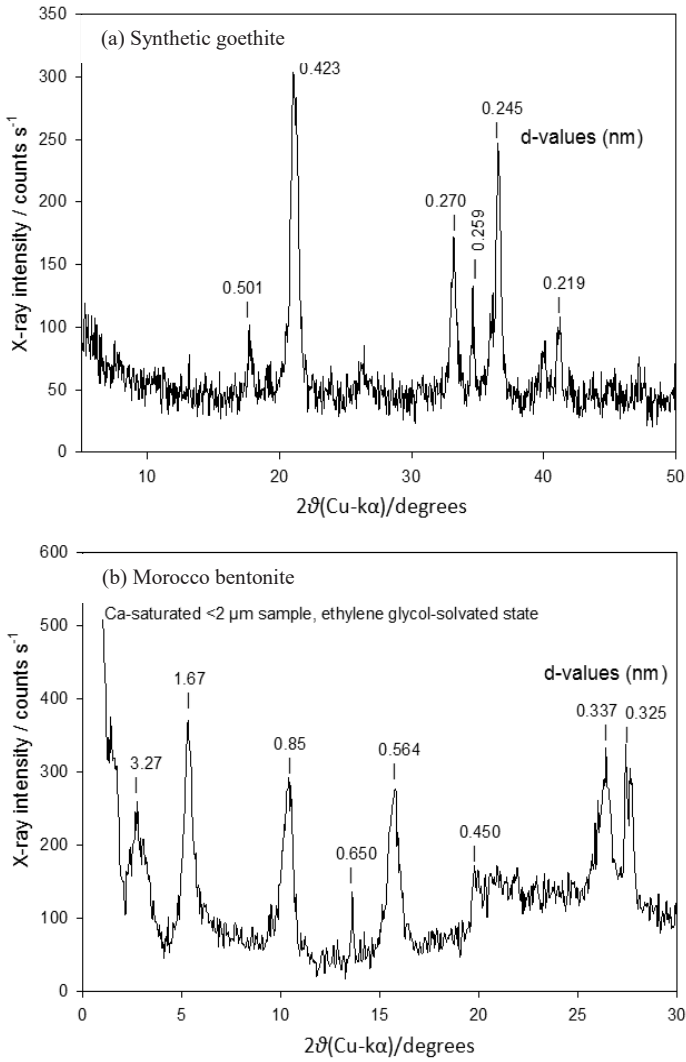


Figure B1 X-ray diffraction patterns of (a) the synthetic goethite and (b) the < 2 μm fraction of Morocco bentonite.

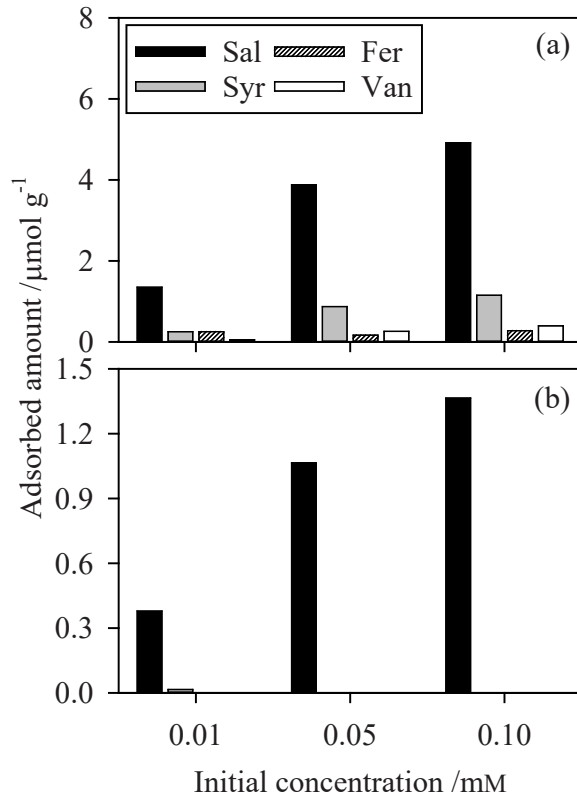


Figure B2 Adsorption of individual PAs (Sal, Syr, Fer and Van) on (a) goethite and (b) montmorillonite in the control experiments. The results are presented as mean values without transformation ($n = 3$). Sal, salicylic acid; Syr, syringic acid; Fer, ferulic acid; Van, vanillic acid.

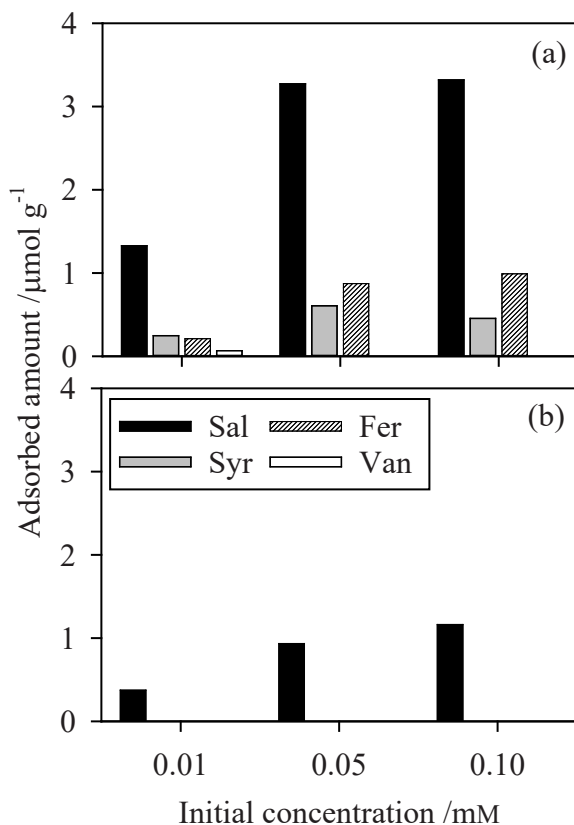


Figure B3 Adsorption of individual PAs (Sal, Syr, Fer and Van) on (a) goethite and (b) montmorillonite in the competition experiment. The results are presented as mean values without transformation ($n = 3$). Sal, salicylic acid; Syr, syringic acid; Fer, ferulic acid; Van, vanillic acid.

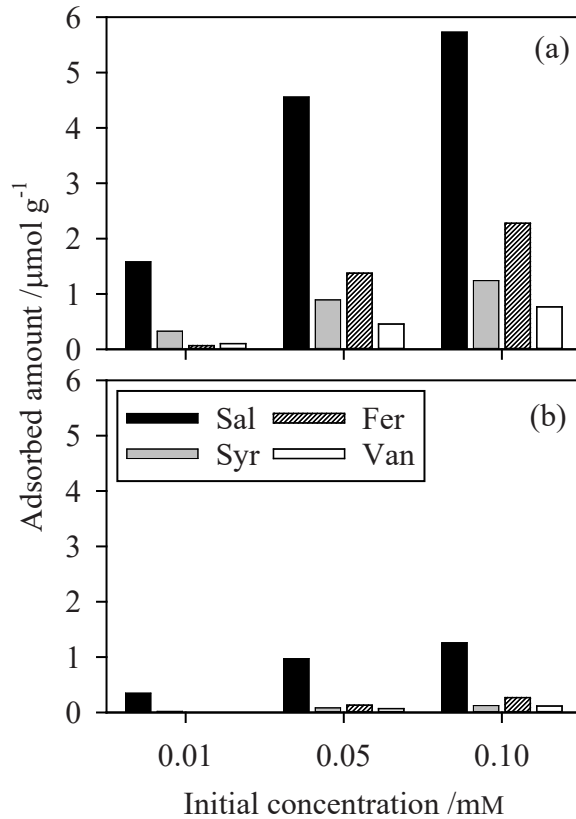


Figure B4 Adsorption of individual PAs (Sal, Syr, Fer and Van) on (a) goethite and (b) montmorillonite after adsorption of AAs. The results are presented as mean values without transformation ($n = 3$). Sal, salicylic acid; Syr, syringic acid; Fer, ferulic acid; Van, vanillic acid.

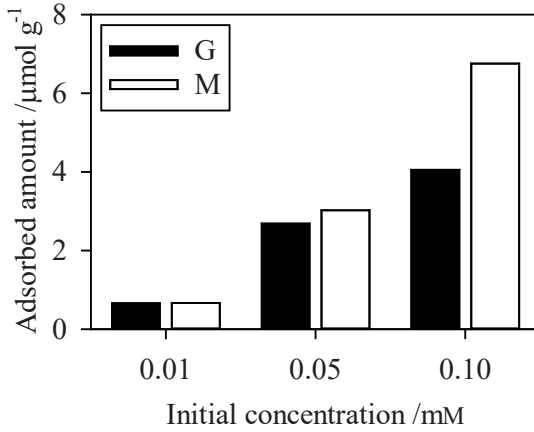


Figure B5 Adsorption of AAs on goethite (G) and montmorillonite (M) after adsorption of PAs. The results are presented as mean values without transformation (SE = 0.321, 12 d.f.). SE: standard error of mean.

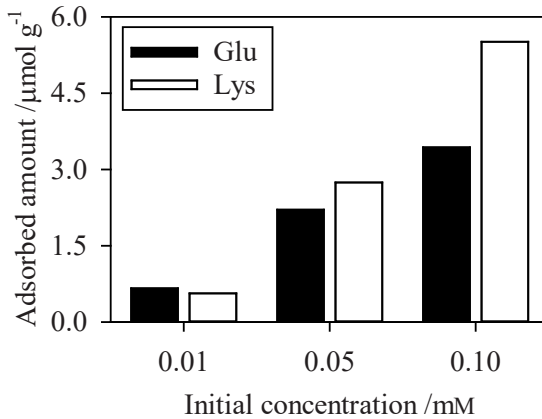


Figure B6 Adsorption of glutamic acid (Glu) on goethite after conditioning with PAs, and lysine (Lys) on montmorillonite after conditioning with PAs. The results are presented as mean values without transformation ($n = 3$). Transformed mean values were used for ANOVA analysis (SE = 0.025, 12 d.f., $P < 0.05$ for the initial concentration of 0.05 and 0.1 mM). SE: standard error of mean.

Appendix (C) to Chapter 5

Measurement of PAs

The standard mixture solution of four PAs and internal standard (IS) were prepared in ultrapure H₂O. Separation was done with a LiChrospher/Superspher RP-18 100-Å column (125 mm × 2 mm, 4 μm; Phenomenex, Torrance, CA, USA) and an RP-18 4-μm guard column. The mobile phase was solvent A (MeOH, 0.1% FA, v/v%) and solvent B (ultrapure H₂O, 0.1% FA, v/v%) with an isocratic elution of 27% solvent A for 15 minutes. Solvent A (90%) was used to wash the column between injections for 5 minutes, followed by a 15-minute equilibration period. The rate of flow of the mobile phase was 0.3 ml minute⁻¹. The injection volume was 10 μl and the oven temperature was 35 °C. Sal, Van, Syr, Fer and Eva were detected at 240, 260, 270, 320 and 280 nm, respectively.

Calibration lines were made by plotting the ratio of analyte to IS concentration versus analyte to IS peak area. Quantification of all measurements was performed with a eight point calibration line. For each different level of analyte concentration, the IS concentration was the same (4 mg l⁻¹). The high coefficients of determination (r^2) in Table C1 indicated the reliability of the calibration line over a wide range of concentration.

Table C1 Regression linear range and coefficients of determination of the PAs.

Analyte	IS	Linear range /mg l ⁻¹	r^2
Van	Eva	0.1–20	0.9999
Syr	Eva	0.1–20	0.9999
Fer	Eva	0.1–20	0.9998
Sal	Eva	0.1–20	0.9998

Table C2 Accuracies of the analytical methods for mixture of PAs and AAs.

Analyte	Concentration /mM		
	0.01	0.05	0.10
PAs			
Van	90 (4)	92 (5)	91 (5)
Syr	92 (4)	91 (5)	92 (5)
Fer	86 (2)	93 (15)	94 (13)
Sal	87 (3)	93 (4)	94 (5)
AAs			
Leu	105 (9)	100 (8)	108 (10)
Glu	99 (6)	115 (8)	110 (5)
Lys	93 (12)	107 (12)	99 (11)
Phe	101 (8)	110 (7)	107 (7)

Notes: The accuracies (%) are calculated as the ratio of measured value to calculated value. The results are presented as mean values with standard deviation ($n = 6$).

Table C3 Desorption of adsorbed OC from OM-coated minerals^a.

Mineral	Adsorbed OC /mg g ⁻¹	First cycle		Second cycle	
		Desorbed OC /mg g ⁻¹	Desorbed fraction /%	Desorbed OC /mg g ⁻¹	Desorbed fraction /%
L-G ^b	8.85 (0.01)	0.30 (0.02)	3.4 (0.2)	ND	ND
O-G ^c	18.2 (0.02)	1.51 (0.04)	8.3 (0.2)	0.33 (0.00)	1.8 (0.0)
L-K ^d	1.07 (0.00)	0.07 (0.00)	6.4 (0.4)	ND	ND
O-K ^e	1.13 (0.00)	0.12 (0.02)	10.2 (2.0)	ND	ND
L-M ^f	0.73 (0.00)	0.19 (0.01)	26.7 (0.7)	0.02 (0.00)	2.1 (0.6)
O-M ^g	0.80 (0.00)	0.18 (0.02)	22.2 (2.0)	0.01 (0.00)	1.7 (0.3)

^a The results are presented as mean values with standard deviation ($n = 3$). ^b Goethite coated with L-DOM; ^c Goethite coated with O-DOM; ^d Kaolinite coated with L-DOM; ^e Kaolinite coated with O-DOM; ^f Montmorillonite coated with L-DOM; ^g Montmorillonite coated with O-DOM; ND: not detectable.

Table C4 Desorption of previously adsorbed PAs and AAs after addition of AAs and PAs, respectively, in the conditioning experiment^a.

Mineral	DOM coating	Compounds	IC ^g /mM	Desorption / $\mu\text{mol g}^{-1}$	Desorbed proportion /%	
G ^b	L ^e	PAs	CK ^h	ND		
			0.01	0.17 (0.01)	73 (7)	
			0.05	0.56 (0.00)	70 (1)	
				0.10	0.85 (0.03)	96 (6)
		AAs	CK	0.12 (0.01)		
			0.01	0.17 (0.04)	8 (6)	
			0.05	0.46 (0.04)	18 (12)	
				0.10	0.72 (0.30)	21 (13)
		O ^f	PAs	CK	ND	
	0.01			NA		
	0.05			NA		
	0.10			NA		
	AAs		CK	0.01 (0.00)		
			0.01	ND		
			0.05	ND		
0.10			ND			
K ^c	L	PAs	CK	ND		
			0.01	0.07 (0.00)	43 (1)	
			0.05	0.23 (0.00)	49 (2)	
				0.1	0.35 (0.00)	60 (1)
		AAs	CK	0.02 (0.00)		
			0.01	0.10 (0.01)	15 (1)	
			0.05	0.26 (0.05)	10 (2)	
			0.10	0.41 (0.10)	11 (4)	

(Continued)

Table C4 Desorption of previously adsorbed PAs and AAs after addition of AAs and PAs, respectively, in the conditioning experiment (continued)^a.

Mineral	DOM coating	Compounds	IC /mM	Desorption / $\mu\text{mol g}^{-1}$	Desorbed proportion /%	
K	O	PAs	CK	ND		
			0.01	0.05 (0.00)	74 (9)	
			0.05	0.19 (0.00)	81 (10)	
		0.10	0.30 (0.00)	101 (3)		
		AAs	CK	ND		
			0.01	0.06 (0.01)	11 (1)	
	0.05		0.24 (0.03)	11 (1)		
	M ^d	L	PAs	CK	ND	
				0.01	0.11 (0.00)	52 (1)
				0.05	0.39 (0.01)	57 (1)
			0.10	0.64 (0.01)	68 (1)	
			AAs	CK	0.02 (0.00)	
0.01				0.07 (0.02)	7 (2)	
0.05		0.21 (0.01)		6 (0)		
O		PAs	CK	ND		
			0.01	0.11 (0.00)	44 (1)	
			0.05	0.39 (0.00)	49 (1)	
		0.10	0.64 (0.01)	58 (1)		
		AAs	CK	ND		
	0.01		0.06 (0.00)	9 (0)		
0.05	0.28 (0.02)		8 (1)			
			0.10	0.60 (0.07)	11 (1)	

^a The results are presented as mean values with standard deviation ($n = 3$); ^b Goethite; ^c Kaolinite; ^d Montmorillonite; ^e L-DOM; ^f O-DOM; ^g Initial concentration; ^h Desorption from adsorbed OM on mineral surface; NA: not applicable due to no adsorption of PAs; ND: not detectable.

Table C5 Recovery of PAs and AAs spiked to the solutions desorbed from OM-coated minerals^a.

Compound	OM-coated minerals						
	L-G ^b	O-G ^c	L-K ^d	O-K ^e	L-M ^f	O-M ^g	
PAs	Van	90.9 (1.6)	91.4 (0.6)	91.1 (1.2)	90.9 (0.9)	90.9 (0.6)	91.0 (0.1)
	Syr	91.4 (1.3)	91.9 (0.4)	91.6 (1.0)	91.4 (0.7)	91.3 (0.8)	91.4 (0.4)
	Fer	92.5 (1.2)	93.1 (0.4)	92.8 (1.1)	92.6 (0.7)	92.4 (0.8)	92.6 (0.5)
	Sal	91.9 (1.1)	92.4 (2.0)	91.9 (2.3)	92.2 (1.8)	91.7 (3.4)	92.0 (2.6)
AAs	Leu	91.0 (6.6)	85.7 (6.2)	88.7 (6.7)	93.5 (3.8)	87.5 (8.0)	90.6 (6.0)
	Glu	92.3 (7.3)	87.8 (10.7)	90.4 (9.3)	97.2 (4.7)	87.9 (8.4)	92.7 (6.8)
	Lys	98.5 (9.1)	88.8 (12.6)	95.3 (9.4)	101.3 (4.1)	92.2 (9.1)	96.4 (4.6)
	Phe	89.4 (7.1)	85.3(7.4)	87.8 (4.2)	92.7 (5.2)	87.7 (8.9)	91.1 (7.8)

^a The results (in %) are presented as mean values of four different spiking concentrations with standard deviation. ^b Goethite coated with L-DOM; ^c Goethite coated with O-DOM; ^d Kaolinite coated with L-DOM; ^e Kaolinite coated with O-DOM; ^f Montmorillonite coated with L-DOM; ^g Montmorillonite coated with O-DOM.

Table C6 Langmuir parameters obtained by fitting the adsorption isotherms of L-DOM (L) and O-DOM (O) on goethite (G), kaolinite (K) and montmorillonite (M).

Mineral	DOM	$Q_{max}/\text{mg C g}^{-1}$	$Q_{max}/\text{mg C m}^{-2}$	$k/\text{g mg}^{-1}$	r^2
G	L	14.29	0.205	0.1203	0.9985
	O	31.15	0.447	0.0834	0.9968
K	L	1.70	0.068	1.1351	0.9990
	O	1.96	0.078	1.4140	0.9993
M	L	1.45	0.015	0.1752	0.9805
	O	1.44	0.015	0.8933	0.9996

Note: The equilibrium concentration of adsorbates after adsorption referred to the ratio of the amount of remaining OC in the solution to the amount of minerals in fitting of adsorption data. Q_{max} = adsorption capacity, k = affinity coefficient.

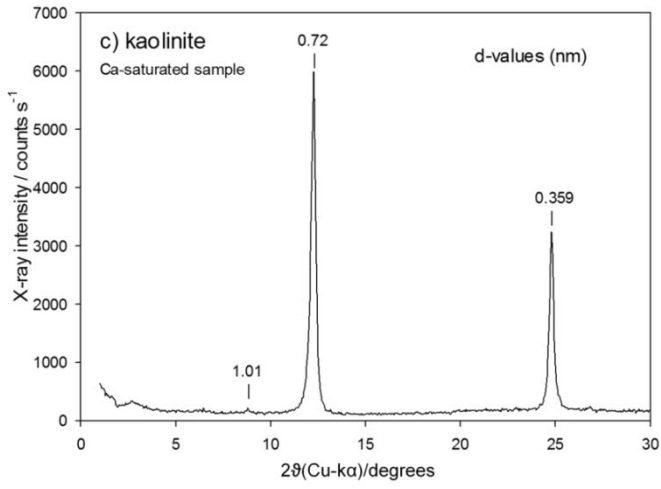


Figure C1 X-ray diffraction patterns of kaolinite.

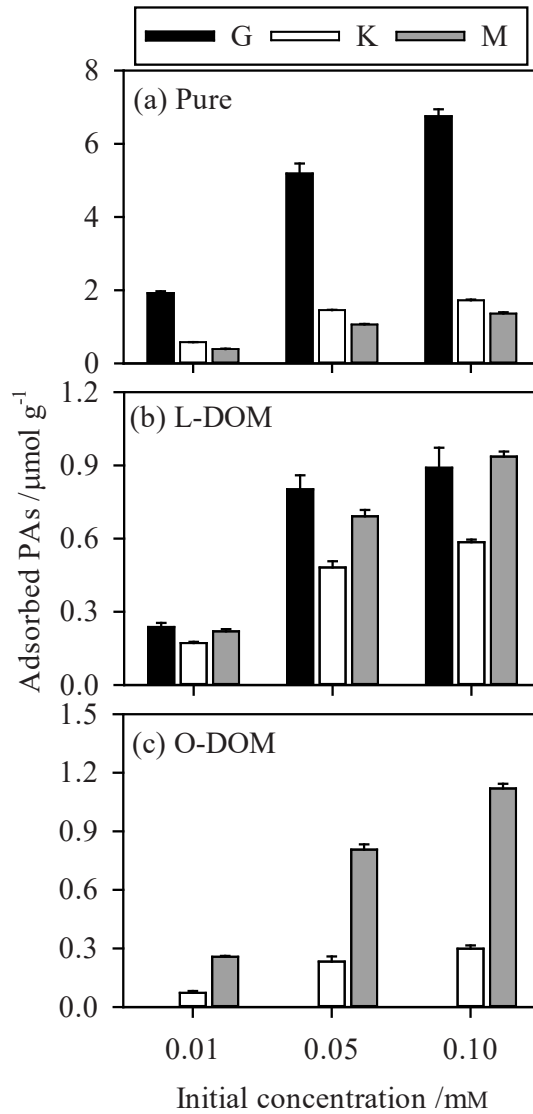


Figure C2 Adsorption of PAs on (a) pure minerals, (b) coated minerals with L-DOM and (c) coated minerals with O-DOM. Data are presented as mean values with 95% confidence intervals ($n = 3$). G, goethite; K, kaolinite; M, montmorillonite.

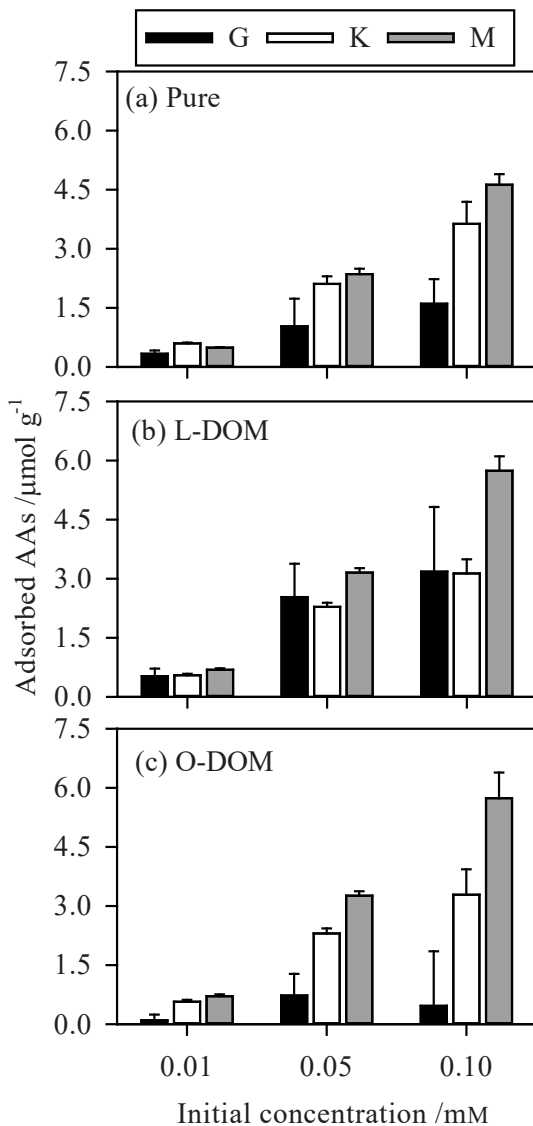


Figure C3 Adsorption of AAs on (a) pure minerals, (b) coated minerals with L-DOM and (c) coated minerals with O-DOM. Data are presented as mean values with 95% confidence intervals ($n = 3$). G, goethite; K, kaolinite; M, montmorillonite.

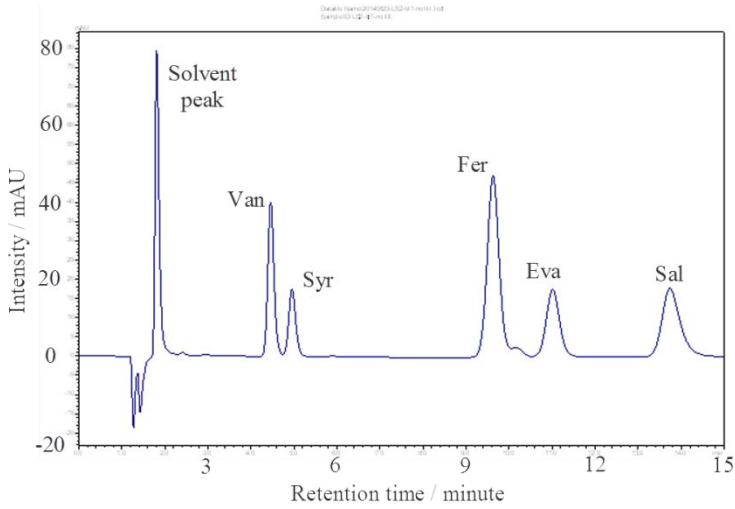


Figure C4 Typical chromatograms of the targeted PAs and IS (Eva) obtained from a mixture solution of PAs and AAs. The injection concentrations of targeted PAs and IS were 0.05 and 0.03 mM, respectively. The wavelength of the detection was 240 nm.

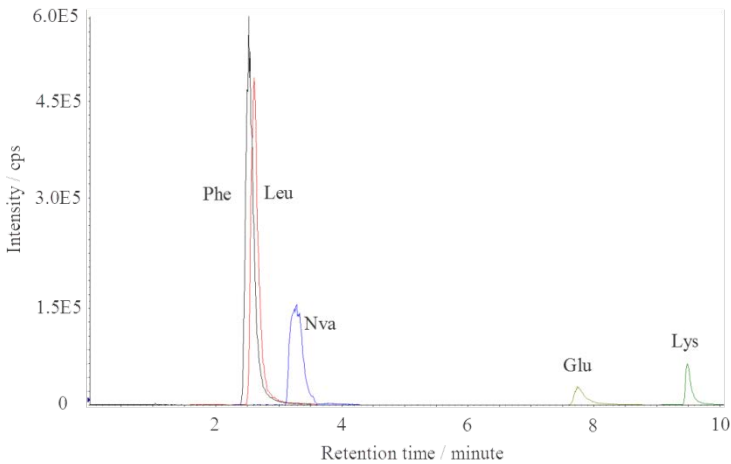


Figure C5 Typical chromatograms of the targeted AAs and IS (Nva) obtained from a mixture solution of PAs and AAs. The injection concentrations of targeted AAs and IS were 1.0 and 0.9 μM , respectively.

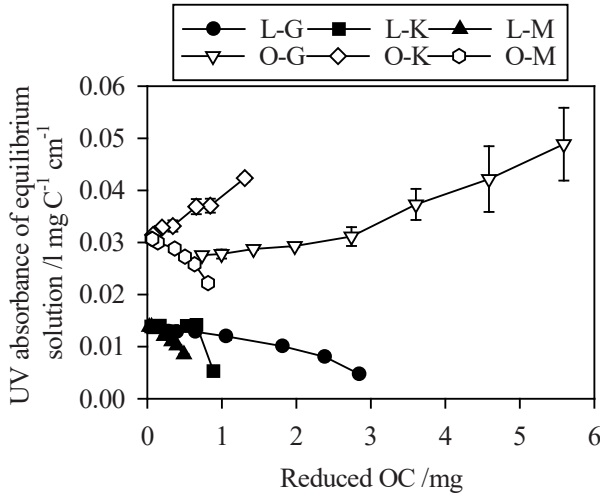


Figure C6 Changes of the UV absorbance (280 nm) of equilibrium solution with reduced OC in solution for all combinations of minerals and DOM. The results are presented as mean values with standard deviation ($n = 2$). G, goethite; K, kaolinite; M, montmorillonite; L, L-DOM; O, O-DOM.

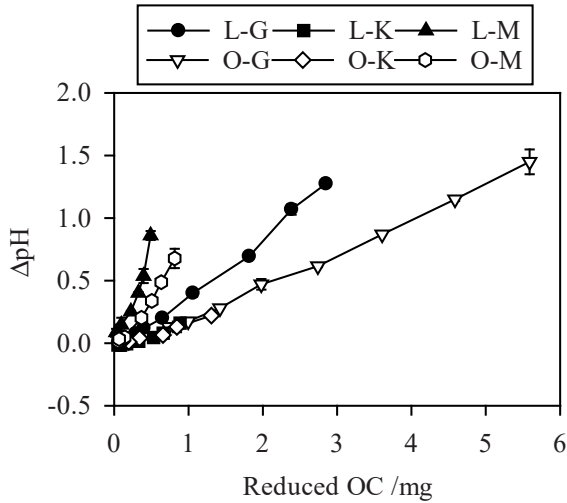


Figure C7 Changes of equilibrium solution pH with reduced OC in the solution for all combinations of minerals and DOM. The results are presented as mean values with standard deviation ($n = 2$). G, goethite; K, kaolinite; M, montmorillonite; L, L-DOM; O, O-DOM.

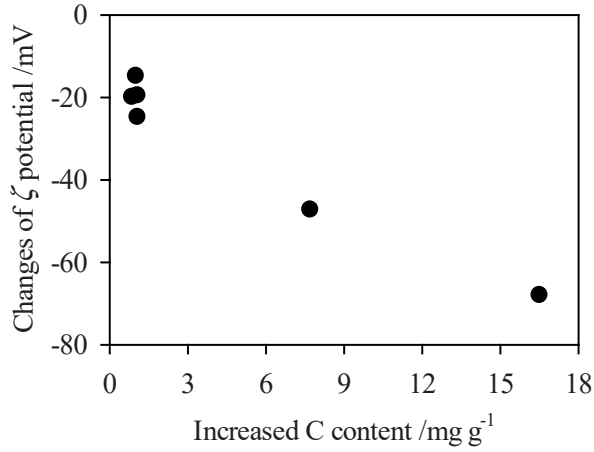


Figure C8 Relation between the increased C content of all OM-coated minerals and the changes of ζ potential.

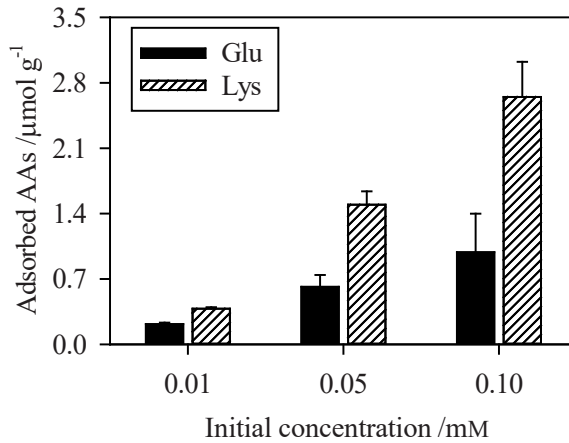


Figure C9 Adsorption of Glu and Lys on kaolinite. The results are presented as mean values with standard deviation ($n = 3$). Glu, glutamic acid; Lys, lysine.

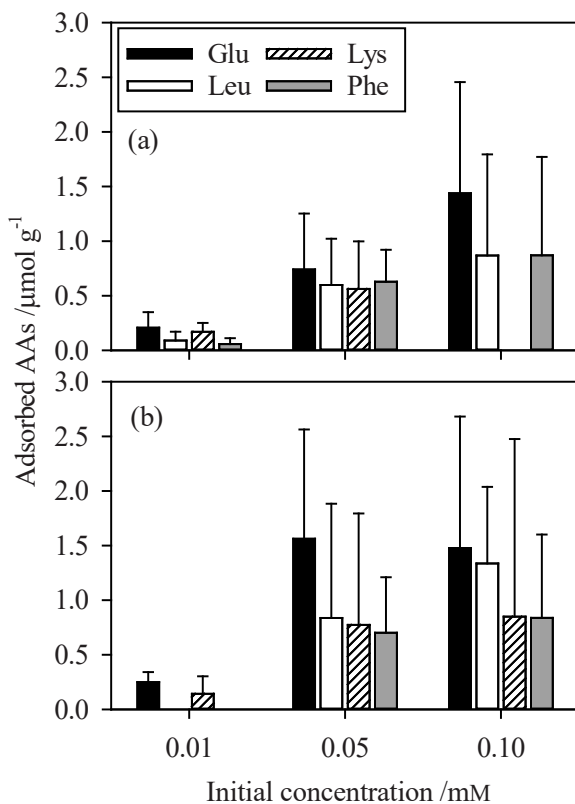


Figure C10 Adsorption of individual AA on (a) L-goethite and (b) L-goethite with pre-conditioning by PAs. The results are presented as mean values with standard deviation ($n = 3$). Glu, glutamic acid; Leu, leucine; Lys, lysine; Phe, phenylalanine.

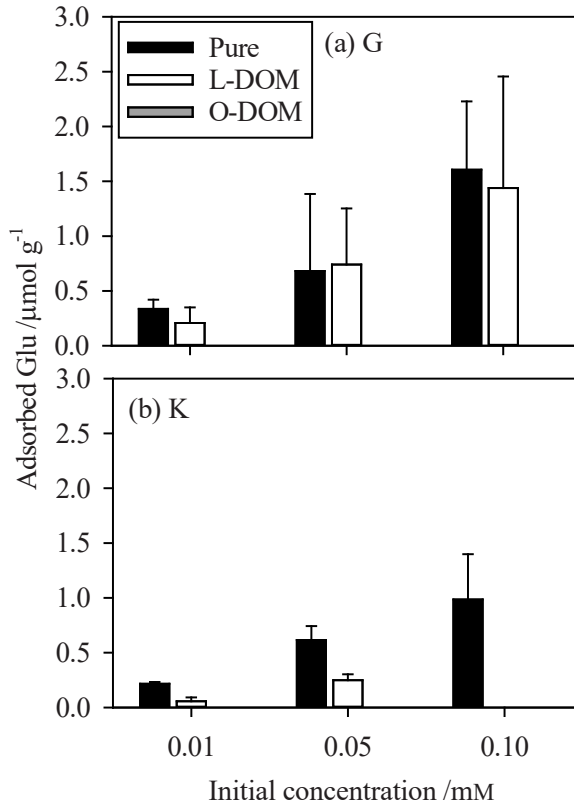


Figure C11 Adsorption of Glu on (a) pure and coated goethite with L-DOM and O-DOM and (b) pure and coated kaolinite with L-DOM and O-DOM. The results are presented as mean values with standard deviation ($n = 3$). No adsorption was observed on O-goethite and O-kaolinite for all initial concentrations and L-kaolinite at the high initial concentration. G, goethite; K, kaolinite.

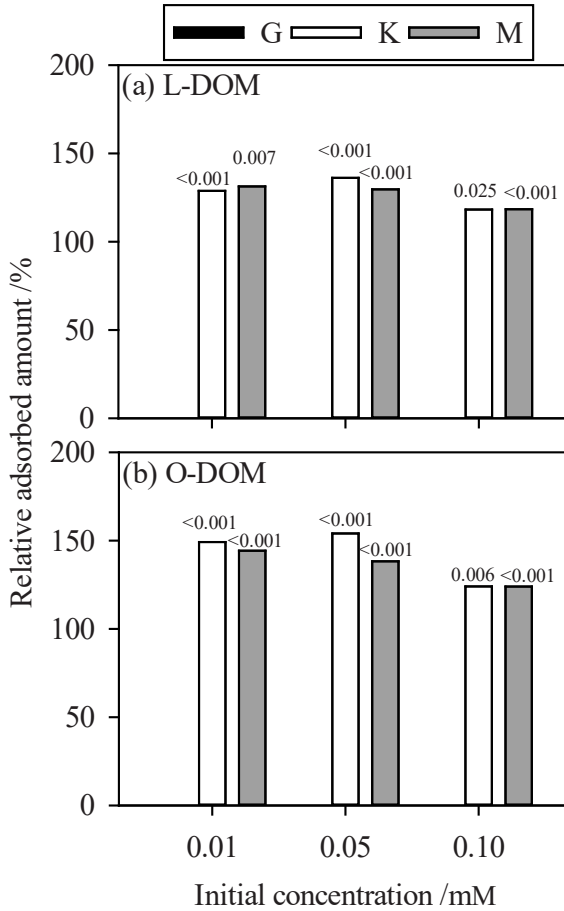


Figure C12 Relative adsorption of Lys on (a) coated minerals with L-DOM and (b) coated minerals with O-DOM. The results are expressed relative to the adsorption (mean value) on pure minerals (reference, expressed as horizontal line). Data are presented as mean values ($n = 3$). P values above each column indicate significant level of differences compared with the references. The adsorption results on coated goethite were not displayed because the values of the references were zero. G, goethite; K, kaolinite; M, montmorillonite.

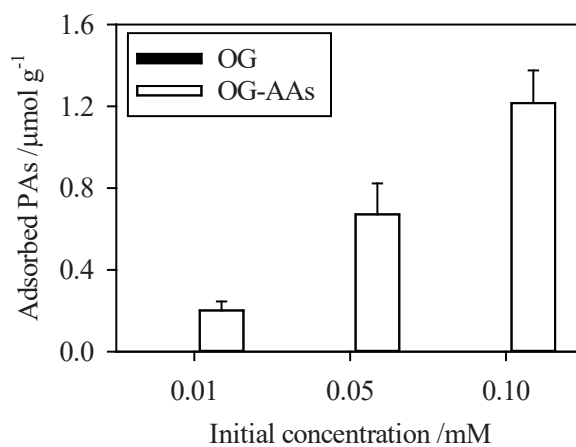


Figure C13 Adsorption of PAs on O-goethite (OG) and after pre-conditioning by AAs (OG-AAs). The results are presented as mean values with standard deviation ($n = 3$). No adsorption of PAs was observed on OG.

References

- Achtenhagen, J., Goebel, M.-O., Miltner, A., Woche, S.K. & Kästner, M. 2015. Bacterial impact on the wetting properties of soil minerals. *Biogeochemistry* 122, 269–280.
- Annesley, T.M. 2003. Ion suppression in mass spectrometry. *Clinical Chemistry* 49, 1041–1044.
- Araujo, M.A., Zinn, Y.L. & Lal, R. 2017. Soil parent material, texture and oxide contents have little effect on soil organic carbon retention in tropical highlands. *Geoderma* 300, 1–10.
- Armstrong, M., Jonscher, K. & Reisdorph, N.A. 2007. Analysis of 25 underivatized amino acids in human plasma using ion-pairing reversed-phase liquid chromatography / time-of-flight mass spectrometry. *Rapid Communications in Mass Spectrometry* 21, 2717–2726.
- Arnarson, T. & Keil, R.G. 2001. Organic-mineral interactions in marine sediments studies using density fractionation and X-ray photoelectron spectroscopy. *Organic Geochemistry* 32, 1401–1415.
- Atkinson, R.J., Posner, A.M. & Quirk, J.P. 1967. Adsorption of potential-determining ions at the ferric oxide-aqueous electrolyte interface. *The Journal of Physical Chemistry*, 71, 550–558.
- Aufdenkampe, A.K., Hedges, J.I., Richey, J.E., Krusche, A.V. & Llerena, C.A. 2001. Sorptive fractionation of dissolved organic nitrogen and amino acids onto fine sediments within the Amazon Basin. *Limnology and Oceanography* 46, 1921–1935.
- Avneri-Katz, S., Young, R.B., McKenna, A.M., Chen, H., Corilo, Y.E., et al. 2017. Adsorptive fractionation of dissolved organic matter (DOM) by mineral soil: Macroscale approach and molecular insight. *Organic Geochemistry* 103, 113–124.
- Bachmann, J., Guggenberger, G., Baumgartl, T., Ellerbrock, R.H., Urbanek, E., Goebel, M.O., et al. 2008. Physical carbon-sequestration mechanisms under special consideration of soil wettability. *Journal of Plant Nutrition and Soil Science* 171, 14–26.
- Barbera, V., Poma, I., Gristina, L., Novara, A. & Egli, M. 2012. Long-term cropping systems and tillage management effects on soil organic carbon stock and steady state level of C sequestration rates in a semiarid environment. *Land Degradation & Development* 23, 82–91.

- Barbera, V., Raimondi, S., Egli, M. & Plötze, M. 2008. The influence of weathering processes on labile and stable organic matter in Mediterranean volcanic soils. *Geoderma* 143, 191–205.
- Barré, P., Fernandez-Ugalde, O., Virto, I., Velde, B. & Chenu, C. 2014. Impact of phyllosilicate mineralogy on organic carbon stabilization in soils: incomplete knowledge and exciting prospects. *Geoderma* 235–236, 382–395.
- Barrett G.C. 1985. Chemistry and biochemistry of amino acids. In: *The Protein Amino Acids*, (Ed Hardy P.M.), pp. 9. Chapman and Hall, London.
- Bimüller, C., Mueller, C.W., von Lütow, M., Kreyling, O., Kölbl, A., Haug, S., et al. 2014. Decoupled carbon and nitrogen mineralization in soil particle size fractions of a forest topsoil. *Soil Biology & Biochemistry* 78, 263–273.
- Bingham, A.H. & Cotrufo, M.F. 2016. Organic nitrogen storage in mineral soil: Implications for policy and management. *Science of the Total Environment* 551–552, 116–126.
- Bonina, F., Giannossi, M., Medici, L., Puglia, C., Summa, V. & Tateo, F. 2007. Adsorption of salicylic acid on bentonite and kaolin and release experiments. *Applied Clay Science* 36, 77–85.
- Bonnard, P., Basile-Doelsch, I., Balesdent, J., Masion, A., Borschneck, D. & Arrouays, D. 2012. Organic matter content and features related to associated mineral fractions in an acid, loamy soil. *European Journal of Soil Science* 63, 625–636.
- Borden, D. & Giese, R.E. 2001. Baseline studies of the clay minerals society source clays: Cation exchange capacity measurements by the ammonia-electrode method. *Clays and Clay Minerals* 49, 444–445.
- Brüggemann, N., Gessler, A., Kayler, Z., Keel, S.G., Badeck, F., Barthel, M., et al. 2011. Carbon allocation and carbon isotope fluxes in the plant-soil-atmosphere continuum: A review. *Biogeosciences* 8, 3457–3489.
- Brunauer, S., Emmett, P.H. & Teller, E. 1938. Adsorption of gases in multimolecular layers. *Journal of the American Chemical Society*, 60, 309–319.
- Burke, I.C., Yonker, C.M., Parton, W.J., Cole, C. V., Schimel, D.S. & Flach, K. 1989. Texture, climate, and cultivation effects on soil organic matter content in U.S. grassland soils. *Soil Science Society of America Journal* 53, 800.
- Buszewski, B. & Noga, S. 2012. Hydrophilic interaction liquid chromatography (HILIC) – a powerful separation technique. *Analytical and Bioanalytical Chemistry* 402, 231–247.

- Calderón-Santiago, M., Priego-Capote, F., Galache-Osuna, J.G. & Luque de Castro, M.D. 2012. Determination of essential amino acids in human serum by a targeting method based on automated SPE-LC-MS/MS: discrimination between atherosclerotic patients. *Journal of pharmaceutical and biomedical analysis* 70, 476–484.
- Callejón, R.M., Troncoso, A.M. & Morales, M.L. 2010. Determination of amino acids in grape-derived products: a review. *Talanta* 81, 1143–1152.
- Cammeraat, E.L.H. 2004. Scale dependent thresholds in hydrological and erosion response of a semi-arid catchment in southeast Spain. *Agriculture, Ecosystems & Environment* 104, 317–332.
- Casella, I.G. & Contursi, M. 2003. Isocratic ion chromatographic determination of underivatized amino acids by electrochemical detection. *Analytica Chimica Acta* 478, 179–189.
- Castanha, C., Trumbore, S. & Amundson, R. 2008. Methods of separating soil carbon pools affect the chemistry and turnover time of isolated fractions. *Radiocarbon* 50, 83–97.
- Cecchi, A.M., Koskinen, W.C., Cheng, H.H. & Haider, K. 2004. Sorption-desorption of phenolic acids as affected by soil properties. *Biology and Fertility of Soils* 39, 235–242.
- Celis R., Real M., Hermosin M.C. & Cornejo J. 2005. Sorption and leaching behaviour of polar aromatic acids in agricultural soils by batch and column leaching tests. *European Journal of Soil Science*, 56, 287–297.
- Cerli, C., Celi, L., Bosio, P., Motta, R. & Grassi, G. 2009. Effect of land use change on soil properties and carbon accumulation in the Ticino Park (North Italy). *Studi Trent. Sci. Nat.* 85, 83–92.
- Cernei, N., Zitka, O., Ryvolova, M., Adam, V., Masarik, M., Jaromir, H. & Reze, K. 2012. Spectrometric and electrochemical analysis of sarcosine as a potential prostate carcinoma marker. *International Journal of Electrochemical Science* 7, 4286–4301.
- Chefetz, B., Eldad, S. & Polubesova, T. 2011. Interactions of aromatic acids with montmorillonite: Ca²⁺- and Fe³⁺-saturated clays versus Fe³⁺-Ca²⁺-clay system. *Geoderma*, 160, 608–613.
- Chen, C., Dynes, J.J., Wang, J., Karunakaran, C. & Sparks, D.L. 2014. Soft X-ray spectromicroscopy study of mineral-organic matter associations in pasture soil clay fractions. *Environmental Science & Technology* 48, 6678–6686.

- Chenu, C. & Plante, A.T. 2006. Clay-sized organo-mineral complexes in a cultivation chronosequence: revisiting the concept of the "primary organo-mineral complex." *European Journal of Soil Science* 57, 596–607.
- Chorover, J. & Amistadi, M.K. 2001. Reaction of forest floor organic matter at goethite, birnessite and smectite surfaces. *Geochimica et Cosmochimica Acta* 65, 95–109.
- Cismasu, A.C., Williams, K.H. & Nico, P.S. 2016. Iron and carbon dynamics during aging and reductive transformation of biogenic ferrihydrite. *Environmental Science & Technology* 50, 25–35.
- Creamer, C.A., Filley, T.R., Olk, D.C., Plante, A., Peltre, C., Top, S.M. & Boutton, T.W. 2012. Degree of woody encroachment into grasslands controls soil carbohydrate and amino compound changes during long term laboratory incubation. *Organic Geochemistry* 52, 23–31.
- Creamer, C.A., Filley, T.R., Olk, D.C., Stott, D.E., Dooling, V. & Boutton, T.W. 2013. Changes to soil organic N dynamics with leguminous woody plant encroachment into grasslands. *Biogeochemistry* 113, 307–321.
- Croteau, R., Kutchan T.M. & Lewis N.G. 2000. Natural products (secondary metabolites). In: *Biochemistry and molecular biology of plants*, (eds Buchanan B., Gruissem W., Jones R.), pp. 1250–1318. American Society of Plant Physiologists, Rockville, MD.
- Cuba-Chiem, L.T., Huynh, L., Ralston, J. & Beattie, D.A. 2008. In situ particle film ATR FTIR spectroscopy of carboxymethyl cellulose adsorption on talc: binding mechanism, pH effects, and adsorption kinetics. *Langmuir* 24, 8036–8044.
- Cusack, D.F., Chadwick, O.A., Ladefoged, T. & Vitousek, P.M. 2013. Long-term effects of agriculture on soil carbon pools and carbon chemistry along a Hawaiian environmental gradient. *Biogeochemistry* 112, 229–243.
- Daou, I., Zegaoui, O., Chfaira, R., Ahlafi, H. & Moussout, H. 2015. Physico-chemical characterization and kinetic study of methylene blue adsorption onto a Moroccan Bentonite. *International Journal of Scientific and Research Publications*, 5, 1–9.
- Davis, J.A. 1982. Adsorption of natural dissolved organic matter at the oxide/water interface. *Geochimica et Cosmochimica Acta* 46, 2381–2393.
- Ddani, M., Meunier, A., Zahraoui, M., Beaufort, D., El Wartiti, M., Fontaine, C., Boukili, B. & El Mahi, B. 2005. Clay mineralogy and chemical composition of bentonites from the Gourougou volcanic massif (northeast Morocco). *Clays and Clay Minerals* 53, 250–267.
- Dell'mour, M., Jaitz, L., Oburger, E., Puschenreiter, M., Koellensperger, G. & Hann, S. 2010. Hydrophilic interaction LC combined with electrospray MS for highly

- sensitive analysis of underivatized amino acids in rhizosphere research. *Journal of Separation Science* 33, 911–922.
- Desiderio, C., Iavarone, F., Rossetti, D.V., Messina, I. & Castagnola, M. 2010. Capillary electrophoresis-mass spectrometry for the analysis of amino acids. *Journal of separation science* 33, 2385–2393.
- Diehl, D., Ellerbrock, R.H. & Schaumann, G.E. 2009. Influence of drying conditions on wettability and DRIFT spectroscopic C-H band of soil samples. *European Journal of Soil Science* 60, 557–566.
- Du, C., Goynes, K.W., Miles, R.J. & Zhou, J. 2014. A 1915–2011 microscale record of soil organic matter under wheat cultivation using FTIR-PAS depth-profiling. *Agronomy for Sustainable Development*, 34, 803–811.
- Dümig, A., Häusler, W., Steffens, M. & Kögel-Knabner, I. 2012. Clay fractions from a soil chronosequence after glacier retreat reveal the initial evolution of organo-mineral associations. *Geochimica et Cosmochimica Acta* 85, 1–18.
- Egli, M., Favilli, F., Krebs, R., Pichler, B. & Dahms, D. 2012. Soil organic carbon and nitrogen accumulation rates in cold and alpine environments over 1 Ma. *Geoderma* 183–184, 109–123.
- Egli, M., Merkli, C., Sartori, G., Mirabella, A. & Plötze, M. 2008. Weathering, mineralogical evolution and soil organic matter along a Holocene soil toposequence developed on carbonate-rich materials. *Geomorphology* 97, 675–696.
- European Commission (EC). 2006. Communication from the Commission to the Council, the European Parliament, the European Economic and Social Committee and the Committee of the Regions, Thematic Strategy for Soil Protection. COM231 Final. Brussels.
- FAO and ITPS. 2015. Status of the world's soil resources – technical summary. Rome, Italy.
- Favilli, F., Egli, M., Cherubini, P., Sartori, G., Haeberli, W. & Delbos, E. 2008. Comparison of different methods of obtaining a resilient organic matter fraction in Alpine soils. *Geoderma* 145, 355–369.
- Feng, W., Plante, A.F., Aufdenkampe, A.K. & Six, J. 2014. Soil organic matter stability in organo-mineral complexes as a function of increasing C loading. *Soil Biology & Biochemistry* 69, 398–0405.

- Feng, X., Simpson, A.J. & Simpson, M.J. 2005. Chemical and mineralogical controls on humic acid sorption to clay mineral surfaces. *Organic Geochemistry* 36, 1553–1566.
- Fischlin, A., Midgley, G.F., Price, J.T., Leemans, R., Gopal, B., Turley, C., et al. 2007: Ecosystems, their properties, goods, and services. Climate Change 2007: Impacts, Adaptation and Vulnerability. *Contribution of Working Group II to the Fourth Assessment Report of the Intergovernmental Panel on Climate Change*, M.L. Parry, O.F. Canziani, J.P. Palutikof, P.J. van der Linden and C.E. Hanson, Eds., Cambridge University Press, Cambridge, 211-272.
- Gao, J., Helmus, R., Cerli, C., Jansen, B., Wang, X. & Kalbitz, K. 2016. Robust analysis of underivatized free amino acids in soil by hydrophilic interaction liquid chromatography coupled with electrospray tandem mass spectrometry. *Journal of Chromatography A*, 1449, 78–88.
- Gao, J., Jansen, B., Cerli, C., Helmus, R., Mikutta R., Dultz S., et al. 2017. Competition and surface conditioning alter the adsorption of phenolic acids and amino acids on soil minerals. *European Journal of Soil Science*, 68, 667–677.
- Gatta, G.D. 1985. Direct determination of adsorption heats. *Thermochimica Acta* 96, 349–363.
- Goebel, M.O., Bachmann, J., Reichstein, M., Janssens, I.A. & Guggenberger, G. 2011. Soil water repellency and its implications for organic matter decomposition - is there a link to extreme climatic events? *Global Change Biology* 17, 2640–2656.
- Gökmen, V., Serpen, A. & Mogol, B.A. 2012. Rapid determination of amino acids in foods by hydrophilic interaction liquid chromatography coupled to high-resolution mass spectrometry. *Analytical and Bioanalytical Chemistry* 403, 2915–2922.
- Gu, B., Mehlhorn, T.L., Liang, L. & McCarthy, J.F. 1996. Competitive adsorption, displacement, and transport of organic matter on iron oxide: II. Displacement and transport. *Geochimica et Cosmochimica Acta*, 60, 2977–2992.
- Gu, B.H., Schmitt, J., Chen, Z.H., Liang, L.Y. & McCarthy, J.F. 1994. Adsorption and desorption of natural organic-matter on iron-oxide - mechanisms and models. *Environmental Science & Technology* 28, 38–46.
- Guan, X.H., Shang, C. & Chen, G.H. 2006. ATR-FTIR investigation of the role of phenolic groups in the interaction of some NOM model compounds with aluminum hydroxide. *Chemosphere*, 65, 2074–2081.
- Guggenberger, G. & Zech, W. 1994. Composition and dynamics of dissolved carbohydrates and lignin-degradation products in two coniferous forests, N.E. Bavaria, Germany. *Soil Biology & Biochemistry* 26, 19–27.

- Guo, S., Duan, J., Qian, D., Tang, Y., Qian, Y., Wu, D., Su, S. & Shang, E. 2013. Rapid determination of amino acids in fruits of *Ziziphus jujube* by hydrophilic interaction ultra-high-performance liquid chromatography coupled with triple-quadrupole mass spectrometry. *Journal of agriculture and food chemistry* 61, 2709–2719.
- Hagedorn, F., Bruderhofer, N., Ferrari, A. & Niklaus, P.A. 2015. Tracking litter-derived dissolved organic matter along a soil chronosequence using ^{14}C imaging: Biodegradation, physico-chemical retention or preferential flow? *Soil Biology & Biochemistry*, 88, 333–343.
- Han, L., Sun, K., Jin, J. & Xing, B. 2016. Some concepts of soil organic carbon characteristics and mineral interaction from a review of literature. *Soil Biology & Biochemistry* 94, 107–121.
- Hanke, A., Cerli, C., Muhr, J., Borcken, W. & Kalbitz, K. 2013. Redox control on carbon mineralization and dissolved organic matter along a chronosequence of paddy soils. *European Journal of Soil Science* 64, 476–487.
- Hansson, K., Kleja, D.B., Kalbitz, K. & Larsson, H. 2010. Amounts of carbon mineralised and leached as DOC during decomposition of Norway spruce needles and fine roots. *Soil Biology & Biochemistry* 42, 178–185.
- Hatton, P.J., Remusat, L., Zeller, B., Brewer, E.A. & Derrien, D. 2015. NanoSIMS investigation of glycine-derived C and N retention with soil organo-mineral associations. *Biogeochemistry* 125, 303–313.
- Hatton, P.-J., Remusat, L., Zeller, B. & Derrien, D. 2012. A multi-scale approach to determine accurate elemental and isotopic ratios by nano-scale secondary ion mass spectrometry imaging. *Rapid Communications in Mass Spectrometry* 26, 1363–1371.
- He, W., Chen, M., Schlautman, M.A. & Hur, J. 2016. Dynamic exchanges between DOM and POM pools in coastal and inland aquatic ecosystems: A review. *Science of the Total Environment* 551–552, 415–428.
- Heister, K., Höschen, C., Pronk, G.J., Mueller, C.W. & Kögel-Knabner, I. 2012. NanoSIMS as a tool for characterizing soil model compounds and organomineral associations in artificial soils. *Journal of Soils and Sediments* 12, 35–47.
- Helassa, N., Quiquampoix, H., Noinville, S., Szponarski, W. & Staunton, S. 2009. Adsorption and desorption of monomeric Bt (*Bacillus thuringiensis*) Cry1Aa toxin on montmorillonite and kaolinite. *Soil Biology & Biochemistry* 41, 498–504.
- Henrichs, S.M. & Sugai, S.F. 1993. Adsorption of amino acids and glucose by sediments of Resurrection Bay, Alaska, USA: Functional group effects. *Geochimica et Cosmochimica Acta* 57, 823–835.

- Herold, N., Schöning, I., Michalzik, B., Trumbore, S. & Schrumpf, M. 2014. Controls on soil carbon storage and turnover in German landscapes. *Biogeochemistry* 119, 435–451.
- Hobbie, J.E. & Hobbie, E.A. 2012. Amino acid cycling in plankton and soil microbes studied with radioisotopes: measured amino acids in soil do not reflect bioavailability. *Biogeochemistry* 107, 339–360.
- Horne, D. & McIntosh, J. 2000. Hydrophobic compounds in sands in New Zealand—extraction, characterisation and proposed mechanisms for repellency expression. *Journal of Hydrology* 231–232, 35–46.
- Huang, P.M., Wang, T.S.C., Wang, M.K., Wu, M.H. & Hsu, N.W. 1977. Retention of phenolic acids by noncrystalline hydroxy-aluminum and -iron compounds and clay minerals of soils. *Soil Science* 123, 213–219.
- Hunter, R.J. 1981. In: *Zeta Potential in Colloid Science: Principles and Applications*. Academic Press, New York, pp.232.
- Hunter, R.J. 2001. *Foundations of colloid science* (second edition), Oxford University Press.
- Inagaki, S., Tano, Y., Yamakata, Y., Higashi, T., Min, J.Z. & Toyo'oka, T. 2010. Highly sensitive and positively charged precolumn derivatization reagent for amines and amino acids in liquid chromatography/electrospray ionization tandem mass spectrometry. *Rapid Communications in Mass Spectrometry* 24, 1358–1364.
- Ingerslev, M. 1997. Effects of liming and fertilization on growth, soil chemistry and soil water chemistry in a Norway spruce plantation on a nutrient-poor soil in Denmark. *Forest Ecology and Management* 92, 55–66.
- Jandera, P. 2011. Stationary and mobile phases in hydrophilic interaction chromatography: a review. *Analytica Chimica Acta* 692, 1–25.
- Jansen, B., Nierop, K.G.J. & Verstraten, J.M. 2005. Mechanisms controlling the mobility of dissolved organic matter, aluminium and iron in podzol B horizons. *European Journal of Soil Science* 56, 537–550.
- Jardine, P.M., McCarthy, J.F. & Weber, N.L. 1989. Mechanisms of Dissolved Organic Carbon Adsorption on Soil. *Soil Science Society of America Journal* 53, 1378.
- John, B., Yamashita, T., Ludwig, B. & Flessa, H. 2005. Storage of organic carbon in aggregate and density fractions of silty soils under different types of land use. *Geoderma* 128, 63–79.

- Jones, D.L. & Hodge, A. 1999. Biodegradation kinetics and sorption reactions of three differently charged amino acids in soil and their effects on plant organic nitrogen availability. *Soil Biology & Biochemistry* 31, 1331–1342.
- Jones, D.L., Owen, A.G. & Farrar, J.F. 2002. Simple method to enable the high resolution determination of total free amino acids in soil solutions and soil extracts. *Soil Biology & Biochemistry* 34, 1893–1902.
- Jones, D.L., Shannon, D., Murphy, D. V. & Farrar, J. 2004. Role of dissolved organic nitrogen (DON) in soil N cycling in grassland soils. *Soil Biology & Biochemistry* 36, 749–756.
- Kaiser, K. & Guggenberger, G. 2000. The role of DOM sorption to mineral surfaces in the preservation of organic matter in soils. *Organic Geochemistry*, 31, 711–725.
- Kaiser, K. & Guggenberger, G. 2007. Sorptive stabilization of organic matter by microporous goethite: Sorption into small pores vs. surface complexation. *European Journal of Soil Science* 58, 45–59.
- Kaiser, K. & Kalbitz, K. 2012. Cycling downwards - dissolved organic matter in soils. *Soil Biology & Biochemistry* 52, 29–32.
- Kaiser, K. & Guggenberger, G. 2000. The role of DOM sorption to mineral surfaces in the preservation of organic matter in soils. *Organic Geochemistry* 31, 711–725.
- Kaiser, K. & Guggenberger, G. 2003. Mineral surfaces and soil organic matter. *European Journal of Soil Science* 54, 219–236.
- Kaiser, K., Guggenberger, G., Haumaier, L. & Zech, W. 1997. Dissolved organic matter sorption on subsoils and minerals studied by ¹³C-NMR and DRIFT spectroscopy. *European Journal of Soil Science* 48, 301–310.
- Kaiser, K., Guggenberger, G., Haumaier, L. & Zech, W. 2001. Seasonal variations in the chemical composition of dissolved organic matter in organic forest floor layer leachates of old-growth Scots pine (*Pinus sylvestris* L.) and European beech (*Fagus sylvatica* L.) stands in northeastern Bavaria, Germany. *Biogeochemistry* 55, 103–143.
- Kaiser, M., Kleber, M. & Berhe, A.A. 2015. How air-drying and rewetting modify soil organic matter characteristics: An assessment to improve data interpretation and inference. *Soil Biology & Biochemistry* 80, 324–340.
- Kaiser, M., Zederer, D.P., Ellerbrock, R.H., Sommer, M. & Ludwig, B. 2016. Effects of mineral characteristics on content, composition, and stability of organic matter fractions separated from seven forest topsoils of different pedogenesis. *Geoderma* 263, 1–7.

- Kalbitz, K., Schwesig, D., Rethemeyer, J. & Matzner, E. 2005. Stabilization of dissolved organic matter by sorption to the mineral soil. *Soil Biology & Biochemistry*, 37, 1319–1331.
- Kalbitz, K., Schwesig, D., Schmerwitz, J., Kaiser, K., Haumaier, L., Glaser, B., Ellerbrock, R. & Leinweber, P. 2003. Changes in properties of soil-derived dissolved organic matter induced by biodegradation. *Soil Biology & Biochemistry* 35, 1129–1142.
- Kaspar, H., Dettmer, K., Gronwald, W. & Oefner, P.J. 2009. Advances in amino acid analysis. *Analytical and bioanalytical chemistry* 393, 445–452.
- Keesstra, S.D., Bouma, J., Wallinga, J., Tiftonell, P., Smith, P., Cerdà, A., et al. 2016. The significance of soils and soil science towards realization of the United Nations Sustainable Development Goals. *SOIL* 2, 111–128.
- Keiluweit, M. & Kleber, M. 2009. Molecular-level interactions in soils and sediments: the role of aromatic π -systems. *Environmental Science & Technology*, 43, 3421–3429.
- Kielland, K. 1995. Landscape patterns of free amino acids in arctic tundra soils. *Biogeochemistry* 31, 85–98.
- Kitadai, N., Yokoyama, T. & Nakashima, S. 2009. In situ ATR-IR investigation of L-lysine adsorption on montmorillonite. *Journal of Colloid and Interface Science*, 338, 395–401.
- Kleber, M., Eusterhues, K., Keiluweit, M., Mikutta, C., Mikutta, R. & Nico, P.S. 2014. Mineral-organic associations: formation, properties, and relevance in soil environments. *Advances in Agronomy* 130, 1–140.
- Kleber, M., Sollins, P. & Sutton, R. 2007. A conceptual model of organo-mineral interactions in soils: Self-assembly of organic molecular fragments into zonal structures on mineral surfaces. *Biogeochemistry*, 85, 9–24.
- Klotzbücher, T., Kaiser, K., Filley, T.R. & Kalbitz, K. 2013. Processes controlling the production of aromatic water-soluble organic matter during litter decomposition. *Soil Biology & Biochemistry* 67, 133–139.
- Knicker, H. 2011. Soil organic N - An under-rated player for C sequestration in soils? *Soil Biology & Biochemistry* 43, 1118–1129.
- Kögel-Knabner, I., Guggenberger, G., Kleber, M., Kandeler, E., Kalbitz, K., Scheu, S., et al. 2008. Organo-mineral associations in temperate soils: Integrating biology, mineralogy, and organic matter chemistry. *Journal of Plant Nutrition and Soil Science* 171, 61–82.

- Koopmans, C.J., Tietema, A. & Verstraten, J.M. 1997. Effects of reduced N deposition on litter decomposition and N cycling in two N saturated forests in the Netherlands. *Soil Biology & Biochemistry* 30, 141–151.
- Kothawala, D.N., Roehm, C., Blodau, C. & Moore, T.R. 2012. Selective adsorption of dissolved organic matter to mineral soils. *Geoderma* 189–190, 334–342.
- Kramer, M.G., Sanderman, J., Chadwick, O.A., Chorover, J. & Vitousek, P.M. 2012. Long-term carbon storage through retention of dissolved aromatic acids by reactive particles in soil. *Global Change Biology* 18, 2594–2605.
- Kubicki, J.D., Itoh, M.J., Schroeter, L.M. & Apitz, S.E. 1997. Bonding mechanisms of salicylic acid adsorbed onto illite clay: An ATR-FTIR and molecular orbital study. *Environmental Science & Technology*, 31, 1151–1156.
- Kvitvang, H.F.N., Andreassen, T., Adam, T., Villas-Bôas, S.G. & Bruheim, P. 2011. Highly sensitive GC/MS/MS method for quantitation of amino and nonamino organic acids. *Analytical Chemistry* 83, 2705–2711.
- Lal, R. 2004. Soil carbon sequestration impacts on global climate change and food security. *Science* 304, 1623–1627.
- Langrock, T., Czihal, P. & Hoffmann, R. 2006. Amino acid analysis by hydrophilic interaction chromatography coupled on-line to electrospray ionization mass spectrometry. *Amino Acids* 30, 291–297.
- Le Quéré, C., Raupach, M.R., Canadell, J.G., Marland, G., Bopp, L., Ciais, P., et al. 2009. Trends in the sources and sinks of carbon dioxide. *Nature Geoscience* 2, 831–836.
- Le, A., Ng, A., Kwan, T., Cusmano-Ozog, K. & Cowan, T.M. 2014. A rapid, sensitive method for quantitative analysis of underivatized amino acids by liquid chromatography-tandem mass spectrometry (LC-MS/MS). *Journal of Chromatography B* 944, 166–74.
- Lehmann, J. & Kleber, M. 2015. The contentious nature of soil organic matter. *Nature*, 528, 60–68.
- Lehmann, J., Kinyangi, J. & Solomon, D. 2007. Organic matter stabilization in soil microaggregates: Implications from spatial heterogeneity of organic carbon contents and carbon forms. *Biogeochemistry* 85, 45–57.
- Lehmann, J., Solomon, D., Kinyangi, J., Dathe, L., Wirrick, S. & Jacobsen, C. 2008. Spatial complexity of soil organic matter forms at nanometre scales. *Nature Geoscience* 1, 238–242.

- Leinemann, T., Mikutta, R., Kalbitz, K., Schaarschmidt, F. & Guggenberger, G. 2016. Small scale variability of vertical water and dissolved organic matter fluxes in sandy Cambisol subsoils as revealed by segmented suction plates. *Biogeochemistry* 131, 1–15.
- Lin, L.H. & Simpson, M.J. 2016. Enhanced extractability of cutin- and suberin-derived organic matter with demineralization implies physical protection over chemical recalcitrance in soil. *Organic Geochemistry* 97, 111–121.
- Liu, D.L., Beegle, L.W. & Kanik, I., 2008. Analysis of underivatized amino acids in geological samples using ion-pairing liquid chromatography and electrospray tandem mass spectrometry. *Astrobiology* 8, 229–241.
- Liu, S.Y., Kleber, M., Takahashi, L.K., Nico, P., Keiluweit, M. & Ahmed, M. 2013. Synchrotron-based mass spectrometry to investigate the molecular properties of mineral-organic associations. *Analytical Chemistry* 85, 6100–6106.
- Liu, X., Lu, X., Wang, R., Zhou, H. & Xu, S. 2008. Surface complexes of acetate on edge surfaces of 2:1 type phyllosilicate: Insights from density functional theory calculation. *Geochimica et Cosmochimica Acta* 72, 5896–5907.
- Liu, Z. & Lee, C. 2007. The role of organic matter in the sorption capacity of marine sediments. *Marine Chemistry* 105, 240–257.
- Luo, Y., Keenan, T.F. & Smith, M. 2015. Predictability of the terrestrial carbon cycle. *Global Change Biology* 21, 1737–1751.
- Lützw, M. V., Kögel-Knabner, I., Ekschmitt, K., Matzner, E., Guggenberger, G., Marschner, B. & Flessa, H. 2006. Stabilization of organic matter in temperate soils: Mechanisms and their relevance under different soil conditions - a review. *European Journal of Soil Science* 57, 426–445.
- Macías, F. & Arbestain, M.C. 2010. Soil carbon sequestration in a changing global environment. *Mitigation and Adaptation Strategies for Global Change* 15, 511–529.
- Martens, D.A. & Loeffelmann, K.L. 2003. Soil amino acid composition quantified by acid hydrolysis and anion chromatography-pulsed amperometry. *Journal of agriculture and food chemistry*, 51, 6521–6529.
- Martens, D.A., Jaynes, D.B., Colvin, T.S., Kaspar, T.C. & Karlen, D.L. 2006. Soil Organic Nitrogen Enrichment Following Soybean in an Iowa Corn–Soybean Rotation. *Soil Science Society of America Journal* 70, 382.
- Mayer, L.M. & Xing, B. 2001. Organic matter – surface area relationships in acid soils. *Soil Science Society of America Journal* 65, 250–258.

- Mayes, M.A., Heal, K.R., Brandt, C.C., Phillips, J.R. & Jardine, P.M. 2012. Relation between soil order and sorption of dissolved organic carbon in temperature subsoils. *Soil Science Society of America Journal* 76, 1027–1037.
- McDowell, W.H. & Likens, G.E. 1988. Origin, composition, and flux of dissolved organic carbon in the Hubbard Brook Valley. *Ecological Monographs* 58, 177–195.
- Meier, M., Namjesnik-Dejanovic, K., Maurice, P.A., Chin, Y.P. & Aiken, G.R. 1999. Fractionation of aquatic natural organic matter upon sorption to goethite and kaolinite. *Chemical Geology* 157, 275–284.
- Mikutta, R., Kaiser, K., Dörr, N., Vollmer, A., Chadwick, O.A., Chorover, J., Kramer, M.G. & Guggenberger, G. 2010. Mineralogical impact on organic nitrogen across a long-term soil chronosequence (0.3–4100 kyr). *Geochimica et Cosmochimica Acta* 74, 2142–2164.
- Mikutta, R., Kleber, M., Kaiser, K. & Jahn, R. 2005. Review: Organic matter removal from soils using hydrogen peroxide. *Soil Science Society of America Journal* 69, 120–135.
- Mikutta, R., Kleber, M., Torn, M.S. & Jahn, R. 2006. Stabilization of soil organic matter: Association with minerals or chemical recalcitrance? *Biogeochemistry* 77, 25–56.
- Mikutta, R., Lorenz, D., Guggenberger, G., Haumaier, L. & Freund, A. 2014. Properties and reactivity of Fe-organic matter associations formed by coprecipitation versus adsorption: Clues from arsenate batch adsorption. *Geochimica et Cosmochimica Acta*, 144, 258–276.
- Mikutta, R., Mikutta, C., Kalbitz, K., Scheel, T., Kaiser, K. & Jahn, R. 2007. Biodegradation of forest floor organic matter bound to minerals via different binding mechanisms. *Geochimica et Cosmochimica Acta*, 71, 2569–2590.
- Mikutta, R., Schaumann, G.E., Gildemeister, D., Bonneville, S., Kramer, M.G., Chorover, J., et al. 2009. Biogeochemistry of mineral-organic associations across a long-term mineralogical soil gradient (0.3–4100 kyr), Hawaiian Islands. *Geochimica et Cosmochimica Acta* 73, 2034–2060.
- Mikutta, R., Zang, U., Chorover, J., Haumaier, L. & Kalbitz, K. 2011. Stabilization of extracellular polymeric substances (*Bacillus subtilis*) by adsorption to and coprecipitation with Al forms. *Geochimica et Cosmochimica Acta* 75, 3135–3154.
- Minasny, B., Malone, B.P., McBratney, A.B., Angers, D.A., Arrouays, D., Chambers, A., et al. 2017. Soil carbon 4 per mille. *Geoderma* 292, 59–86.
- Mota, F.L., Queimada, A.J., Pinho, S.P. & Macedo, E.A. 2008. Aqueous solubility of some natural phenolic compounds. *Industrial and Engineering Chemistry*

- Research*, 47, 5182–5189.
- Murphy, E.M., Zachara, J.M. & Smith, S.C. 1990. Influence of mineral-bound humic substances on the sorption of hydrophobic organic compounds. *Environmental Science & Technology* 24, 1507–1516.
- Näsholm, T., Huss-Danell, K. & Högberg, P. 2000. Uptake of organic nitrogen in the field by four agriculturally important plant species. *Ecology* 81, 1155–1161.
- Nave, L.E., Vance, E.D., Swanston, C.W. & Curtis, P.S. 2009. Impacts of elevated N inputs on north temperate forest soil C storage, C/N, and net N-mineralization. *Geoderma* 153, 231–240.
- Nieder, R., Benbi, D.K. & Scherer, H.W. 2011. Fixation and defixation of ammonium in soils: A review. *Biology and Fertility of Soils* 47, 1–14.
- Noubigh, A., Abderrabba, M. & Provost, E. 2007. Temperature and salt addition effects on the solubility behaviour of some phenolic compounds in water. *Journal of Chemical Thermodynamics*, 39, 297–303.
- O'Brien, S.L. & Jastrow, J.D., 2013. Physical and chemical protection in hierarchical soil aggregates regulates soil carbon and nitrogen recovery in restored perennial grasslands. *Soil Biology & Biochemistry* 61, 1–13.
- Olk, D.C. 2008. Improved analytical techniques for carbohydrates, amino compounds, and phenols: tools for understanding soil processes. *Soil Science Society of America Journal* 72, 1672–1682.
- Olk, D.C., Fortuna, A. & Honeycutt, C.W. 2008. Using anion chromatography–pulsed amperometry to measure amino compounds in dairy manure-amended soils. *Soil Science Society of America Journal* 72, 1711–1720.
- Omoike, A. & Chorover, J. 2006. Adsorption to goethite of extracellular polymeric substances from *Bacillus subtilis*. *Geochimica et Cosmochimica Acta* 70, 827–838.
- Orgill, S.E., Condon, J.R., Kirkby, C.A., Orchard, B.A., Conyers, M.K., Greene, R.S.B. & Murphy, B.W. 2017. Soil with high organic carbon concentration continues to sequester carbon with increasing carbon inputs. *Geoderma* 285, 151–163.
- Parbhakar, A., Cuadros, J., Sephton, M.A., Dubbin, W., Coles, B.J. & Weiss, D. 2007. Adsorption of L-lysine on montmorillonite. *Colloids and Surfaces A: Physicochemical and Engineering Aspects*, 307, 142–149.
- Paul, E.A. 2016. The nature and dynamics of soil organic matter: Plant inputs, microbial transformations, and organic matter stabilization. *Soil Biology and Biochemistry* 98, 109–126.

- Perakis, S.S. & Hedin, L.O. 2002. Nitrogen loss from unpolluted South American forests mainly via dissolved organic compounds. *Nature* 415, 416–419.
- Philippe, A. & Schaumann, G.E. 2014. Interactions of dissolved organic matter with natural and engineered inorganic colloids: A review. *Environmental Science & Technology* 48, 8946–8962.
- Piraud, M., Vianey-Saban, C., Petritis, K., Elfakir, C., Steghens, J.P. & Bouchu, D. 2005. Ion-pairing reversed-phase liquid chromatography/electrospray ionization mass spectrometric analysis of 76 underivatized amino acids of biological interest: a new tool for the diagnosis of inherited disorders of amino acid metabolism. *Rapid Communications in Mass Spectrometry* 19, 1587–1602.
- Polubesova, T., Chen, Y., Navon, R. & Chefetz, B. 2008. Interactions of hydrophobic fractions of dissolved organic matter with Fe^{3+} - and Cu^{2+} -montmorillonite. *Environmental Science & Technology* 42, 4797–4803.
- Polubesova, T., Chen, Y., Stefan, C., Selle, M., Werner, P. & Chefetz, B. 2009. Sorption of polyaromatic compounds by organic matter-coated Ca^{2+} - and Fe^{3+} -montmorillonite. *Geoderma* 154, 36–41.
- Polubesova, T., Eldad, S. & Chefetz, B. 2010. Adsorption and oxidative transformation of phenolic acids by $\text{Fe}(\text{III})$ -montmorillonite. *Environmental Science & Technology*, 44, 4203–4209.
- Preinerstorfer, B., Schiesel, S., Lämmerhofer, M. & Lindner, W. 2010. Metabolic profiling of intracellular metabolites in fermentation broths from beta-lactam antibiotics production by liquid chromatography-tandem mass spectrometry methods. *Journal of chromatography A* 1217, 312–328.
- Quiquampoix, H., Abadie, J., Baron, M.H., Leprince, F., Matumoto-Pintro, P.T., Ratcliffe, R.G. & Staunton, S. 1995. Mechanisms and consequences of protein adsorption on soil mineral surfaces. In: *Proteins at interfaces*, pp. 321-333. Washington, USA : ACS - American Chemical Society.
- Ragnar, M., Lindgren, C.T. & Nilvebrant, N.O. 2000. pK_a -values of guaiacyl and syringyl phenols related to lignin. *Journal of Wood Chemistry and Technology*, 20, 277–305.
- Ramos, A.C.H. & McBride, M.B. 1996. Goethite dispersibility in solutions of variable ionic strength and soluble organic matter content. *Clays and Clay Minerals* 44, 286–296.
- Ransom, B., Bennett, R.H., Baerwald, R. & Shea, K. 1997. TEM study of in situ organic matter on continental margins: occurrence and the “monolayer” hypothesis. *Marine Geology* 138, 1–9.

- Remusat, L., Hatton, P.J., Nico, P.S., Zeller, B., Kleber, M. & Derrien, D. 2012. NanoSIMS study of organic matter associated with soil aggregates: Advantages, limitations, and combination with STXM. *Environmental Science & Technology* 46, 3943–3949.
- Ruddiman, W.F. 2003. The anthropogenic greenhouse era began thousands of years ago. *Climatic Change* 61, 261–293.
- Saidy, A.R., Smernik, R.J., Baldock, J.A., Kaiser, K. & Sanderman, J. 2013. The sorption of organic carbon onto differing clay minerals in the presence and absence of hydrous iron oxide. *Geoderma* 209–210, 15–21.
- Sánchez-Hernández, L., Marina, M.L. & Crego, A.L. 2011. A capillary electrophoresis-tandem mass spectrometry methodology for the determination of non-protein amino acids in vegetable oils as novel markers for the detection of adulterations in olive oils. *Journal of chromatography A* 1218, 4944–4951.
- Sanderman, J., Baldock, J.A. & Amundson, R. 2008. Dissolved organic carbon chemistry and dynamics in contrasting forest and grassland soils. *Biogeochemistry* 89, 181–198.
- Sarazin, C., Delaunay, N., Costanza, C., Eudes, V., Mallet, J. & Gareil, P. 2011. New avenue for mid-UV-range detection of underivatized carbohydrates and amino Acids in capillary electrophoresis. *Analytical Chemistry* 83, 7381–7387.
- Schimel, J.P. & Bennett, J. 2004. Nitrogen mineralization: challenges of a changing paradigm. *Ecology*, 85, 591–602.
- Schlautman, M.A. & Morgan, J.J. 1994. Adsorption of aquatic humic substances on colloidal-size aluminum oxide particles: Influence of solution chemistry. *Geochimica et Cosmochimica Acta* 58, 4293–4303.
- Schmidt, C.F., Zimmermann, R.M. & Gaub, H.E. 1990. Multilayer adsorption of lysozyme on a hydrophobic substrate. *Biophysical Journal* 57, 577–588.
- Schmidt, M.W.I., Torn, M.S., Abiven, S., Dittmar, T., Guggenberger, G., Janssens, I.A., et al. 2011. Persistence of soil organic matter as an ecosystem property. *Nature* 478, 49–56.
- Schneider, M.P.W., Scheel, T., Mikutta, R., Van Hees, P., Kaiser, K. & Kalbitz, K. 2010. Sorptive stabilization of organic matter by amorphous Al hydroxide. *Geochimica et Cosmochimica Acta* 74, 1606–1619.
- Schrumpf, M. & Kaiser, K. 2015. Large differences in estimates of soil organic carbon turnover in density fractions by using single and repeated radiocarbon inventories. *Geoderma* 239–240, 168–178.

- Servagent-Noirville, S., Revault, M., Quiquampoix, H. & Baron, M. 2000. Conformational Changes of Bovine Serum Albumin Induced by Adsorption on Different Clay Surfaces: FTIR Analysis. *Journal of Colloid and Interface Science* 221, 273–283.
- Siewert, C. & Kučerík, J. 2015. Practical applications of thermogravimetry in soil science. Part 3: I interrelations between soil components and unifying principles of pedogenesis. *Journal of Thermal Analysis and Calorimetry* 120, 471–480.
- Six, J., Bossuyt, H., Degryze, S. & Denef, K. 2004. A history of research on the link between (micro)aggregates, soil biota, and soil organic matter dynamics. *Soil & Tillage Research* 79, 7–31.
- Sleutel, S., Leinweber, P., Van Ranst, E., Kader, M.A. & Jegajeevagan, K. 2011. Organic matter in clay density fractions from sandy cropland soils with differing land-use history. *Soil Science Society of America Journal* 75, 521–532.
- Smith, P., Martino, D., Cai, Z., Gwary, D., Janzen, H., Kumar, P., et al. 2008. Greenhouse gas mitigation in agriculture. *Philosophical Transactions of the Royal Society B: Biological Sciences* 363, 789–813.
- Sollins, P., Swanston, C., Kleber, M., Filley, T., Kramer, M., Crow, S., et al. 2006. Organic C and N stabilization in a forest soil: Evidence from sequential density fractionation. *Soil Biology & Biochemistry* 38, 3313–3324.
- Solomon, D., Lehmann, J., Harden, J., Wang, J., Kinyangi, J., Heymann, K., et al. 2012. Micro- and nano-environments of carbon sequestration: Multi-element STXM-NEXAFS spectromicroscopy assessment of microbial carbon and mineral associations. *Chemical Geology* 329, 53–73.
- Souza, I.F., Archanjo, B.S., Hurtarte, L.C.C., Oliveros, M.E., Gouvea, C.P., Lidizio, L.R., et al. 2017. Al-/Fe-(hydr)oxides–organic carbon associations in Oxisols — from ecosystems to submicron scales. *Catena* 154, 63–72.
- Sposito, G. 2008. *The chemistry of soil* (second edition). Oxford University Press, New York.
- Štefanić, I., Ljubić, I., Bonifačić, M., Sabljčić, A., Asmus, K.-D. & Armstrong, D.A. 2009. A surprisingly complex aqueous chemistry of the simplest amino acid. A pulse radiolysis and theoretical study on H/D kinetic isotope effects in the reaction of glycine anions with hydroxyl radicals. *Physical Chemistry Chemical Physics* 11, 2256–2267.
- Stevenson, F.J. 1994. *Humus chemistry: genesis, composition, reactions* (2nd Edition), Wiley.

- Stockmann, U., Adams, M.A., Crawford, J.W., Field, D.J., Henakaarchchi, N., Jenkins, M., et al. 2013. The knowns, known unknowns and unknowns of sequestration of soil organic carbon. *Agriculture, Ecosystems and Environment* 164, 80–99.
- Swenson, T.L., Bowen, B.P., Nico, P.S. & Northen, T.R. 2015. Competitive sorption of microbial metabolites on an iron oxide mineral. *Soil Biology & Biochemistry* 90, 34–41.
- Swift, R.S. 1999. Macromolecular properties of soil humic substances: Fact, fiction, and opinion. *Soil Science* 164, 790–802.
- Tang, X., Gu, Y., Nie, J., Fan, S. & Wang, C. 2014. Quantification of amino acids in rat urine by solid-phase extraction and liquid chromatography/electrospray tandem mass spectrometry: Application to radiation injury rat model. *Journal of Liquid Chromatography & Related Technologies* 37, 951–973.
- Thomas, J.E. & Kelley, M.J. 2010. A study of competitive adsorption of organic molecules onto mineral oxides using DRIFTS. *Journal of Colloid and Interface Science*, 342, 474–478.
- Tombácz, E., Libor, Z., Illés, E., Majzik, A. & Klumpp, E. 2004. The role of reactive surface sites and complexation by humic acids in the interaction of clay mineral and iron oxide particles. *Organic Geochemistry*, 35, 257–267.
- Torn, M.S., Kleber, M., Zavaleta, E.S., Zhu, B., Field, C.B. & Trumbore, S.E. 2013. A dual isotope approach to isolate soil carbon pools of different turnover times. *Biogeosciences* 10, 8067–8081.
- Vázquez-Ortega, A., Hernandez-Ruiz, S., Amistadi, M.K., Rasmussen, C. & Chorover, J. 2014. Fractionation of dissolved organic matter by (oxy)hydroxide-coated sands: Competitive sorbate displacement during reactive transport. *Vadose Zone Journal* 13, 1–13.
- Vogel, C., Mueller, C.W., Höschen, C., Buegger, F., Heister, K., Schulz, S., et al. 2014. Submicron structures provide preferential spots for carbon and nitrogen sequestration in soils. *Nature Communications* 5, 1–7.
- Von Lütow, M., Kögel-Knabner, I., Ludwig, B., Matzner, E., Flessa, H., Ekschmitt, K., et al. 2008. Stabilization mechanisms of organic matter in four temperate soils: Development and application of a conceptual model. *Journal of Plant Nutrition and Soil Science* 171, 111–124.
- Walsch, J. & Dultz, S. 2010. Effects of pH, Ca- and SO₄-concentration on surface charge and colloidal stability of goethite and hematite – consequences for the adsorption of anionic organic substances. *Clay Minerals*, 45, 1–13.

- Wang, K. & Xing, B. 2005. Structural and sorption characteristics of adsorbed humic acid on clay minerals. *Journal of Environmental Quality* 34, 342–349.
- Wang, X., Cammeraat, E.L.H., Romeijn, P. & Kalbitz, K. 2014. Soil organic carbon redistribution by water erosion – the role of CO₂ emissions for the carbon budget. *PLoS ONE* 9, 1–13.
- Wang, X., Lu, J., Xu, M. & Xing, B. 2008. Sorption of pyrene by regular and nanoscaled metal oxide particles: Influence of adsorbed organic matter. *Environmental Science & Technology* 42, 7267–7272.
- Wang, X.C. & Lee, C. 1993. Adsorption and desorption of aliphatic amines, amino acids and acetate by clay minerals and marine sediments. *Marine Chemistry* 44, 1–23.
- Weng, L., Van, W.H., Hiemstra, T. & Quality, S. 2008. Humic nanoparticles at the oxide-water interface: Interactions with phosphate ion adsorption. *Environmental Science & Technology* 42, 8747–8752.
- Wershaw, R.L. 1993. Model for humus in soils and sediments. *Environmental Science & Technology* 27, 814–816.
- Woche, S.K., Goebel, M.-O., Mikutta, R., Schurig, C., Kaestner, M., Guggenberger, G. & Bachmann, J. 2017. Soil wettability can be explained by the chemical composition of particle interfaces - An XPS study. *Scientific Reports* 7, 42877.
- Yang, S., Synovec, R.E., Kalyuzhnaya, M.G. & Lidstrom, M.E. 2011. Development of a solid phase extraction protocol coupled with liquid chromatography mass spectrometry to analyze central carbon metabolites in lake sediment microcosms. *Journal of separation science* 34, 3597–605.
- Yang, Y., Wang, S., Xu, Y., Zheng, B. & Liu, J. 2016. Molecular-scale study of aspartate adsorption on goethite and competition with phosphate. *Environmental Science & Technology*, 50, 2938–2945.
- Yeasmin, S., Singh, B., Kookana, R.S., Farrell, M., Sparks, D.L. & Johnston, C.T. 2014. Influence of mineral characteristics on the retention of low molecular weight organic compounds: A batch sorption-desorption and ATR-FTIR study. *Journal of Colloid and Interface Science*, 432, 246–257.
- Yost, E.C., Tejedor-tejedor, M.I. & Anderson, M.A. 1990. In situ CIR-FTIR characterization of salicylate complexes at the goethite/aqueous solution interface. *Environmental Science & Technology*, 24, 822–828.
- Zaia, D.A.M. 2004. A review of adsorption of amino acids on minerals: Was it important for origin of life? *Amino Acids*, 27, 113–118.
- Zhang, L., Luo, L. & Zhang, S. 2012. Integrated investigations on the adsorption

- mechanisms of fulvic and humic acids on three clay minerals. *Colloids and Surfaces A: Physicochemical and Engineering Aspects*, 406, 84–90.
- Zhang, W., Liang, C., Kao-Kniffin, J., He, H., Xie, H., Zhang, H. & Zhang, X. 2015. Differentiating the mineralization dynamics of the originally present and newly synthesized amino acids in soil amended with available carbon and nitrogen substrates. *Soil Biology & Biochemistry* 85, 162–169.
- Zhao, H., Bhattacharjee, S., Chow, R., Wallace, D., Masliyah, J.H. & Xu, Z. 2008. Probing surface charge potentials of clay basal planes and edges by direct force measurements. *Langmuir* 24, 12899–12910.
- Zhou, G., Pang, H., Tang, Y., Yao, X., Mo, X., Zhu, S. et al. 2013. Hydrophilic interaction ultra-performance liquid chromatography coupled with triple-quadrupole tandem mass spectrometry for highly rapid and sensitive analysis of underivatized amino acids in functional foods. *Amino acids* 44, 1293–1305.
- Zhuang, J. & Yu, G.R. 2002. Effects of surface coatings on electrochemical properties and contaminant sorption of clay minerals. *Chemosphere* 49, 619–628.
- Zollinger, B., Alewell, C., Kneisel, C., Meusbürger, K., Gärtner, H., Brandová, D., et al. 2013. Effect of permafrost on the formation of soil organic carbon pools and their physical-chemical properties in the Eastern Swiss Alps. *Catena* 110, 70–85.

Summary

The bioavailability and dynamics of soil organic matter (SOM) depend largely on the association with mineral particles. However, no consensus exists on the formation, composition and structure of the mineral–organic associations (MOAs). A multilayer conceptual model was proposed ten years ago to clarify the role of SOM and minerals in the formation of MOAs and visualize their spatial structure. Although the multilayer model has seen extensive adoption as research motivation and theoretical explanation for the experimental results in soil science and related fields, the experimental evidence for this multilayer model was still lacking. Thus, the main objective of this study was to test the multilayer model with well-defined soil minerals and natural organic compounds via batch adsorption experiments. Goethite, kaolinite and montmorillonite were selected to represent important minerals derived from soils. Phenolic acids (PAs) and amino acids (AAs) were used to represent the degradation products of lignin and proteinaceous compounds respectively, which are widespread in the natural environment. The fate of these highly oxidized monomers was expected to be affected by the interaction with soil minerals to a larger extent than the original polymers.

First, this study summarized the applicability of the multilayer model and evaluated its validity based on current knowledge and experimental evidence (**chapter 2**). To date, the direct and reliable evidence for the multilayer model was still missing. The multilayer model was widely used to explain experimental observations in terms of the retention and turnover of OM in soils. In fact, many of these experimental findings can be explained by simpler explanations instead of the multilayer model, like aggregation effects for the storage of SOM and differences in the availability of reactive mineral surfaces for the positive relationship between SOC content and the content of specific minerals. The patchy distribution of adsorbed organic compounds on mineral surfaces has been visualized and verified using advanced submicron spectroscopy. However, this cannot be treated as direct evidence for the multilayer model. The current evidence does not support the idea that N-rich organic compounds are generally enriched on mineral surfaces by preferential adsorption. The enrichment of N could be dependent on mineral surfaces. It is still challenging to directly visualise the spatial organization of associated OM on mineral surfaces

at the molecular scale and unravel the mechanisms involved. Some state-of-the-art techniques have great potential to address these issues, including XPS depth profiling, NanoSIMS and STXM-NEXAFS. However, more works is needed to improve the feasibility and reliability of these techniques regarding the spatial resolution, sample preparation, control of radiation damage and spectral quantification.

We developed a HILIC-MS/MS technique to achieve precise quantification of free AAs in aqueous samples and subsequently applied it to measure 20 free AAs in soil extracts (**chapter 3**). A solid phase extraction (SPE) procedure was needed to clean up and concentrate the AAs in soil extracts. We achieved similar recoveries of individual AA over the SPE procedure within each group of acidic, basic and neutral AAs. This supported our selection strategy of the tested AAs in the adsorption experiments (**chapters 4 and 5**). The SPE recoveries of a few AAs (Arg and Met) were readily affected by the composition of soil extracts. Thus further study was needed to eliminate the varied SPE recoveries of Arg and Met for different soils. In brief, the method shows great promise for the routine analysis of free AAs extracted from soils.

In the batch adsorption experiments (**chapter 4**), we found selective adsorption of organic compounds depended largely on the properties of the soil minerals. Phenolic acids were preferentially adsorbed on goethite, whereas the phyllosilicates (kaolinite and montmorillonite) were a better adsorbent for AAs. Varied adsorption behaviour was also observed for some PAs and AAs. Among all tested PAs (Sal, Syr, Fer and Van), Sal was preferentially adsorbed on all minerals. For the AAs, Glu was preferentially adsorbed on goethite and Lys on phyllosilicates. Little adsorption of neutral AAs (Leu and Phe) was observed on all minerals. Similarly, in **chapter 5** we demonstrated the adsorption of natural DOM depended on both the mineral and DOM sources. The adsorption of DOM on different minerals followed the order of goethite >> kaolinite > montmorillonite. Higher adsorption of O-DOM (derived from the O-horizon of forest soil) was observed on goethite than L-DOM (derived from forest leaf litter). Similar adsorption of O-DOM and L-DOM was observed on kaolinite and montmorillonite. Our findings contrasted with the general conclusion that aromatic compounds are preferentially adsorbed on soil particles, which is most likely controlled by soil mineralogy and composition of natural DOM.

Moreover, in **chapter 4**, we observed the AAs were more competitive than PAs and partially suppressed the adsorption of PAs on goethite and montmorillonite. The adsorption of PAs or AAs on both minerals was enhanced by surface conditioning with the other group, with larger effects for goethite than

montmorillonite. In **chapter 5**, the results illustrated that coating of various minerals with both DOM sources (O-DOM and L-DOM) reduced the adsorption of PAs and acidic AA (Glu), but enhanced the adsorption of basic AA (Lys). The effect of organic coating depended strongly on the amount of adsorbed OM. The strong bonds between AAs and OM-coated minerals resulted in generally enhanced adsorption of PAs with surface conditioning by AAs. This is in accordance with the results for pure minerals. These findings offer indirect evidence for the multilayer model of MOAs. The results suggest that the amount and composition of OM coatings affect the adsorption of PAs and AAs on soil particles and thus their dynamics in soils. Adsorbed organic matter on soil mineral phases might be subject to a self-strengthening effect via sequential adsorption of different classes of organic compounds. It is worthwhile to investigate the adsorbed PAs and AAs using advanced spectroscopy in future studies to unravel the adsorption mechanism and the molecular structure of the produced MOAs.

To conclude, our works increased the knowledge on the adsorption behaviour of natural organic compounds on soil minerals, especially the importance of the interplay between different OM components in the formation of MOAs. We propose that the adsorptive interaction with mineral phase should be perceived as an important factor in the cycling of SOM and the cycling of different components of SOM can affect each other via competitive or sequential adsorption on mineral phase. The experimental results of this study provide indirect evidence of the spatial multilayer organization of associated OM on mineral surfaces. More testing, however, remains necessary to verify the multilayer model. Since large uncertainties remain in the composition and spatial structure of MOAs, we suggest being more cautious in applying this model. More efforts remain needed to improve the feasibility and reliability of current techniques in examining the molecular composition of associated OM on mineral surfaces and the underlying mechanisms.

Samenvatting

De bio-beschikbaarheid en dynamiek van organisch materiaal in de bodem (SOM) is grotendeels afhankelijk van de associatie met minerale deeltjes. Er is echter geen consensus over de formatie, compositie en de structuur van de resulterende mineraal-organische deeltjes (MOAs). Tien jaar geleden is er een multilayer conceptueel model voorgesteld welke de rol van SOM en mineralen in de formatie van MOAs zou moeten verduidelijken, en daarnaast hun ruimtelijke structuur zou moeten visualiseren. Hoewel het multilayer model al wel veelvuldig is geadopteerd als onderzoeksmotivatie en theoretische onderbouwing voor experimentele resultaten in bodemkunde en gerelateerde velden, blijft de experimentele onderbouwing voor dit multilayer model incompleet.

Het doel van deze studie was het testen van het multilayer model met behulp van goed gedefinieerde bodemmineralen en natuurlijke organische verbindingen in een set adsorptie experimenten. Goethiet, Kaoliniet en Montmorilloniet zijn geselecteerd als goede representanten van belangrijke bodemmineralen. Fenolzuren (PAs) en aminozuren (AAs) representeerden de afbraakproducten van Lignine en andere proteïneverbindingen, welke veelvuldig aanwezig zijn in natuurlijke bodemomstandigheden. De verwachting was dat deze zwaar geoxideerde monomeren eerder beïnvloed zouden worden door interactie met bodemmineralen dan de oorspronkelijke polymeren.

Als eerste hebben we de toepasbaarheid van het multilayer model samengevat, en vervolgens de validiteit van het model geëvalueerd op basis van de huidige kennis en het huidige beschikbare experimentele bewijs (Hoofdstuk 2). Tot op heden ontbreekt direct en betrouwbaar bewijs voor het multilayer model. Het multilayer model is veelvoudig gebruikt voor het onderbouwen van experimentele observaties in betrekking tot het vasthouden en het omzetten van OM in de bodem. Veel van de experimentele bevindingen kunnen echter ook verklaard worden met simpelere theorieën dan het multilayer model, zoals de aggregatie effecten voor de opslag van SOM, en de verschillen in de beschikbaarheid van reactieve minerale oppervlakten voor de positieve relatie tussen de hoeveelheid bodemorganisch koolstof en de hoeveelheid specifieke mineralen.

De onregelmatige verdeling van geadsorbeerde organische verbindingen op minerale oppervlaktes is gevisualiseerd en geverifieerd door middel van geavanceerde submicron spectroscopie. Echter, de resultaten hiervan kunnen niet worden gezien als direct bewijs voor het multilayer model. Het idee dat stikstofrijke organische verbindingen verrijkt worden op de minerale oppervlakten door preferentiële adsorptie wordt niet ondersteund door het huidige beschikbare bewijs. De verrijking van stikstof is mogelijk afhankelijk van minerale oppervlaktes. Het is nog steeds een uitdaging om de ruimtelijke organisatie van geassocieerd OM op minerale oppervlaktes op een moleculair niveau direct te visualiseren en de betrokken mechanismes te ontrafelen. De nieuwste technieken, zoals XPS depth profiling, NanoSIMS en STXM-NEXAFS, kunnen mogelijk toegepast worden om deze barrières te slechten. Om dit ook werkelijk te bewerkstelligen zal echter de haalbaarheid en de betrouwbaarheid van deze technieken op het gebied van ruimtelijke resolutie, monstervoorbewerking, beperking van stralingsschade, en spectrale kwantificatie moeten worden verbeterd.

We hebben een HILIC-MS/MS techniek ontwikkeld voor precieze kwantificatie van vrije AAs in watermonsters en deze vervolgens toegepast op 20 vrije AAs in bodemextracten (Hoofdstuk 3). Een solid phase extraction (SPE) procedure was nodig om de extracten op te schonen en de AAs in de extracten te concentreren. Met de SPE procedure hebben we voor de individuele AAs, binnen de verschillende milieus, zuur, basisch en neutraal, vergelijkbare opbrengsten weten te realiseren. Dit resultaat ondersteunde onze geselecteerde strategie van de geteste AAs in de adsorptie experimenten (Hoofdstuk 4 en 5). De SPE opbrengst van een aantal AAs (Arg en Met) werd duidelijk beïnvloed door de samenstelling van de bodemextracten. Het vereiste verder onderzoek om de variatie in SPE opbrengst voor Arg en Met in verschillende bodems te elimineren. Tot slot, toont deze methode grote potentie voor de routine analyse van vrije AAs geëxtraheerd uit bodems.

In de adsorptie experimenten (Hoofdstuk 4) vonden we dat de selectieve adsorptie van organische verbindingen grotendeels afhankelijk is van de karakteristieken van de bodemmineralen. Fenolzuren werden preferentieel geadsorbeerd op Goethiet, terwijl de AAs preferentieel adsorbeerden op de phyllosilicaten (Kaoliniet en Montmorilloniet). Gevarieerd adsorptie gedrag voor PAs en AAs werd ook geobserveerd. Onder alle geteste PAs (Sal, Syr, Fer en Van) werd Sal preferentieel geadsorbeerd door alle mineralen. Onder de AAs adsorbeerde Glu preferentieel op Goethiet, en Lys op phyllosilicaten. Neutrale AAs (Leu en Phe) werden weinig geadsorbeerd op de mineralen. In Hoofdstuk

5 demonstreerden we de adsorptie van natuurlijke DOM, afhankelijk van de oorsprong van het mineraal en de DOM. De adsorptie van DOM op verschillende mineralen verliep met de volgorde Goethiet >> Kaolinite >> Montmorillonite. Bij O-DOM (afkomstig uit de O-horizon van een bosbodem) werd een hogere adsorptie op Goethiet waargenomen dan bij L-DOM (afkomstig uit boomblad litter). Vergelijkbare adsorptie van O-DOM en L-DOM is waargenomen op Kaolinite en Montmorillonite. Onze bevindingen contrasteren met de algemene conclusie dat aromatische verbindingen preferentieel adsorberen op bodemdeeltjes. De reden is hoogstwaarschijnlijk een afhankelijkheid van de bodemmineralogie en de compositie van het aangewende natuurlijke DOM.

In Hoofdstuk 4 vonden we dat AAs in grotere mate competitief zijn dan PAs en leiden tot gedeeltelijke onderdrukking van de adsorptie van PAs op Goethiet en Montmorillonite. De adsorptie van PAs of AAs op beide mineralen werd versterkt door het conditioneren van het oppervlakte met de andere groep, met grotere effectiviteit voor Goethiet dan bij Montmorillonite. In hoofdstuk 5 illustreerden de resultaten dat door de mineralen te voorzien van een coating van DOM (O-DOM of L-DOM) de adsorptie van PAs en zure AA (Glu) wordt gereduceerd, maar de adsorptie van basische AA (Lys) versterkt wordt. Het effect van de organische coating is sterk afhankelijk van de hoeveelheid geadsorbeerd OM. De sterke verbindingen tussen AAs en OM-gecoate mineralen resulteren in het algemeen in versterkte adsorptie van PAs bij oppervlakte conditionering door AAs. Dit is in overeenstemming met de resultaten voor pure mineralen. Deze bevindingen bieden indirect bewijs voor het multilayer model van MOAs. Het resultaat suggereert dat de hoeveelheid en compositie van OM coatings de adsorptie van PAs en AAs op bodemmineralen beïnvloed en daarbij ook hun dynamiek in bodems. De adsorptie van organisch materiaal op bodemmineralen is mogelijk onderhevige aan een zelfversterkend effect via een sequentiële adsorptie van verschillende klassen van organische verbindingen. In toekomstig onderzoek zou het waardevol zijn om de geadsorbeerde PAs en AAs met behulp van geavanceerde spectroscopie te onderzoeken om zo het adsorptiemechanisme en de moleculaire structuur van de geproduceerde MOAs beter te begrijpen.

Ter conclusie, draagt ons onderzoek bij aan de kennis over adsorptiegedrag van natuurlijke organische verbindingen op bodemmineralen, en dan met name met betrekking tot het belang van de wisselwerking tussen verschillende OM componenten in de formatie van MOAs. We stellen voor dat de adsorptie wisselwerking met de minerale fase zou moeten worden gezien als een

belangrijke factor in de omzetting van SOM en dat de omzetting van verschillende componenten van SOM elkaar kan beïnvloeden door middel van competitie of sequentiële adsorptie op de minerale fase. De experimentele resultaten van dit onderzoek leveren indirecte bewijzen voor de ruimtelijke organisatie van geassocieerde OM op minerale oppervlaktes in laagjes. Verder onderzoek blijft echter nodig om het multilayer model verder te verifiëren. Aangezien er grote onzekerheden blijven ten opzichte van de samenstelling en ruimtelijke structuur van MOAs raden we voorzichtigheid aan bij het toepassen van dit model. Er zal verder onderzoek nodig zijn om de bruikbaarheid en de betrouwbaarheid van de huidige technieken in het bestuderen van de moleculaire samenstelling van geassocieerd OM op minerale oppervlaktes en de onderliggende mechanismen te verbeteren.

Acknowledgements

It was a great moment when Prof. Jianbin Zhou (Northwest A&F University) informed me that there was an opportunity to do my PhD research in the University of Amsterdam (UvA) about 5 years ago. Another great moment is coming soon, because I will be qualified for a doctor as a reward for the time and efforts I spent during the last 5 years. This is a challenging work with high and low moments, but I really enjoy them. The title is important for me if I want to continue my career in academic research. This is also the wish of the China Scholarship Council and the behind government. They paid a big portion of my living expense as the support and strong desire to improve the national level in teaching and research. They deserve my lifelong thanks and respects. My thanks also should go to the UvA and Deutsche Forschungsgemeinschaft DFG (FOR1806, "The Forgot-ten Part of Carbon Cycling: Organic Matter Storage and Turnover in Subsoils (SUBSOM)", which funded my doctoral research works.

I'm deeply grateful to my supervisor Prof. Karsten Kalbitz and Dr. Boris Jansen. You helped me get funding after my CSC scholarship expired, gave me lots of inspiring ideas in designing experiment, addressing troubles, doing oral presentation, writing and revising academic paper. I cannot reach this step without your consistent and remarkable guidance. What I learnt from you will be together with me for the rest of my life and pave my way to be a qualified and confident member not only in pursuing my research career but also as a common individual of the whole society. I really appreciate the support of Prof. Peter de Ruiter, as my formal promoter to replace Karsten after he went back to work in Germany in the middle of 2014.

My sincere gratitude should be extended to Prof. Georg Guggenberger, Dr. Stefan Dultz and Susanne K. Woche from Leibniz Universitaet Hannover for conducting mineral sample analysis and reviewing my paper, and Prof. Robert Mikutta from Martin Luther University Halle-Wittenberg for the constructive suggestions and comments on my paper. I was impressed by your scientific spirits. Your rigorous attitude, solid expertise and background knowledge would inspire me to move up continuously with strong incentives. I really appreciate the substantial lab works carried out in Hannover by Susanne for the XPS analysis. Although, the seven months' efforts spent in the XPS measurement did not result in some expected rewards. This gave me chance to touch and

learn the advanced and promising techniques. I would definitely benefit from this over time.

Many thanks to all my skilled technician colleagues from UvA that participated in sample analysis, especially to Rick Helmus, Chiara Cerli, Joke Westerveld, Leo Hoitinga, Peter Serne, Jorien Schoorl and Rutger van Hall. They taught me the advanced and reliable techniques to measure samples and made great contributions to settle the problems I met in sample analysis. Special thanks should go to Rick, he taught me and helped me a lot in learning HPLC and analysing samples.

I would like to thank all the managers and secretaries of IBED for helping me searching house and applying for residence permission, my PhD researcher colleagues for their suggestions on my research project and efforts in creating a comfortable working environment, my international flatmates and Chinese friends for dealing with the daily life issues, filling my travel time around Europe with wonderful moments as companions and inspiring me when I was trapped in troubles. There are lots of enjoyable experiences. All your conscious and unconscious support enabled me to make progress continuously in conducting research and social life over the last few years. The lasting benefits were already absorbed into my blood and will drive me move forward forever.

Undoubtedly, I have to thank my family for their selfless love and support ever since I was born. You will underpin my life forever and give me power to take responsibilities and make progress.

Amsterdam

30 June 2017

Publications

- Gao, J.**, Helmus, R., Cerli, C., Jansen, B., Wang, X. & Kalbitz, K. 2016. Robust analysis of underivatized free amino acids in soil by hydrophilic interaction liquid chromatography coupled with electrospray tandem mass spectrometry. *Journal of Chromatography A*, 1449, 78–88.
- Gao, J.**, Jansen, B., Cerli, C., Helmus, R., Mikutta R., Dultz S., Guggenberger G., Kalbitz K. 2017. Competition and surface conditioning alter the adsorption of phenolic acids and amino acids on soil minerals. *European Journal of Soil Science*, 68, 667–677.
- Kirkels, F.M.S.A., Cerli, C., Federherr, E., **Gao, J.** and Kalbitz, K. 2014. A novel high-temperature combustion based system for stable isotope analysis of dissolved organic carbon in aqueous samples. II: optimization and assessment of analytical performance. *Rapid Communications in Mass Spectrometry*, 28, 2574–2586.

Manuscripts

- Gao, J.**, Jansen, B., Cerli, C., Helmus, R., Mikutta R., Dultz S., Guggenberger G., Vogel C., Kalbitz K. 2017. Organic matter coatings of soil minerals affect adsorptive interactions with phenolic and amino acids. *European Journal of Soil Science*. (submitted)
- Gao, J.**, Jansen, B., Mikutta R., Guggenberger G., Vogel C., Kalbitz K. 2017. Ten-year anniversary of the “multilayer model” — a mini-review. (in preparation)

